USGS
science for a changing world

Prepared in cooperation with the U.S. Department of Defense Strategic Environmental Research and Development Program (SERDP)

Fena Valley Reservoir Watershed and Water-Balance Model Updates and Expansion of Watershed Modeling to Southern Guam

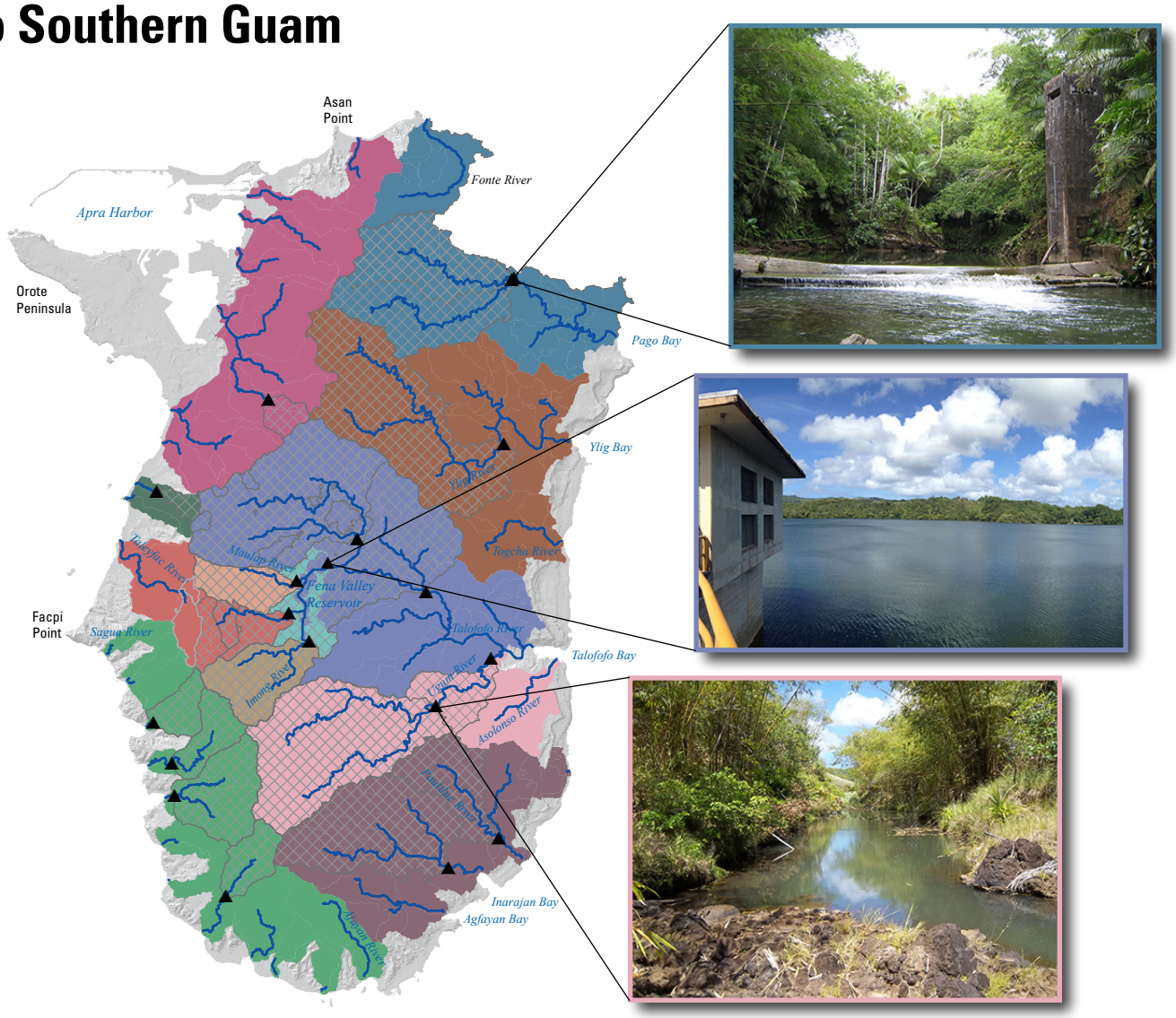

Scientific Investigations Report 2017–5093
Version 1.1, February 2019

U.S. Department of the Interior
U.S. Geological Survey

Cover. Map showing modeled regions, model stream segments, and gaged drainage-basin areas in the PRMS_2016 model. *Top photo*: Looking upstream from the U.S. Geological Survey (USGS) streamflow-gaging station 16865000 on the Pago River near Ordot. Photograph by Marcael Jamison, USGS, 2007. *Center photo*: Looking west from the Fena Valley Reservoir dam near USGS streamflow-gaging station 16849000 Fena Dam Spillway near Agat. Photograph by Sarah N. Rosa, USGS, February 22, 2014. *Bottom photo*: Looking upstream from USGS streamflow-gaging station 16854500 at Ugum River above Talofofo Falls near Talofofo. Photograph by Richard Castro, USGS, April 13, 2012.

Fena Valley Reservoir Watershed and Water-Balance Model Updates and Expansion of Watershed Modeling to Southern Guam

By Sarah N. Rosa and Lauren E. Hay

Prepared in cooperation with the U.S. Department of Defense Strategic Environmental Research and Development Program (SERDP)

Scientific Investigations Report 2017–5093
Version 1.1, February 2019

U.S. Department of the Interior
U.S. Geological Survey

U.S. Department of the Interior
RYAN K. ZINKE, Secretary

U.S. Geological Survey
William H. Werkheiser, Acting Director

U.S. Geological Survey, Reston, Virginia
First release: 2017
Revised: February 2019 (ver. 1.1)

Suggested citation:
Rosa, S.N., and Hay, L.E., 2019, Fena Valley Reservoir watershed and water-balance model updates and expansion of watershed modeling to southern Guam (ver. 1.1, February 2019): U.S. Geological Survey Scientific Investigations Report 2017–5093, 64 p., https://doi.org/10.3133/sir20175093.

ISSN 2328-0328 (online)

Acknowledgments

The authors wish to thank Steve Markstrom, Steve Regan, and Roland Viger from the USGS Modeling of Watershed Systems group for their assistance during the watershed-modeling phase of the study. This work was supported by the U.S. Department of Defense Strategic Environmental Research and Development Program, Project ID RC-2340.

Contents

Figures

Tables

Datum

Vertical coordinate information is referenced to local mean sea level.

Horizontal coordinate information is referenced to the World Geodetic System of 1984 (WGS 84).

Elevation, as used in this report, refers to distance above the vertical datum.

Abbreviations

COOP	cooperative network
DEM	digital elevation model
DOD	U.S. Department of Defense
ENSO	El Niño Southern Oscillation
EPA	U.S. Environmental Protection Agency
FVR	Fena Valley Reservoir
GIS	geographic information system
GWA	Guam Waterworks Authority
HRU	hydrologic response unit
NAS	Naval Air Station
NCDC	National Climatic Data Center
NOAA	National Oceanic and Atmospheric Administration
NRMSE	normalized root mean square error
NS	Nash-Sutcliffe efficiency
NWIS	National Water Information System
PET	potential evapotranspiration
PRMS	Precipitation Runoff Modeling System
SERDP	Strategic Environmental Research and Development Program
SR	solar radiation
USGS	U.S. Geological Survey

Conversion Factors

Inch/Pound to International System of Units

Multiply	By	To obtain
	Length	
inch (in.)	25.4	millimeter (mm)
foot (ft)	0.3048	meter (m)
mile (mi)	1.609	kilometer (km)
	Area	
acre	4,047	square meter (m^2)
acre	0.004047	square kilometer (km^2)
square mile (mi^2)	2.590	square kilometer (km^2)
	Volume	
acre-feet	0.32573	million gallons (Mgal)
gallon (gal)	3.785	liter (L)
gallon (gal)	0.003785	cubic meter (m^3)
million gallons (Mgal)	3,785	cubic meter (m^3)
	Flow rate	
acre-foot per day (acre-ft/d)	0.01427	cubic meter per second (m^3/s)
acre-foot per year (acre-ft/yr)	1,233	cubic meter per year (m^3/yr)
cubic foot per second (ft^3/s)	0.02832	cubic meter per second (m^3/s)
cubic foot per second (ft^3/s)	448.8	gallon per minute
million gallons per day (Mgal/d)	0.04381	cubic meter per second (m^3/s)
	Flow rate—Continued	
inch per hour (in/h)	0.0254	meter per hour (m/h)
inch per year (in/yr)	25.4	millimeter per year (mm/yr)
mile per hour (mi/h)	1.609	kilometer per hour (km/h)
	Potential evapotranspiration	
inch per day (in/d)	25.4	millimeter per day (mm/d)

Temperature in degrees Fahrenheit (°F) may be converted to degrees Celsius (°C) as

$$°C = (°F - 32) / 1.8.$$

Fena Valley Reservoir Watershed and Water-Balance Model Updates and Expansion of Watershed Modeling to Southern Guam

By Sarah N. Rosa and Lauren E. Hay

Abstract

In 2014, the U.S. Geological Survey, in cooperation with the U.S. Department of Defense's Strategic Environmental Research and Development Program, initiated a project to evaluate the potential impacts of projected climate-change on Department of Defense installations that rely on Guam's water resources. A major task of that project was to develop a watershed model of southern Guam and a water-balance model for the Fena Valley Reservoir. The southern Guam watershed model provides a physically based tool to estimate surface-water availability in southern Guam. The U.S. Geological Survey's Precipitation Runoff Modeling System, PRMS-IV, was used to construct the watershed model. The PRMS-IV code simulates different parts of the hydrologic cycle based on a set of user-defined modules. The southern Guam watershed model was constructed by updating a watershed model for the Fena Valley watersheds, and expanding the modeled area to include all of southern Guam. The Fena Valley watershed model was combined with a previously developed, but recently updated and recalibrated Fena Valley Reservoir water-balance model.

Two important surface-water resources for the U.S. Navy and the citizens of Guam were modeled in this study; the extended model now includes the Ugum River watershed and improves upon the previous model of the Fena Valley watersheds. Surface water from the Ugum River watershed is diverted and treated for drinking water, and the Fena Valley watersheds feed the largest surface-water reservoir on Guam. The southern Guam watershed model performed "very good," according to the criteria of Moriasi and others (2007), in the Ugum River watershed above Talofofo Falls with monthly Nash-Sutcliffe efficiency statistic values of 0.97 for the calibration period and 0.93 for the verification period (a value of 1.0 represents perfect model fit). In the Fena Valley watershed, monthly simulated streamflow volumes from the watershed model compared reasonably well with the measured values for the gaging stations on the Almagosa, Maulap, and Imong Rivers—tributaries to the Fena Valley Reservoir—with Nash-Sutcliffe efficiency values of 0.87 or higher. The southern Guam watershed model simulated the total volume of the critical dry season (January to May) streamflow for the entire simulation period within –0.54 percent at the Almagosa River, within 6.39 percent at the Maulap River, and within 6.06 percent at the Imong River.

The recalibrated water-balance model of the Fena Valley Reservoir generally simulated monthly reservoir storage volume with reasonable accuracy. For the calibration and verification periods, errors in end-of-month reservoir-storage volume ranged from 6.04 percent (284.6 acre-feet or 92.7 million gallons) to –5.70 percent (–240.8 acre-feet or –78.5 million gallons). Monthly simulation bias ranged from –0.48 percent for the calibration period to 0.87 percent for the verification period; relative error ranged from –0.60 to 0.88 percent for the calibration and verification periods, respectively. The small bias indicated that the model did not consistently overestimate or underestimate reservoir storage volume.

In the entirety of southern Guam, the watershed model has a "satisfactory" to "very good" rating when simulating monthly mean streamflow for all but one of the gaged watersheds during the verification period. The southern Guam watershed model uses a more sophisticated climate-distribution scheme than the older model to make use of the sparse climate data, as well as includes updated land-cover parameters and the capability to simulate closed depression areas.

The new Fena Valley Reservoir water-balance model is useful as an updated tool to forecast short-term changes in the surface-water resources of Guam. Furthermore, the now spatially complete southern Guam watershed model can be used to evaluate changes in streamflow and recharge owing to climate or land-cover changes. These are substantial improvements to the previous models of the Fena Valley watershed and Reservoir. Datasets associated with this report are available as a U.S. Geological Survey data release (Rosa and Hay, 2017; DOI:10.5066/F7HH6HV4).

Introduction

Guam is a small, remote island with limited water resources that are vulnerable to climate change (Schroeder and others, 2012). Although 80 percent of the potable water in Guam comes from groundwater (Jocson and others, 2002), surface-water resources are important because of the potential increased demand for freshwater as a result of population growth and proposed military expansion (Gingerich, 2013). For over two decades the U.S. Geological Survey (USGS), in cooperation with the U.S. Navy, has provided periodic projections of water availability for the Fena Valley Reservoir (FVR) in south-central Guam (fig. 1). Constructed in 1951 by the U.S. Navy, the FVR is the largest surface-water reservoir on Guam and an important source of potable water for the U.S. Navy and the citizens of Guam.

A severe drought in 1993, associated with an El Niño Southern Oscillation (ENSO) event, prompted the USGS, in cooperation with the U.S. Navy, to develop a two-step modeling procedure using a Precipitation Runoff Modeling System (PRMS) watershed model—from here on referred to as PRMS_1994—and a generalized reservoir water-balance model (Nakama, 1994)—from here on referred to as FVR_1994—to manage water levels in the FVR (fig. 2). In 2004, as a result of the availability and improvement of physiographic and climate data, the watershed model and generalized reservoir water-balance model were updated by Yeung (2004) to address limitations identified in the PRMS_1994 model (Nakama, 1994). The calibrated watershed model of the Fena Valley watershed (Yeung, 2004)— from here on referred to as PRMS_2004—and a water-balance model of the FVR—from here on referred to as FVR_2004—were used by the USGS to provide quarterly projections of water availability for the reservoir for the upcoming 12 months to the Navy Public Works Center on Guam.

In 2014, the USGS initiated a study with the U.S. Department of Defense's (DoD) Strategic Environmental Research and Development Program (SERDP) to evaluate the potential impacts of climate change on DoD installations that depend on Guam's water resources. One of the major tasks of that study was to update the PRMS_2004 model and FVR_2004 water-balance model for the FVR (Yeung, 2004) and expand the watershed model to all of southern Guam, using new data on the FVR storage-capacity (Marineau and Wright, 2015) and the latest version of PRMS, PRMS-IV (Markstrom and others, 2015). These new models are documented in this report. From here on, the new version of the Guam PRMS-IV model will be referred to as PRMS_2016 and the FVR model as FVR_2016. The PRMS_2016 model was not extended to northern Guam because measurable surface runoff does not occur in the northern part of the island owing to karst systems (Ward and others, 1965; fig. 1). The new FVR_2016 model is useful as an updated tool to forecast short-term changes in the surface-water resources of Guam. Furthermore, the now spatially complete PRMS_2016 model can be used to evaluate changes in streamflow and recharge as a result of climate or land-cover changes. These are substantial improvements to the FVR_2004 and PRMS_2004 models.

Purpose and Scope

The purpose of this report is to document the watershed and water-balance models developed by (1) discussing the data and methods used to develop the models; (2) describing the calibration and verification of the PRMS_2016 model for southern Guam; (3) describing the recalibration and verification of the updated FVR_2016 water-balance model; (4) comparing the PRMS_2016 model and the PRMS_2004 model and how output from these models affects results of the FVR_2016 generalized reservoir water balance; and (5) identifying the uncertainties in the models. Potential impacts of projected climate change on Guam's surface-water resources were not simulated as part of this report.

Data from 1951 to 2015 were used to develop the PRMS_2016 and FVR_2016 models. The watershed model covers nearly all of southern Guam (92.5 square miles [mi^2]). The PRMS_2016 model was calibrated using 18 of 21 gaged watersheds, and these 18 watersheds encompass 49.7 mi^2 (54 percent) of southern Guam. The calibrated model parameters of 11 gaged areas (corresponding to the areas with best model performance) were applied to nearby or physiographically similar ungaged areas to complete the model.

Description of Study Area

Guam is the largest island in Micronesia, with an area of approximately 211 mi^2, and is the southernmost of the Mariana Islands in the western Pacific Ocean (fig. 1). Guam is divided into two topographically, geologically, and hydrologically distinct areas by the Adelup Fault, which extends across the center of the island from Pago Bay to Adelup Point (fig.1). Northern Guam is mostly composed of karst which absorbs rainfall quickly, and thus the region has no defined streams (Ward and others, 1965). Southern Guam, the focus of the surface-water availability model, consists primarily of rugged volcanic uplands dissected by streams and gently sloping foothills. A mountain chain running from north to south along the west edge of southern Guam contains Mount Lamlam, the highest peak in southern Guam, with an altitude of 1,332 feet above mean sea level. Terrain from the ridgeline to the western coast is characterized by steep dissected slopes that transition into coastal lowland alluvial-valley floors from Hagåtña Bay to Facpi Point. To the east of the ridgeline the terrain is steeply sloped, but at lower elevations the terrain transitions into gently sloping foothills and limestone plateaus near the coast. Older limestone units overlay the volcanic units in the mountainous areas and in the interior basin. The interior basin is a structural depression that starts at the headwaters of the Maagas River and terminates near the convergence of the Mahlac River with the Talofofo River (Tracey and others, 1964). The interior basin includes the FVR, and the rolling hills and valleys consisting of volcanic, limestone, and alluvial units.

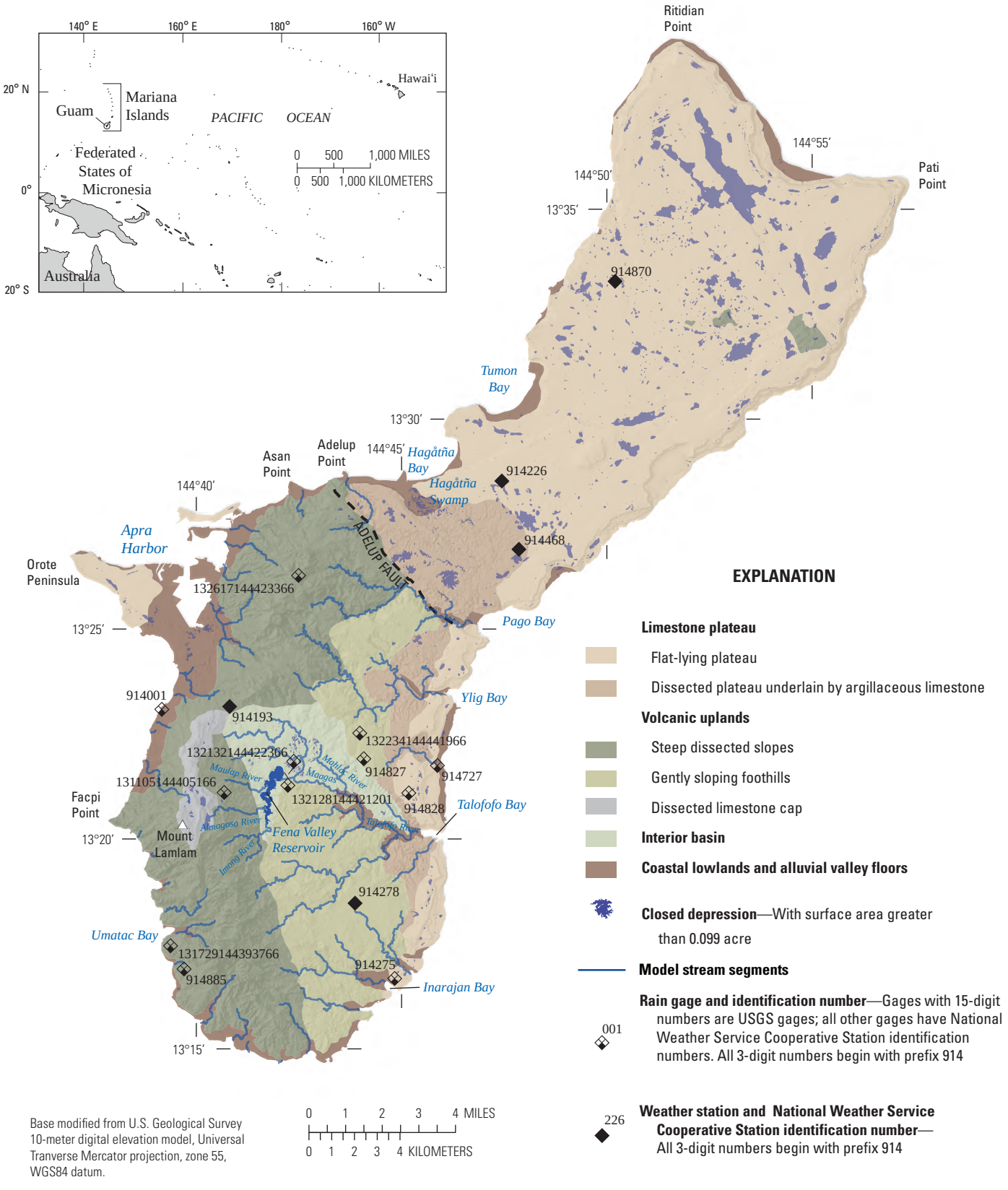

Figure 1. Locations of selected rain gages and weather stations (modified from Johnson, 2012).

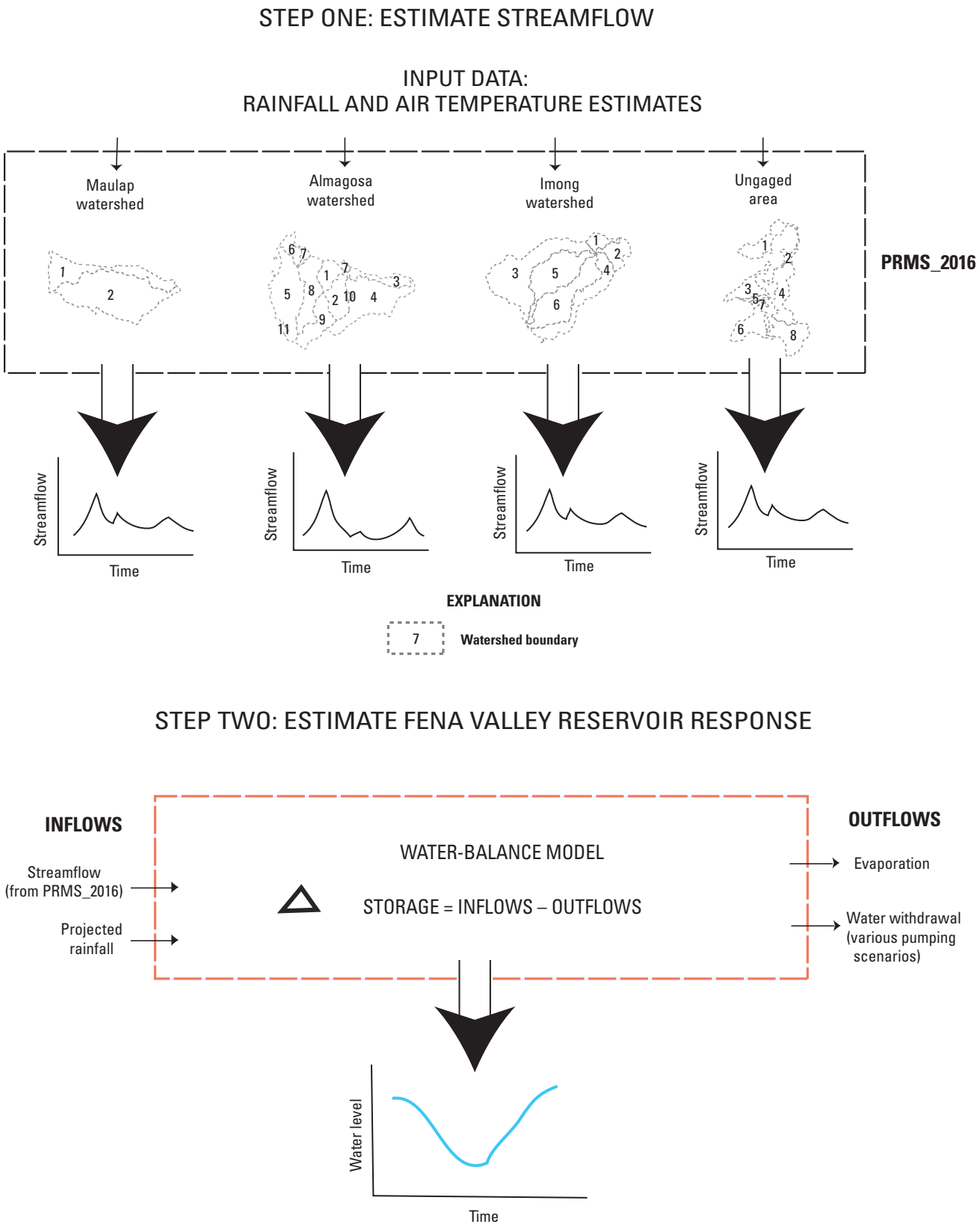

Figure 2. Diagram of the two-step modeling procedure for the Fena Valley watershed, Guam (modified from Yeung, 2004; PRMS, Precipitation Runoff Modeling System).

The FVR is currently the primary source of water for Naval Base Guam and the nearby civilian residents in villages near the southern Guam base (Marineau and Wright, 2015). The FVR has a total storage capacity of approximately 6,915 acre-feet (acre-ft) or 1,936 million gallons (Mgal) and a surface area of 192.6 acres (0.30 mi^2) when at full capacity (Marineau and Wright, 2015). Streamflow from the Fena Valley Watershed's three gaged tributaries, the Maulap, Almagosa, and Imong Rivers, and one ungaged area, a watershed totaling approximately 3,768 acres (5.89 mi^2; only 15 percent of the FVR catchment area is ungaged), is captured by the Fena Valley Reservoir. Over time sediment carried by streamflow into the FVR has reduced the storage capacity of the reservoir, resulting in a change in the relation between reservoir stage and storage capacity. Marineau and Wright (2015) surveyed the FVR in February 2014 as part of the SERDP study to produce new reservoir stage-surface area and reservoir stage-storage capacity curves needed for this study to update and recalibrate the water-balance model. Prior to the 2014 survey, the storage capacity of FVR was last determined in 1990 (Nakama, 1992). FVR total storage capacity decreased about 3.7 percent or 265 acre-ft from 1990 to 2014 as a result of sediment input (Nakama, 1992; Marineau and Wright, 2015).

Climate

Guam's climate is characterized by warm temperatures and humid conditions year-round. Temperatures typically range from the middle or high 80s (in °F) in the afternoon to the 70s at night (fig. 3). Average annual relative humidity typically ranges from 71 percent during the late afternoon to 86 percent during the early morning (Guard and others, 1999). Rainfall, however, varies both seasonally and geographically due to the orographic effect (increasing rainfall with altitude) of the mountain range running from north to south along the western edge of southern Guam (fig. 4). Mean annual rainfall ranges from about 85 inches (in.) near the coastal lowland areas to greater than 115 in. over the mountainous areas in southern Guam (Lander and Guard, 2003). The distinct differences in Guam's wet and dry seasons are defined by the variability in wind and rainfall. Trade winds, blowing from the east, are episodic in Guam (Keener and others, 2012). The temperature of Guam is expected to increase by the end of the century by 3.6 °F and the annual rainfall is expected to increase moderately (8.7 in/year), based on the Intergovernmental Panel on Climate Change's RCP8.5 scenario (Intergovernmental Panel on Climate Change, 2013).

Periodically Guam experiences severe periods of drought due to the highly seasonal rainfall and occurrences of ENSO events. Mean annual rainfall on Guam is about 100 in. with about 70 percent of the annual total occurring in the wet season (July through December) and the remaining 30 percent occurring in the dry season (January through June). Tropical cyclones, or typhoons, during the rainy season can bring high intensity rainfall distributed across the island due to the nature of the storm's structure (Lander and Guard, 2003). Thirty percent of the rainfall on Guam comes from tropical cyclones (Kubota and Wang, 2009), which are less frequent the year after an El Niño event and result in a dry year (Lander and Guard, 2003). Monthly rainfall totals can range from less than 1 in. during February to April to more than 20 in. during August to November, while rainfall during the transitional months of December and June varies from year to year (Lander, 1994).

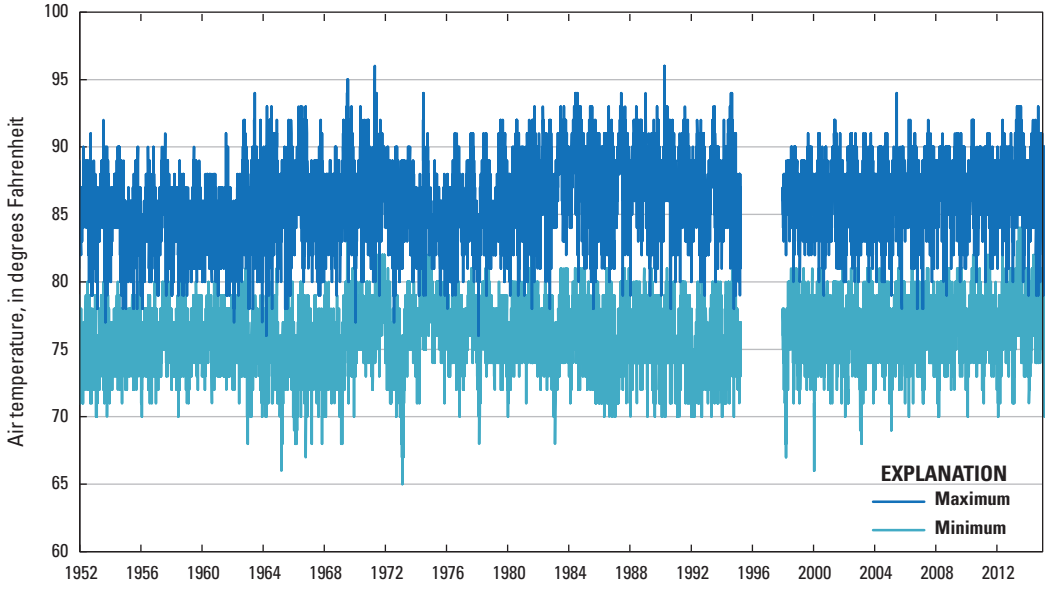

Figure 3. Daily maximum and minimum air temperatures, Naval Air Station Agana (National Climatic Data Center), Guam, 1952–2014.

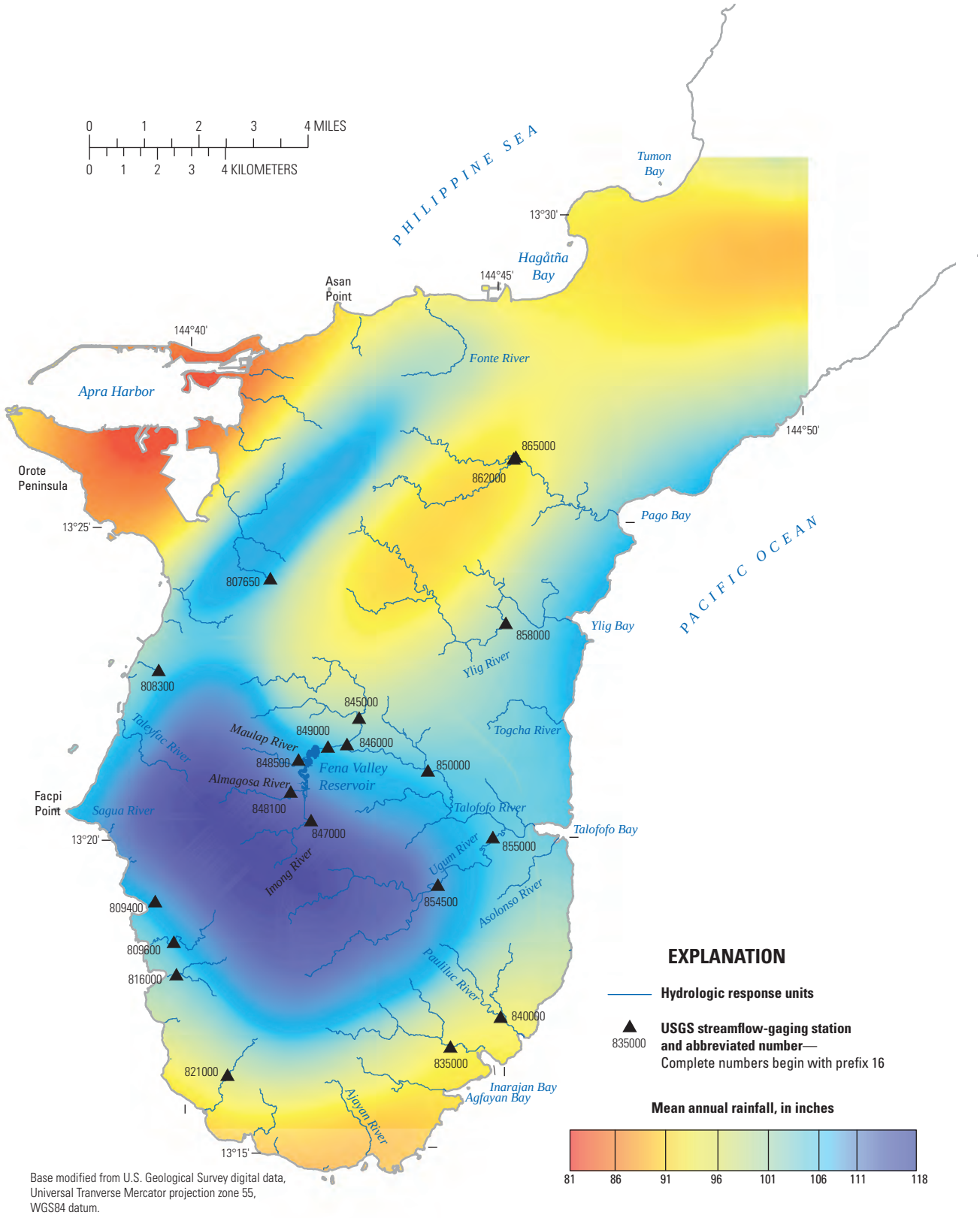

Figure 4. Mean annual rainfall (modified from Heitz, 2015) and locations of U.S. Geological Survey streamflow-gaging stations, Guam.

Geology

The geology underlying the watersheds in southern Guam is predominantly low permeability water-laid volcanic deposits of the Umatac, Alutom, and Facpi Formations (Tracey and others, 1964). Older high-elevation limestone-capped interior areas, as well as lower coastal regions with Hagåtña and Mariana limestones (Siegrist and Reagan, 2007) cover much of the rest of southern Guam and have high porosity and high permeability (fig. 5). The older Alifan Limestone underlies approximately 20 and 31 percent of the Maulap and Almagosa River watersheds, respectively (Nakama, 1994). Near the western drainage divide of the Fena Valley watershed, the older limestone units that overlie the volcanic uplands contain perched groundwater (Mink, 1976). This perched groundwater discharges at the contact with low permeability volcanic rocks in areas like the Almagosa Springs, which is the largest spring in southern Guam. The Navy historically diverted as much as 3.9 cubic feet per second (ft^3/s; 2.5 million gallons per day [Mgal/d]) from Almagosa Springs (Nakama, 1992). However, recent data from the Navy indicate much less of a reliance on water diverted from Almagosa Springs and many days when no water is diverted (at the time of publication, data had not been published by the U.S. Navy). The karst geology of southern Guam also creates many closed and internally drained surface depressions created by dissolution or collapse of the terrain (Taborosi and others, 2004; Taborosi, 2006). Some of the largest closed depressions in southern Guam can be found in the Bonya Limestone at the Naval Magazine, the Alifan Limestone capping the southern mountain ridgeline, and the Mariana Limestone flanking the southeastern coast (Taborosi and others, 2004).

Soils

The soil survey completed by the Soil Conservation Service (Young, 1988) was updated and digitized by the Natural Resources Conservation Service (U.S. Department of Agriculture, 2009). The main physiographic regions primarily dictate how the soil types, and therefore permeability, vary throughout southern Guam (fig. 6). The soil properties below were characterized by Young (1988) and summarized by Johnson (2012). Most of the soils covering the limestone plateaus and bordering coastal plains have moderately rapid to rapid permeability of 2–20 inches per hour (in/h). Soils covering the argillaceous limestone areas are less permeable owing to their higher clay content. Volcanic uplands are covered by soils that generally have moderately slow to moderate permeability of 0.2–2 in/h. Older limestone in the southern highlands of the Fena Valley watersheds is covered by soils with moderately rapid to rapid permeability. Soils covering the valley floors and coastal lowlands that are derived from volcanic alluvium have slow to moderate permeability of 0.01–2 in/h.

Soil thickness across southern Guam tends to vary according to topography and parent material. Soils covering the limestone and volcanic uplands are spatially variable and are typically thicker than 10 in. Soils in closed depressions, valley floors, or coastal lowlands could be several feet thick. The Almagosa watershed closed depression is filled with relatively deep, moderately low-permeability, and high available water holding capacity soils (Nakama, 1994).

Vegetation

According to the U.S. Department of Agriculture (2006) vegetation map (fig. 7), most of southern Guam's land surface is covered by forests and grasslands with some smaller pockets of urban cultivated and urban built-up land. Forest land-cover categories "limestone forest" and "scrub forest" cover much of the rural areas underlain by limestone. Trees within the forests of southern Guam tend to have small diameters owing to a long history of disturbances and typhoon activity (Donnegan and others, 2004). The volcanic uplands in southern Guam are mostly covered by "ravine forest," "limestone forest," or "savanna complex." Barren regions of eroding soil are also present in southern Guam and are of concern for many agencies involved in the management of Guam's nearshore reef environment.

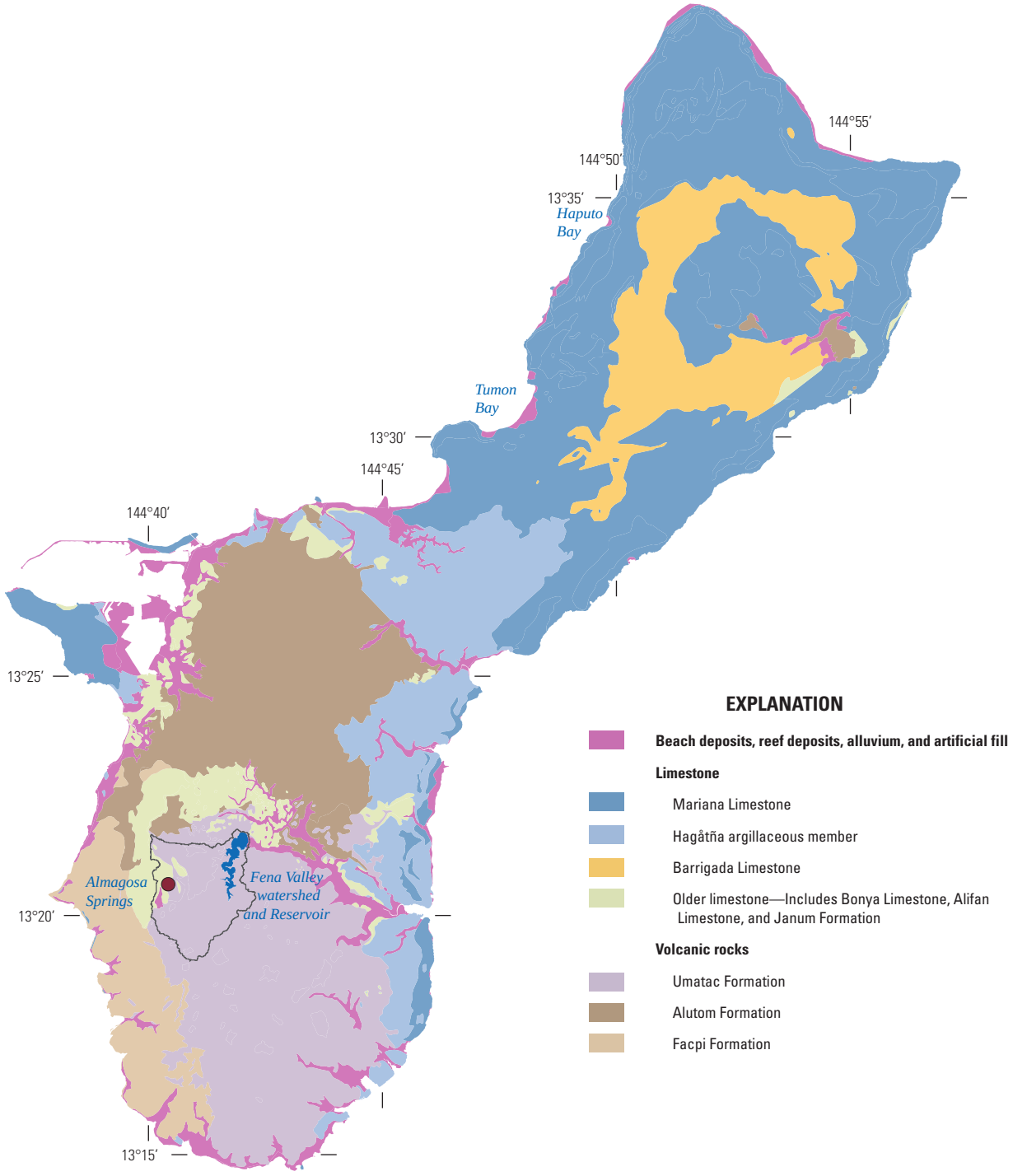

Figure 5. Geologic map of Guam (modified from Tracey and others, 1964; Siegrist and others, 2007; Johnson, 2012). Geologic nomenclature from Siegrist and others (2007).

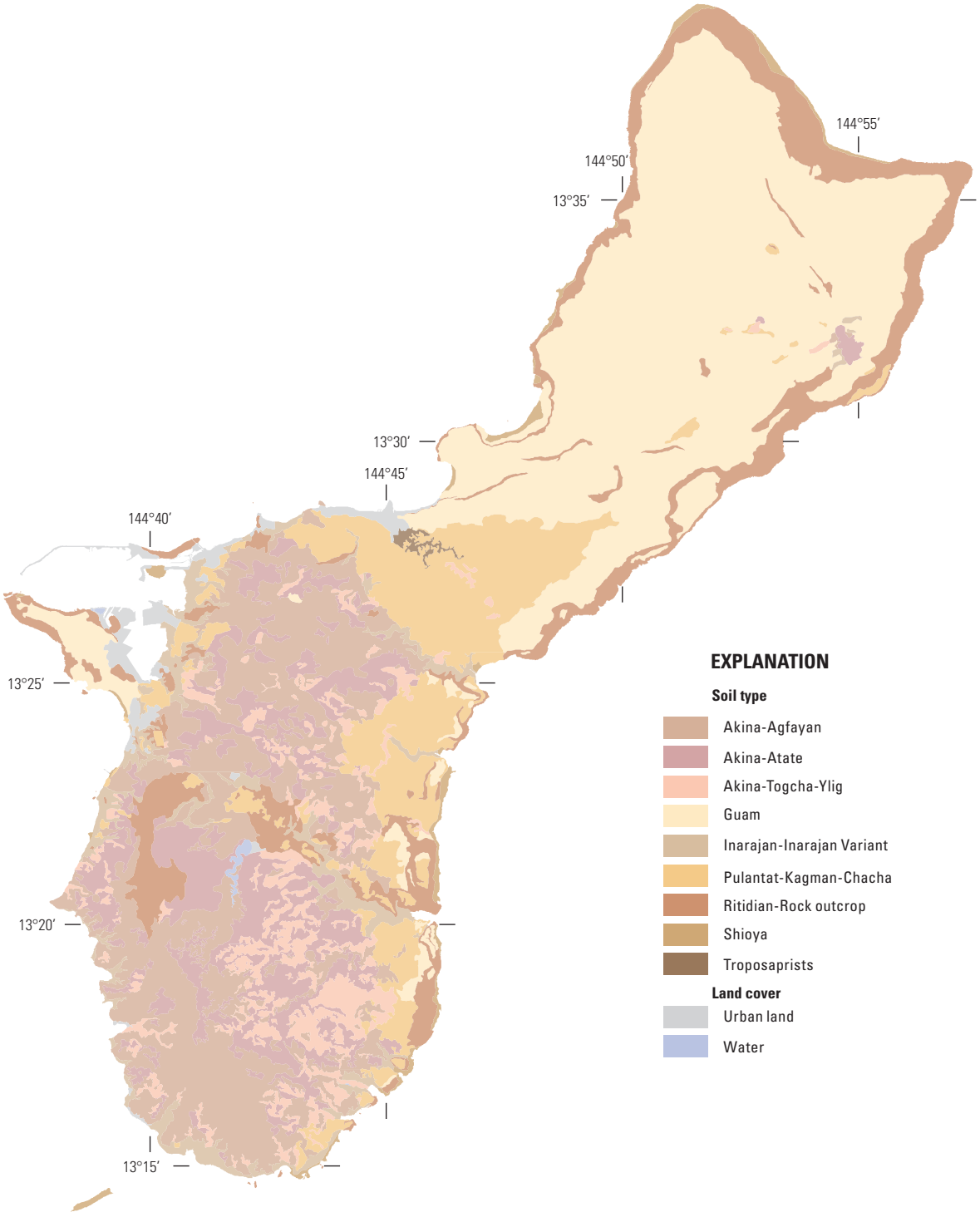

Figure 6. Distribution of soils by general type on Guam documented by Young in 1988 (modified from U.S. Department of Agriculture, 2009).

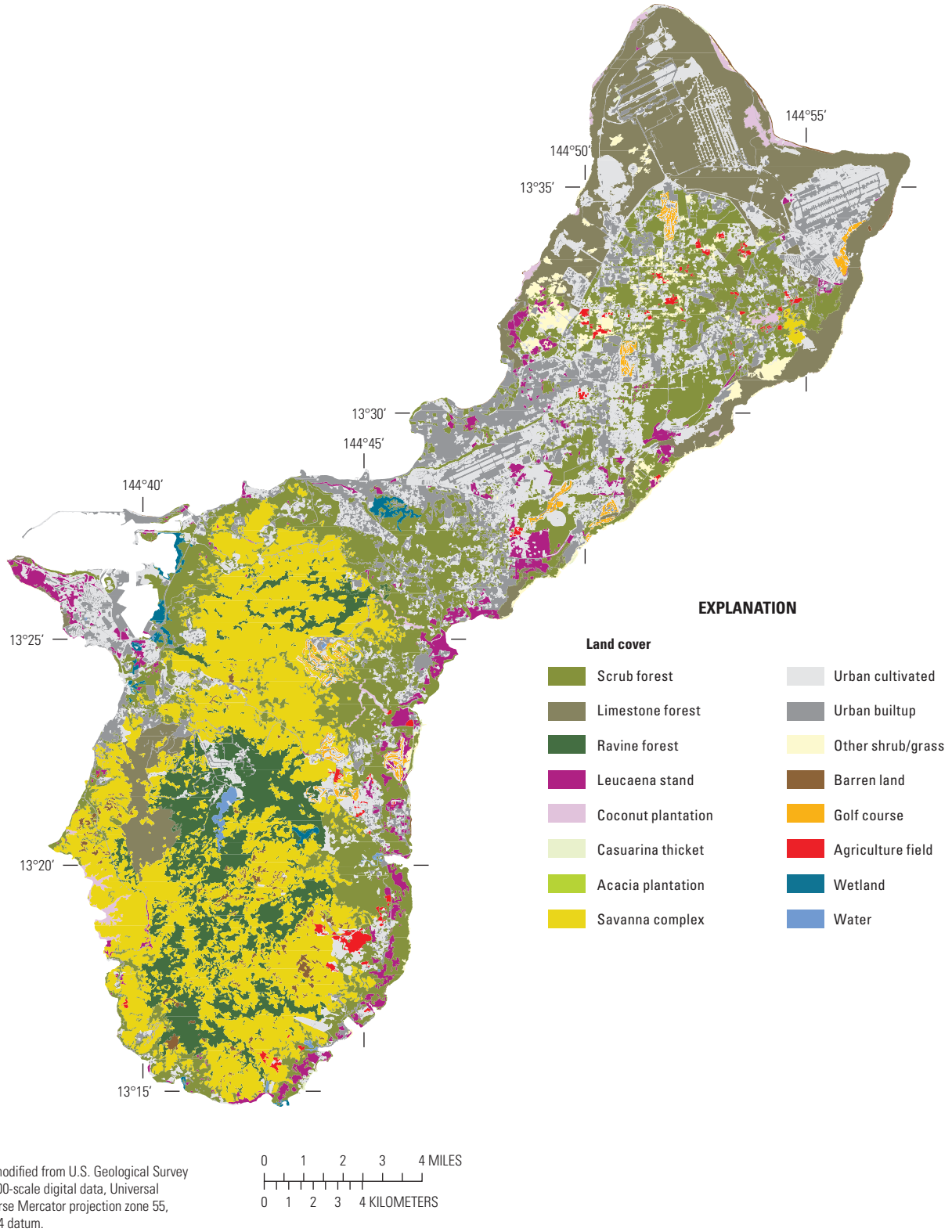

Figure 7. Land cover on Guam (modified from U.S. Department of Agriculture, 2006). Acacia plantation, barren land, and casuarina thicket land covers are difficult to see at this scale (Johnson, 2012).

Streamflow Characteristics

Southern Guam's geology and rainfall distribution heavily influence the streamflow characteristics of each watershed. Streamflow that is not diverted from the Fena Valley watershed is captured by the Fena Valley Reservoir. The three gaged FVR tributaries, the Maulap, Almagosa, and Imong Rivers, along with the gaged Ugum River represent a substantial amount of the surface-water resources currently being used in southern Guam. These watersheds have similar rainfall patterns and geology, which are reflected in the general shape and timing of their hydrographs (fig. 8). The distinctive climatic wet and dry seasons directly translate into seasonal streamflow patterns. For the Fena Valley watersheds these seasonal streamflow patterns also influence the reservoir response (fig. 9). In years when less water is diverted from the FVR system (2011–14) the reservoir is not as dependent on these seasonal flows to replenish it to its full capacity and sharp declines in reservoir levels are not evident.

Streamflow during the dry season is sustained by base flow, which is composed entirely of groundwater discharge from the limestones of southern Guam. In the wet season, streamflow is much flashier, owing to higher rainfall rates in combination with the steep volcanic terrain of these small watersheds, creating direct runoff (Ward and others, 1965). Average streamflow for the four gaged watersheds (fig. 8) during the wet season (July to December) typically ranges from 68 to 78 percent of total annual streamflow for these gages. At these same gages, dry season streamflow (January to June) is typically 19 to 23 percent of annual streamflow, but in general, the streamflow during the dry season varies substantially from stream to stream (Ward and others, 1965).

Flow-duration curves of streamflow for the three gaged basins in the Fena Valley watershed (Maulap, Almagosa, and Imong Rivers) from 2002–14 are shown in figure 10. The discharge data in figure 10 were normalized by dividing discharge by the drainage area at the streamflow-gaging stations so that the data could be directly compared. A flow-duration curve shows the percentage of time a specific discharge is equaled or exceeded in a given period. The shape of a flow-duration curve provides an indication of how the underlying geology, physiography, or rainfall patterns of the watershed affect streamflow. The steep slope and shape of the flow-duration curves for the high to median flows for all three watersheds in the FVR are very similar. These higher flows tend to be controlled by rainfall patterns, physiography, and the land cover of the watershed, which are similar across the three watersheds. However, at the lower-end of the flow range the flow-duration curves diverge. Differences in the low-flow characteristics reflect differences in the underlying geology controlling the base-flow component of flow in the watershed. Even though the Almagosa and Maulap watersheds have very similar underlying geology, the lower flows in Maulap are much smaller than those of Almagosa. For this period of record, the steep slope at the lower-end of Maulap's flow-duration curve is most likely a result of the inclusion of estimated data for a particularly dry period with many extreme low-flow days from February to June 2010. Daily flow from the Almagosa spring diversion (at the time of publication, data had not been published by the U.S. Navy) was added to the daily flow measured at the Almagosa gaging station at the outlet of the basin to account for the effects of the flow diversions. The difference between the two curves reflects the effects of the spring diversions on Almagosa River streamflow. The spring diversion affects low to medium flows in Almagosa, but at higher flows the effects of the diversion are small relative to the discharge.

Precipitation-Runoff Modeling System IV

The PRMS_2004 model for the Fena Valley watershed (Yeung, 2004) was updated and expanded to include all of southern Guam. The updated version of the USGS PRMS-IV model code (Markstrom and others, 2015), was used to construct the PRMS_2016 model. PRMS-IV simulates different parts of the hydrologic cycle based on a set of user-defined modules. Model development requires the delineation and parameterization of watersheds and hydrologic response units (HRUs), and the selection of appropriate PRMS-IV modules suitable for simulating the southern Guam environment.

Description of PRMS-IV

PRMS is a modular, deterministic, distributed-parameter, physical-process simulation code that is used to simulate land-surface hydrologic processes, including evapotranspiration, runoff, and infiltration, and subsurface occurrences of water, including groundwater and soil moisture, based on inputs of distributed daily precipitation and maximum and minimum temperature. PRMS-IV was developed as a tool to evaluate the impact of changing watershed characteristics on surface-water runoff and recharge of a watershed. A detailed description of PRMS-IV can be found in the report by Markstrom and others (2015). PRMS-IV was run using available daily datasets for southern Guam and calibrated and verified based on the watershed model's ability to simulate daily and monthly runoff.

PRMS-IV simulates different parts of the hydrologic cycle through a set of inter-connected user-defined modules. Each component of the hydrologic cycle in PRMS-IV (fig. 11) is calculated by empirical relations or process algorithms (note that snow processes are not used in this model). By taking into account watershed characteristics, including slope, aspect, altitude, land cover, soil type, and temperature and rainfall distribution, the watershed can be divided into homogeneous units called hydrologic response units (HRUs). These HRUs are assumed to be homogeneous with regard to their physical properties and hydrologic response. PRMS-IV utilizes these HRUs to have distributed-parameter capabilities and account

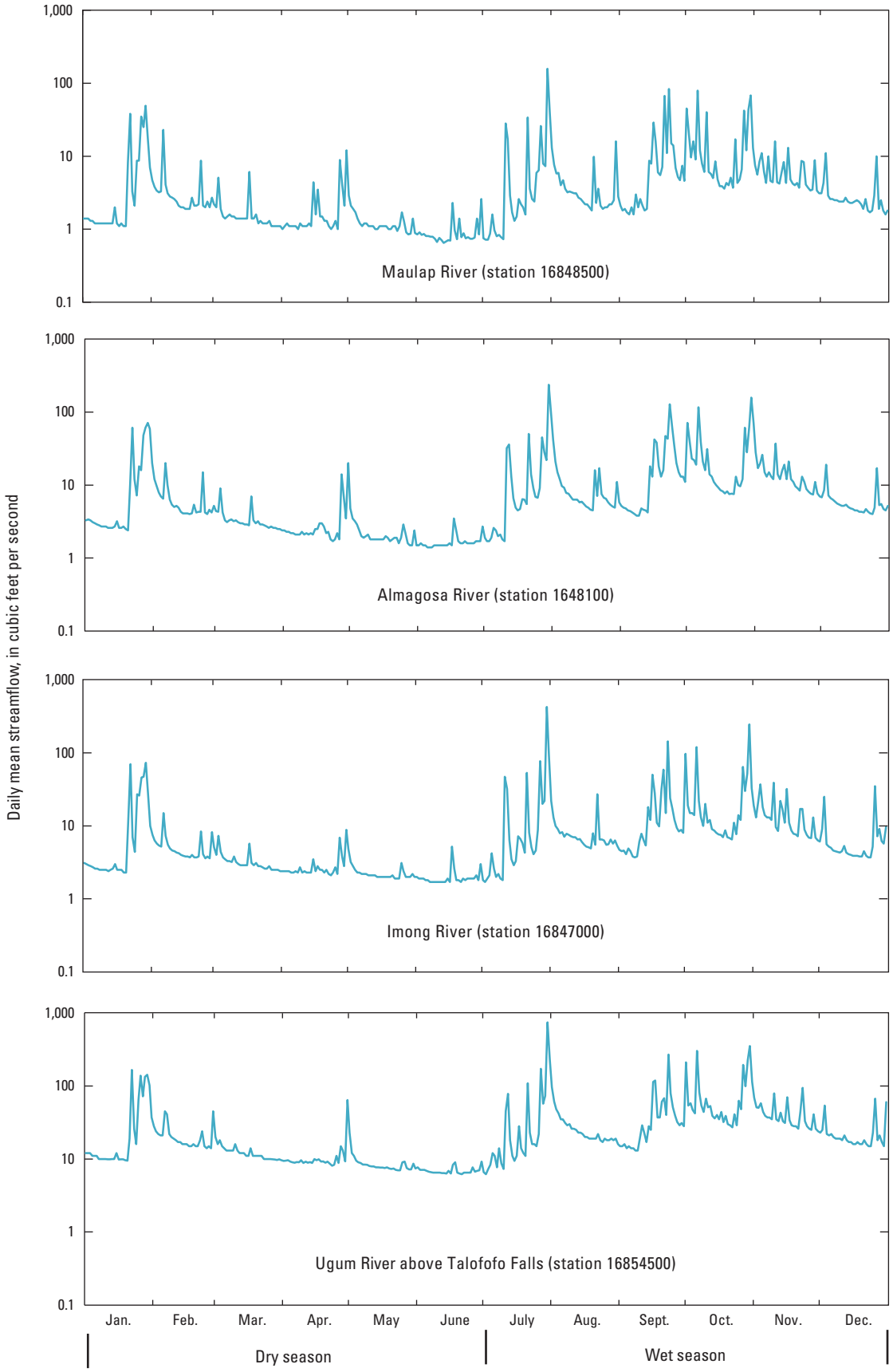

Figure 8. Daily mean streamflow at the Almagosa, Imong, Maulap, and Ugum U.S. Geological Survey streamflow-gaging stations, Guam, 2014.

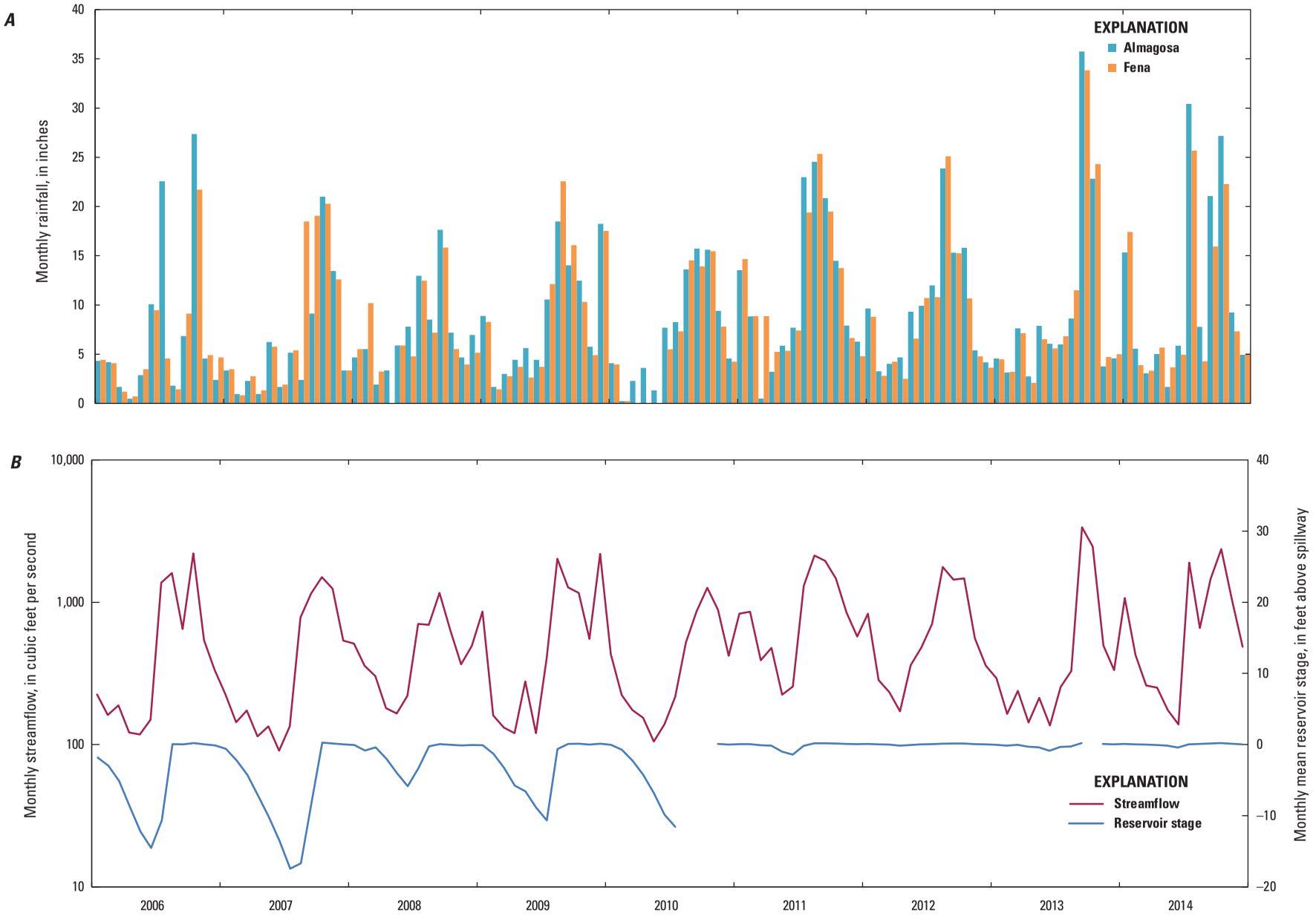

Figure 9. *A.* Monthly rainfall at Almagosa and Fena Pump, January 2006 to December 2014. *B.* Monthly total streamflow (from Almagosa, Maulap, and Imong Rivers) and monthly mean stage of Fena Valley Reservoir (from Fena Dam spillway), Guam, January 2006 to December 2014.

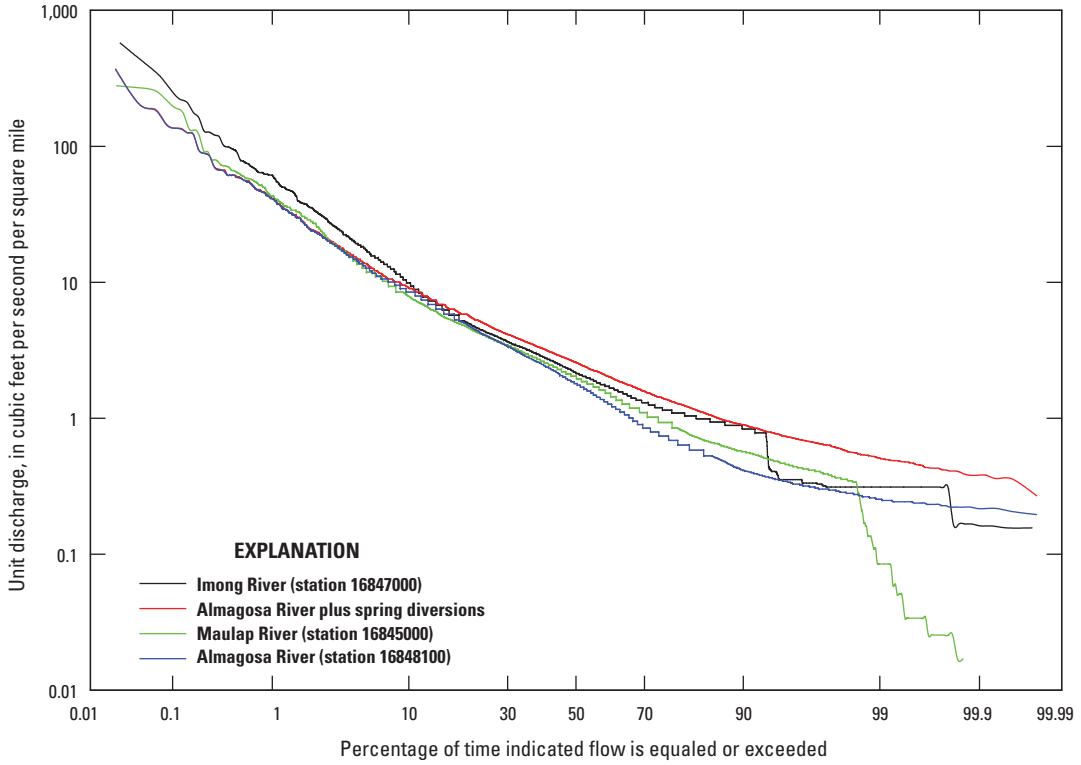

Figure 10. Flow-duration curves for the Maulap, Almagosa, Imong Rivers and the Almagosa River plus spring diversions, Guam (2002–14).

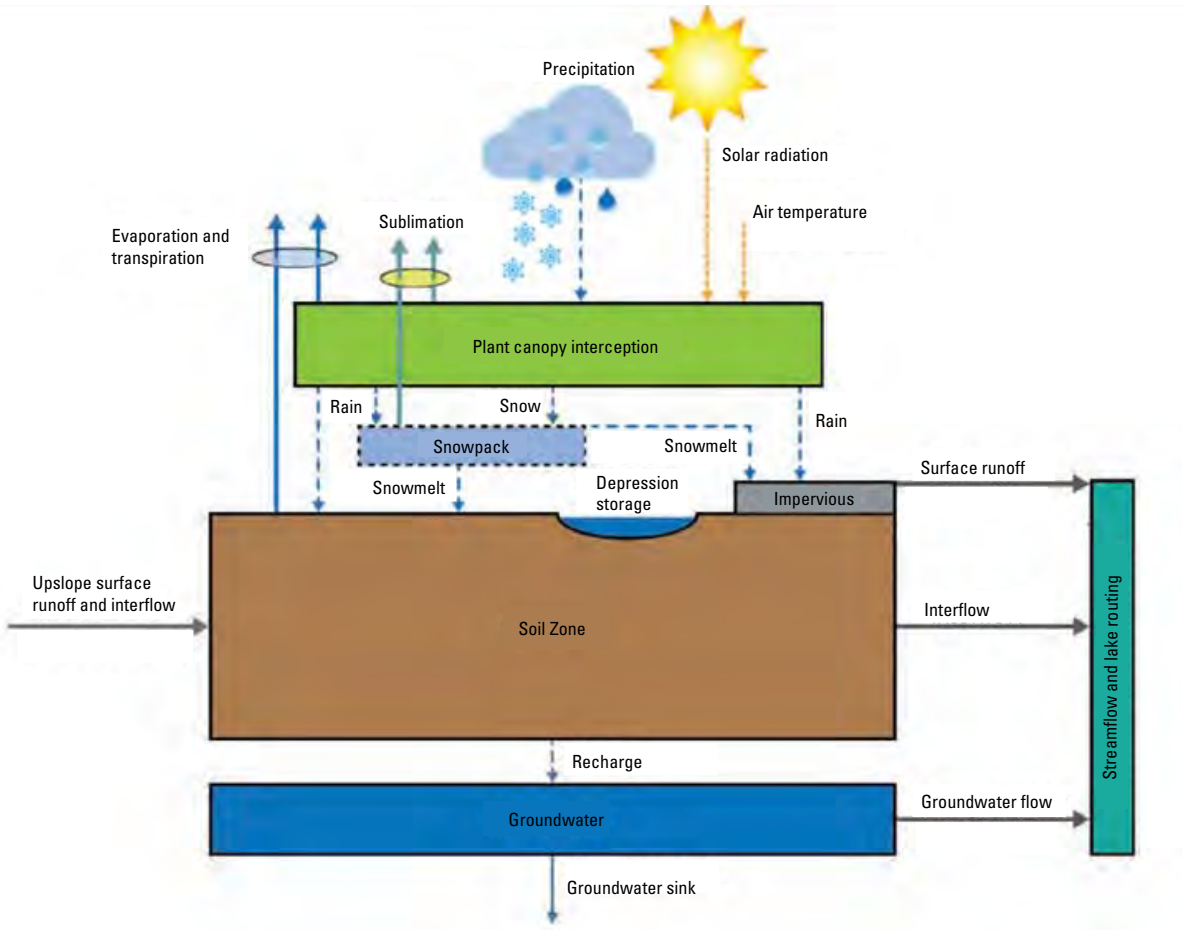

Figure 11. Diagram of the conceptual hydrologic system used in the Precipitation-Runoff Modeling System for southern Guam (modified from Regan and LaFontaine, 2017).

for the spatial variability within a watershed. To account for heterogeneity within a given HRU, area-weighted averages are calculated for each of the appropriate basin characteristics within a HRU (for example an area-weighted average to determine the HRU's slope is not calculated). For each of the HRUs, an energy and water balance is calculated and then the HRU water-budget components are summed or routed to produce the entire watershed's hydrologic response (Markstrom and others, 2015).

PRMS-IV distributes precipitation and minimum and maximum air-temperature data to each HRU as well as estimates of daily shortwave radiation for each HRU. Precipitation in PRMS-IV can either be intercepted by vegetation, evaporated, or continue to the land surface as throughfall that reaches the soil. PRMS-IV also estimates potential evapotranspiration (PET) for each HRU, and actual evapotranspiration is calculated by PRMS-IV as a function of PET, the HRU soil type, the HRU plant-cover type, the water available in the soil zone, and the water-storage capacity of the soil zone. Any rainfall reaching the land surface may then be stored in the impervious-zone reservoir or closed surface-depression areas, infiltrate into the soil zone, evaporate, or contribute to surface runoff.

Surface runoff and infiltration for each HRU are calculated and once water infiltrates into the soil zone, PRMS-IV uses a conceptual three-reservoir system to model soil-zone water content (refer to Markstrom and others [2015] for a detailed description and figure). The capillary reservoir models soil water between the wilting-point and field-capacity thresholds. The gravity reservoir models soil-water content between field capacity and the preferential-flow threshold, and accounts for slow lateral interflow and drainage to the groundwater reservoir. The preferential-flow reservoir also models soil-water content over field capacity, but instead accounts for fast lateral interflow. PRMS-IV calculates the water inflows and outflows of each soil zone for each HRU. Groundwater in PRMS-IV is simulated using another conceptual reservoir called the groundwater reservoir. Any excess infiltration from the soil zone can directly enter the groundwater reservoir as direct recharge or go through the gravity reservoir and be partitioned into gravity drainage from the soil zone or slow interflow. Groundwater may leave the groundwater reservoir but stay in the watershed as groundwater flow to a stream, or leave the groundwater reservoir and be designated to leave the system through a groundwater sink. PRMS-IV calculates the water and energy balances for each HRU and the total for each watershed (Markstrom and others, 2015).

Background Data

Available climate data from October 1, 1951, to February 28, 2015, were used as input to the PRMS_2016 model. Additionally, daily streamflow was used to calibrate the model. Mean monthly pan-evaporation and solar-radiation data were used to calibrate the model's energy budget as an approximation for the seasonal patterns of potential evapotranspiration and solar radiation. Physiographic data were used to parameterize the HRUs.

Climate Data

Daily rainfall, and daily minimum and maximum air temperature data were compiled with the USGS Downsizer application (Ward-Garrison and others, 2009) from available climate-station records from the National Oceanic and Atmospheric Administration's (NOAA) National Weather Service Cooperative Observer Program (National Oceanic and Atmospheric Administration, 2015) into a data file recognized by PRMS-IV. The USGS Downsizer program, which is no longer updated or supported by the USGS, automates the quality-assurance/quality-control (QA/QC) checks while formatting the data into an appropriate file that can be used with PRMS-IV. The data file compiled by the USGS Downsizer application was then supplemented with USGS rainfall data from the National Water Information System (NWIS) that were not in the Downsizer database (U.S. Geological Survey, 2015). Stations are listed in table 1 and periods of record are shown in figure 12.

Rainfall

For the PRMS_2016 model, 11 stations with daily rainfall data with various periods of record ranging from January 1954 to February 2015 (National Oceanic and Atmospheric Administration, 2015) were compiled into the PRMS-IV data file format with the USGS Downsizer (Ward-Garrison and others, 2009). These data were supplemented with data from NWIS (U.S. Geological Survey, 2015) from six additional USGS rain gages (table. 1). The timing of rainfall collected at 5 of the 6 USGS rain gages used in the PRMS_2016 model is similar although the rainfall volumes vary among sites (fig. 13). Data from 2 of the 17 gages considered for the analysis were determined to be unsuitable or insufficient to be used as input to the model and were coded within the model's parameter file to be ignored by the model. Twelve of the 15 remaining stations were located in southern Guam (fig. 1). The other three remaining stations were located in northern Guam. These stations were either located in close proximity to some of the southern Guam watersheds or were the only source of climate data for some watersheds that only had streamflow data in the mid-1950s available for calibration (fig. 14). The elevations of the rain gages used as input to the model ranged from 10 to 830 ft (3 to 253 meters[m]) covering almost the entire elevation range of southern Guam. The daily rainfall data from the rain gages are then distributed to each HRU based on the distribution algorithm designated in PRMS-IV described in the model development section of the report.

Table 1. Rainfall and climate stations in the PRMS_2016 model data file.

[The National Oceanic and Atmospheric Adminitration's Cooperative Observer Program rainfall and climate stations are indicated below according to their six-digit station numbers. U.S. Geological Survey rainfall stations are listed below according to their fifteen-digit station numbers. PRMS, Precipitation Runoff Modeling System; ID, identifier; nr, near; Ag., Agricultural; NASA, National Aeronautics and Space Administration; WSMO, Weather Service Meteorological Office; NAS, Naval Air Station; RG at Res., rain gage at reservoir]

Station number	Station name	Elevation, in feet	Longitude[1]	Latitude[1]	Station ID in PRMS data file
914275	Inarajan Ag. Station	30	13.28530	144.75470	1
914885	Umatac	190	13.28330	144.66670	2
914278	Inarajan NASA	280	13.31140	144.73640	3
914828	Talofofo Village	299	13.35000	144.75000	4
914193	Fena Filter Plant	367	13.36670	144.70000	5
914001	Agat	10	13.38940	144.65750	6
914468	Mangilao	60	13.45280	144.79810	7
914827	Talofofo[2]	250	13.36470	144.73890	8
914870	Guam WSMO	361	13.55970	144.83750	9
914226	NAS-Tiyan	254	13.48330	144.80000	10
914727	Pirates Cove	10	13.35220	144.76690	11
131729144393766	Umatac Rain Gage at Umatac	180	13.29178	144.66220	12
132105144405166	Almagosa Rain Gage nr Santa Rita	600	13.35292	144.68320	13
132128144421201	Fena Dam Rain Gage at Spillway near Agat[2]	113	13.35936	144.70580	14
132132144422366	Fena RG at Res. Pump Station	70	13.30625	144.70890	15
132617144423366	Mount Chachao Rain Gage near Piti	830	13.43947	144.71220	16
132234144441966	Windward Hills Rain Gage near Talofofo	365	13.37717	144.73780	17

[1]Latitude and longitude coordinates in decimal degrees north of the equator and east of the prime meridian and World Geodetic System of 1984.

[2]Station data were not used as input to the model.

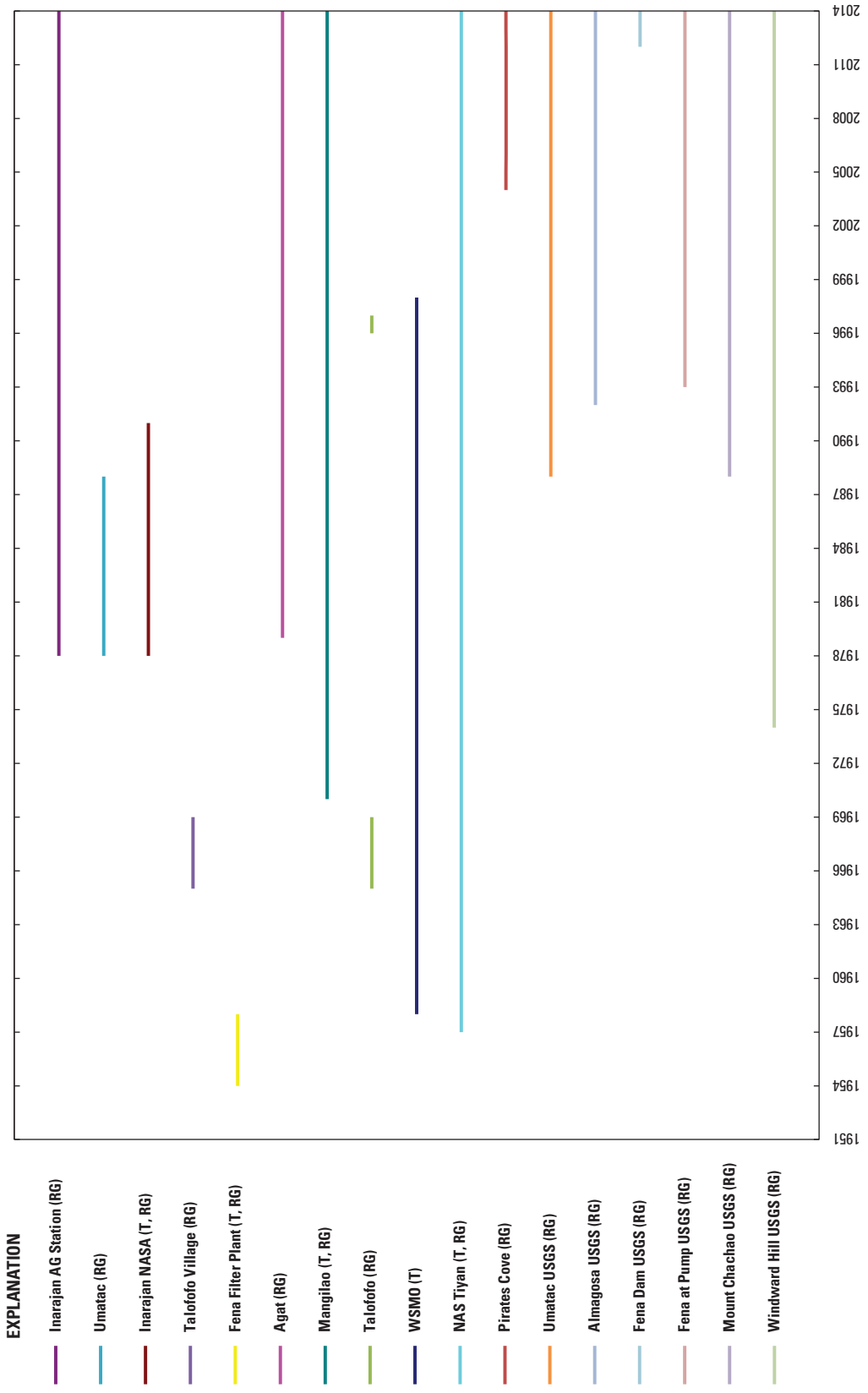

Figure 12. Periods with rain-gage (RG) and minimum and maximum air temperature (T) data, from 1951 to 2014, used in the development of the Precipitation-Runoff Modeling System models for southern Guam. AG, Agricultural; NASA, National Aeronautics and Space Administration; USGS, U.S. Geological Survey.

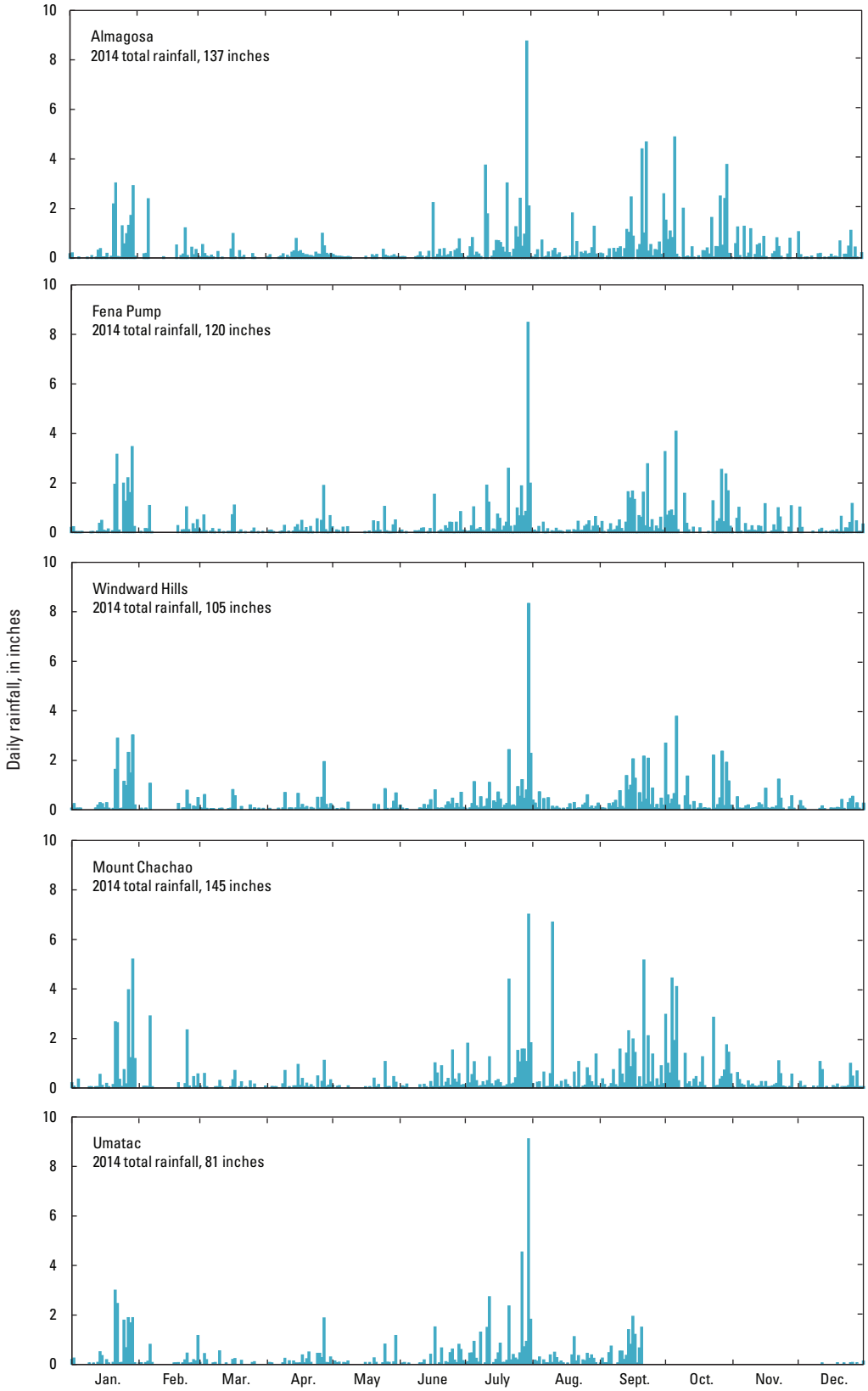

Figure 13. Daily rainfall at the U.S. Geological Survey Almagosa, Fena Pump, Windward Hills, Mount Chachao, and Umatac rain gages, Guam, 2014.

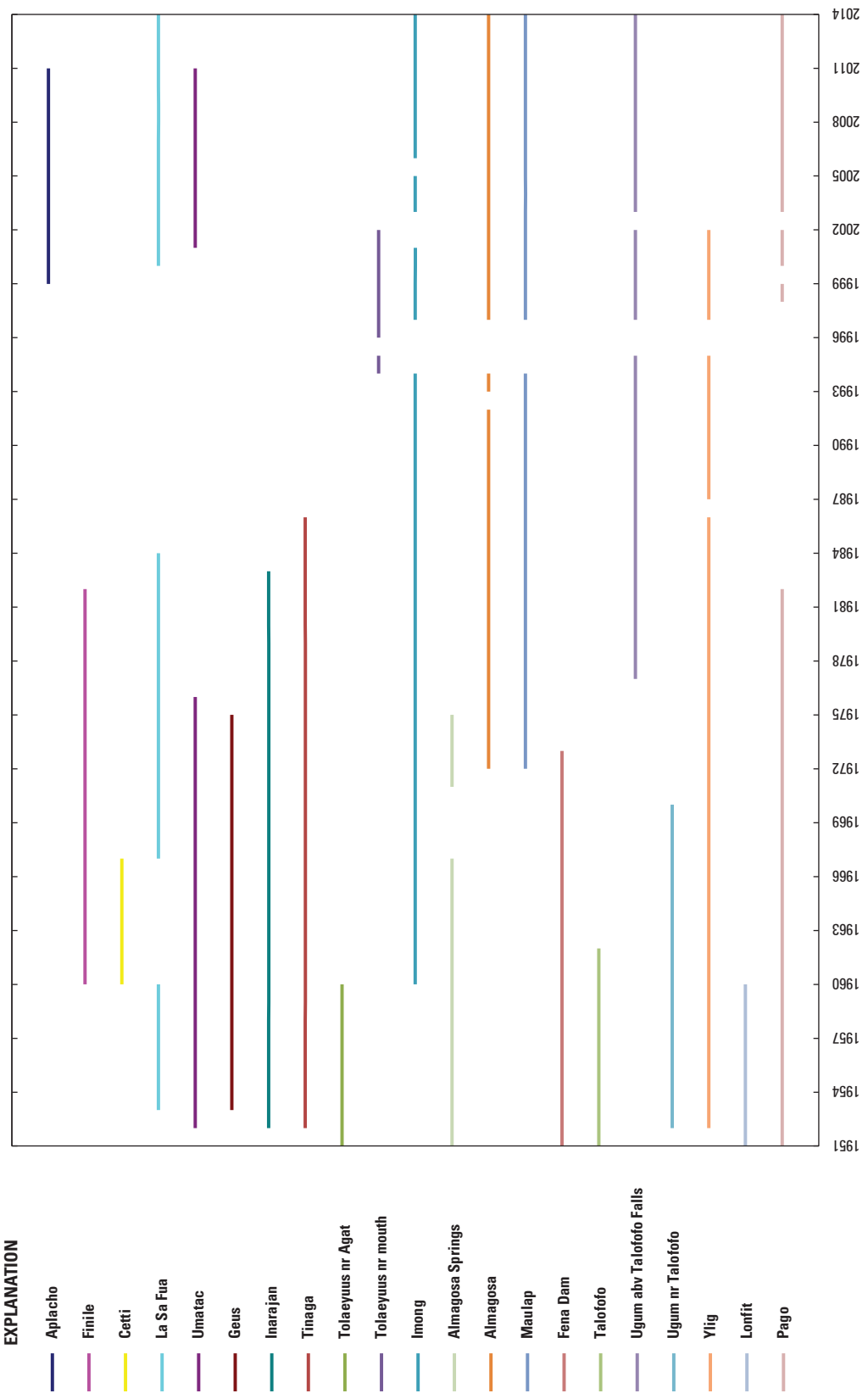

Figure 14. Periods with streamflow data, from 1951 to 2014, used in the development of the Precipitation-Runoff Modeling System models for southern Guam.
Abv, above; nr, near.

Temperature

The air temperature in Guam varies very little (fig. 3). According to Daly and Halbleib (2006), the spatial variability, in any given month, of modeled estimates of average minimum and maximum air temperature is less than 7 °F. The required daily minimum and maximum air temperatures were available at 5 of the 17 climate stations (table. 1; fig. 12).

Streamflow Data

USGS streamflow data stored in NWIS for the 21 available southern Guam streamflow-gaging stations were also compiled using the USGS Downsizer and used to calibrate PRMS_2016. The USGS established a network of streamflow-gaging stations in southern Guam in 1951. During the interval from 1951 to 2015, 21 streamflow-gaging stations were established to collect continuous streamflow data across southern Guam. Three of the available streamflow-gaging stations in southern Guam were not used due to either an insufficient amount of data or streamflow regulation that affected the usability of the data for model calibration (table 2). Measured daily streamflow data were used directly with no adjustments for 17 of the 18 gages used to calibrate the PRMS_2016 model. Five of the 17 streamflow-gaging stations with daily streamflow data that were used directly with no adjustments may have been affected by an upstream diversion at some time during the station's period of record, which could affect lower flows. However, because diversion data were not available the records were left unadjusted, and instead the calibration scheme was adjusted to avoid periods with regulated flows and put more weight on the calibration of monthly flows, which will be discussed later in the report.

The Maulap, Almagosa, and Imong River gages provide a continuous record of inflow to the FVR. These gages in the Fena Valley watershed have been concurrently operated by the USGS since 1972. The Almagosa River gaging station's data, however, do not reflect natural streamflow conditions owing to the Almagosa Springs diversion. Because daily flow data for the Almagosa Springs diversion were available from the U.S. Navy (at the time of publication, data had not been published by the U.S. Navy), the daily diverted flow was added back into the Almagosa streamflow record to account for the effects of the diversion and reconstruct natural-flow conditions. This record reconstruction assumes that the amount of flow diverted at the springs causes an equal amount of reduction of flow at the gaging station located near the outlet of the watershed.

The streamflow records for the 18 gages used to calibrate the PRMS_2016 model ranged in accuracy from "good" to "poor" ratings. A "good" and "fair" rating indicates that about 95 percent of the daily discharges are within 10 and 15 percent of their actual values, respectively. Records that are considered to be less accurate are rated "poor." The accuracy of the Almagosa Springs diversion data supplied by the U.S. Navy is not known.

Evaporation and Solar Radiation Data

Daily PET can be estimated in PRMS-IV using either pan-evaporation data or minimum and maximum air-temperature data. The PRMS_1994 model used pan-evaporation data to estimate PET because of the availability of pan-evaporation data for the duration of the modeled period (Nakama, 1994). However, the PRMS_2004 model used one of the empirical methods in PRMS that estimates PET using minimum and maximum air temperature and possible hours of sunshine, the Hamon (1961) method (Yeung, 2004). For the PRMS_2016 model, the Jensen and Haise method (1963) was used to estimate PET. The Jensen-Haise method uses minimum and maximum temperature, and simulated daily solar radiation (SR) to estimate PET (Markstrom and others, 2015), which is more accurate than the Hamon method. The required daily minimum and maximum air temperatures were available at 5 of the 17 climate stations (table. 1; fig. 12). Even though there is a sparse distribution of gages both spatially and throughout time (figs. 1, 12) the available data were sufficient to estimate PET across southern Guam.

The model's energy budget was calibrated using mean monthly pan-evaporation data from 1958 to 1998 at station WSMO (table 1, fig. 15) as an approximation for the seasonal pattern of potential evapotranspiration. Accuracies associated with the pan-evaporation data and air-temperature data are not known, but the data were adjusted downward by 30 percent to be consistent with the values used by Nakama (1994). The National Weather Service provides data-quality flags which were used to either manually or automatically set the flagged data to "missing" as part of the internal QA/QC process in the USGS Downsizer. Measured mean monthly solar-radiation values were calculated from hourly solar-radiation data for station WSMO (table 1) from 1961 to 1990, obtained from the National Solar Radiation Database (National Renewable Energy Laboratory, 2007; fig. 16) to calibrate the daily solar-radiation model. The calibration process using the available solar-radiation and pan-evaporation data is discussed later in the Energy-Budget Calibration section of the report.

Table 2. Streamflow-gaging stations in the PRMS_2016 model data file.

[PRMS, Precipitation Runoff Modeling System; ID, identifier; nr, near]

Station number	Station name	Elevation, in feet	Longitude[1]	Latitude[1]	Calibrated	Station ID in PRMS data file
16807650	Aplacho River at Apra Heights	250	13.4040	144.6897	yes	1
16808300	Finile Creek at Agat	20	13.3791	144.6596	yes	2
16809400	Cetti River near Umatac	10	13.3175	144.6592	yes	3
16809600	La Sa Fua River near Umatac	120	13.3069	144.6644	yes[2]	4
16816000	Umatac River at Umatac	8	13.2980	144.6652	yes[2]	5
16821000	Geus River nr Merizo	60	13.2714	144.6793	yes[2]	6
16835000	Inarajan River nr Inarajan	15	13.2795	144.7399	yes[2]	7
16840000	Tinaga River nr Inarajan	15	13.2876	144.7534	yes	8
16845000	Tolaeyuus River near Agat	90	13.3669	144.7142	yes	9
16846000	Tolaeyuus River at mouth near Agat	60	13.3598	144.7109	no[2]	10
16847000	Imong River near Agat	120	13.3390	144.7015	yes	11
16848000	Almagosa Springs near Agat	620	13.3469	144.6816	no[2]	12
16848100	Almagosa River near Agat	155	13.3467	144.6955	yes[2]	13
16848500	Maulap River near Agat	130	13.3554	144.6979	yes	14
16849000	Fena Dam Spillway near Agat	111	13.3594	144.7057	no[2]	15
16850000	Talofofo River near Talofofo	20	13.3531	144.7330	yes[2]	16
16854500	Ugum River above Talofofo Falls	130	13.3224	144.7361	yes	17
16855000	Ugum River near Talofofo	3	13.3354	144.7509	yes	18
16858000	Ylig River near Yona	20	13.3926	144.7538	yes	19
16862000	Lonfit River near Ordot	30	13.4364	144.7556	yes	20
16865000	Pago River near Ordot	25	13.4368	144.7560	yes	21

[1]Latitude and longitude coordinates in decimal degrees north of the equator and east of the prime meridian and World Geodetic System of 1984.

[2]Possible low-flow alteration during part of station's period of record.

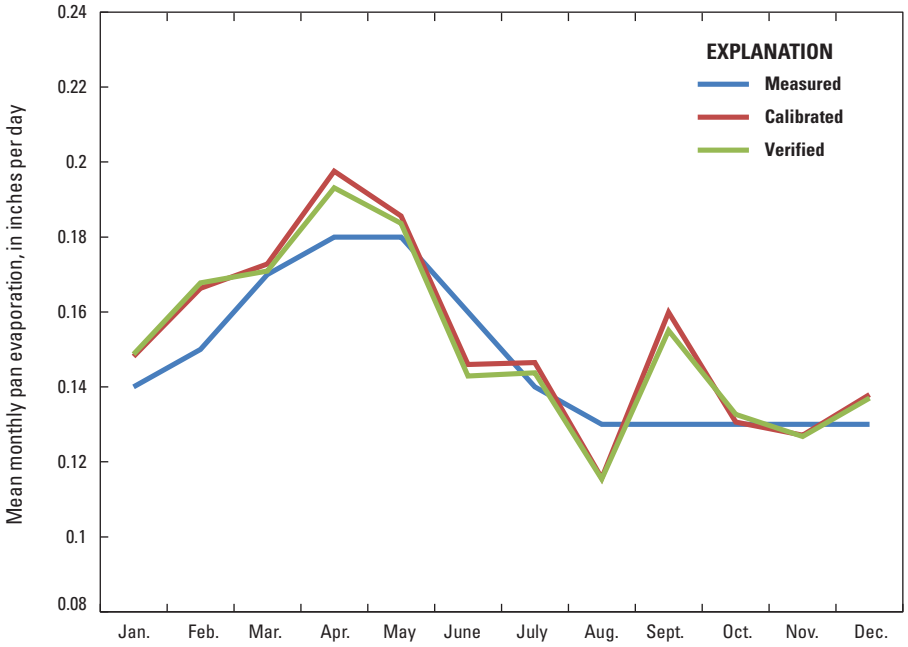

Figure 15. Mean monthly pan evaporation at station WSMO for months with at least one daily record from 1958 to 1998, and the mean potential evapotranspiration calibration and verification results for the Ugum and the Fena Valley watersheds.

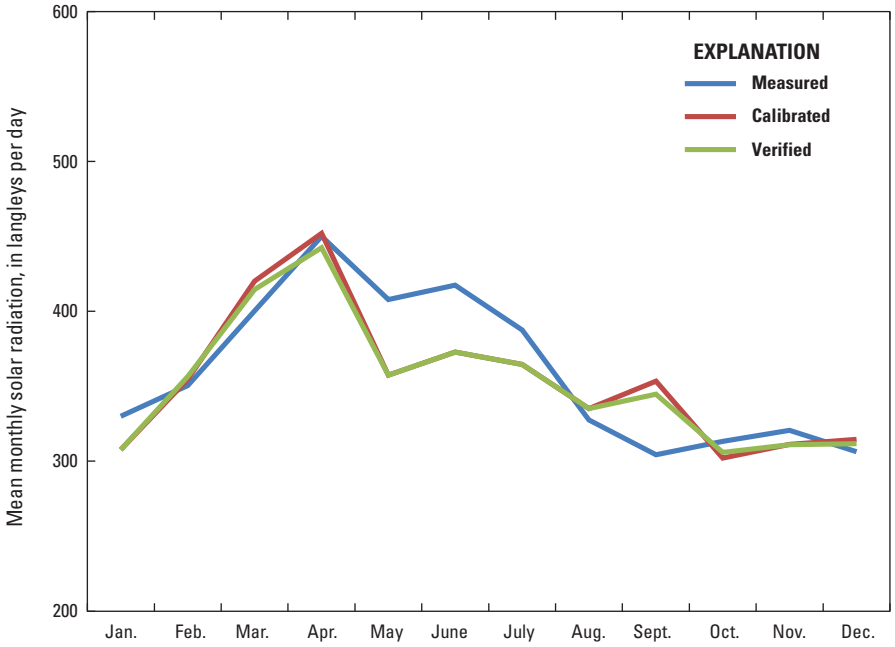

Figure 16. Mean monthly solar radiation at station WSMO from 1961 to 1990 (National Renewable Energy Laboratory, 2007) and the mean solar radiation calibration and verification results for the Ugum and the Fena Valley watersheds.

Physiographic Data

Distributed parameters for physical characteristics for the PRMS_2016 model, including basin area, slope, aspect, and elevation, were estimated from a 5-m digital elevation model (DEM) derived by Johnson (2012) from the Joint Airborne LIDAR (light detection and ranging) Bathymetry Technical Center of Expertise topobathy data (National Oceanic and Atmospheric Administration, 2007). Johnson (2012) used the procedures described in Taylor and Nelson (2008) to derive the DEM and delineate internally drained areas in the karst topography, or areas with closed depressions and their surface drainage basins that contribute runoff to the closed depression (fig. 1). These internally drained areas were defined as separate HRUs and modeled as closed depressions in the PRMS_2016 model. Losses from closed depressions in the PRMS_2016 model include seepage to the groundwater reservoirs as well as evaporative losses based on the PET (Markstrom and others, 2015). Land cover for the PRMS_2016 model was determined using the U.S. Department of Agriculture (2006) detailed vegetation dataset (fig. 7). Soil properties for the model were determined using the updated digital Natural Resources Conservation Service (U.S. Department of Agriculture, 2009) soils dataset originally documented by Young in 1988 (fig. 6). General geologic information was derived from the geologic map of Guam produced by Tracey and others (1964; fig. 5).

Model Development

PRMS-IV simulates different parts of the hydrologic cycle based on a set of user-defined modules. Model development requires the delineation of watersheds and HRUs, and the selection of appropriate modules suitable for simulating the southern Guam hydrologic cycle. The modules selected for the PRMS_2016 model are summarized in table 3 and briefly described below. For a more detailed description of each module and the underlying equations used to approximate each hydrologic process refer to Markstrom and others (2015).

Rainfall and minimum and maximum temperature data for southern Guam are distributed to each HRU using the PRMS-IV inverse distance and elevation-weighting scheme, module ide_dist. This is an improvement over the PRMS_1994 and PRMS_2004 models of the FVR watersheds (Nakama, 1994; Yeung, 2004), which used the arithmetic average of the two closest rainfall stations for the HRU portioned rainfall. This method tends to lower rainfall extremes (Yeung, 2004). However, in order to make it possible to download and process data in a timely manner such that the PRMS_2016 and FVR_2016 models can be used as a forecasting tool for surface-water availability (see section below on "Two-Step Modeling Procedure for Fena Valley Reservoir"), the parts of the PRMS_2016 model covering the Fena Valley watershed (Maulap, Almagosa, Imong, and FVR ungaged areas) are limited to using rainfall data from the USGS Almagosa (132105144405166) and Fena (132132144422366) rain gages and temperature data from the Naval Air Station (914226) in Tiyan (table 1).

For the other processes, module selection is straightforward. Daily shortwave radiation is estimated using the soltab module and distributed to each HRU using a modified degree-day method, module ddsolrad. Interception in PRMS-IV is modeled with the intcp module by calculating the amount of rainfall that is intercepted by vegetation, the amount of evaporation of intercepted rain, and the amount of net rain throughfall that reaches the soil. PET for the PRMS_2016 model is calculated for each HRU using a modified Jensen-Haise approach, module potet_jh. The surface runoff and infiltration for each HRU are calculated using the srunoff_smidx module, a non-linear variable-source-area method. Detailed descriptions and the equations used for each of these modules can be found in the report by Markstrom and others (2015) that documents PRMS-IV.

Watershed and Hydrologic Response Unit Delineation

HRUs were first delineated based on overland-flow planes that contribute to each stream segment using the geographic information system (GIS) Weasel application (Viger and Leavesley, 2007) and the 5-m DEM derived by Johnson (2012). These initial HRUs were then intersected with the closed-depression delineations (Johnson, 2012) to define HRUs in the model that are internally drained to the subsurface and modeled as closed-depression HRUs, resulting in a total of 317 HRUs (fig. 17). Outside of the water-balance model (which does not simulate either the water-levels above the spillway crest or flow over the spillway) the FVR was modeled as an open depression in the PRMS_2016 model to simulate flows downstream of the Fena Dam spillway. In the PRMS_2004 model only two subsurface and groundwater reservoirs per watershed were used to represent subsurface hydrogeologic conditions of each basin, however for the PRMS_2016 model subsurface and groundwater reservoirs were used for every HRU to describe the underlying limestone or volcanic units. Yeung (2004) also added an extra HRU to the Almagosa watershed in the PRMS_2004 model to account for added subsurface and groundwater contributions from the Alifan Limestone at the headwaters of the basin (fig. 5) owing to the disproportionate contribution of groundwater at the Almagosa Springs and the sloping geologic contact favoring flow toward the Almagosa River. For the PRMS_2016 model, flow from two HRUs delineated as closed depressions that originally drained to the west of the mountain range were rerouted by reassigning the stream segments of those HRUs so that they instead contributed subsurface and groundwater flow to the Almagosa watershed (HRUs 5 and 11, fig. 2). These additional closed-depression HRUs added approximately 280 acres of contributing area to the Almagosa watershed.

Table 3. Descriptions of modules used for the PRMS_2016 model

[Table modified from Markstrom and others (2015); HRU, hydrologic response unit]

Module name	Description
Basin definition process	
basin	Defines shared watershed-wide and HRU physical parameters and variables.
Cascading flow process	
cascade	Determines computational order of the HRUs and groundwater reservoirs for routing flow downslope.
Solar table process	
soltab	Compute potential solar radiation and sunlight hours for each HRU for each day of year; modification of soltab_prms.
Time series data process	
obs	Reads and stores observed data from all specified measurement stations.
Combined climate distribution process	
ide_dist	Determines the form of precipitation and distributes precipitation and temperatures to each HRU on the basis of measurements at stations with closest elevation or shortest distance to the respective HRU.
Solar radiation distribution process	
ddsolrad	Distributes solar radiation to each HRU and estimates missing solar radiation data using a maximum temperature per degree-day relation.
Transpiration period process	
transp_tindex	Determines whether the current time step is in a period of active transpiration by the temperature index method.
Potential evapotranspiration process	
potet_jh	Computes the potential evapotranspiration by using the Jensen-Haise formulation (Jensen and Haise, 1963).
Canopy interception process	
intcp	Computes volume of intercepted precipitation, evaporation from intercepted precipitation, and throughfall that reaches the soil.
Surface runoff process	
srunoff_smidx	Computes surface runoff and infiltration for each HRU using a nonlinear variable-source-area method allowing for cascading flow.
Soil zone process	
soilzone	Computes inflows to and outflows from soil zone of each HRU and includes inflows from infiltration, groundwater, and upslope HRUs, and outflows to gravity drainage, interflow, and surface runoff to down-slope HRUs
Groundwater process	
gwflow	Sums inflow to and outflow from PRMS groundwater reservoirs; outflow can be routed to downslope groundwater reservoirs and stream segments.
Streamflow process	
strmflow_in_out	Routes water between segments in the system by setting the outflow to the inflow.
Summary process	
basin_sum	Computes daily, monthly, yearly, and total flow summaries of volumes and flows for all HRUs.

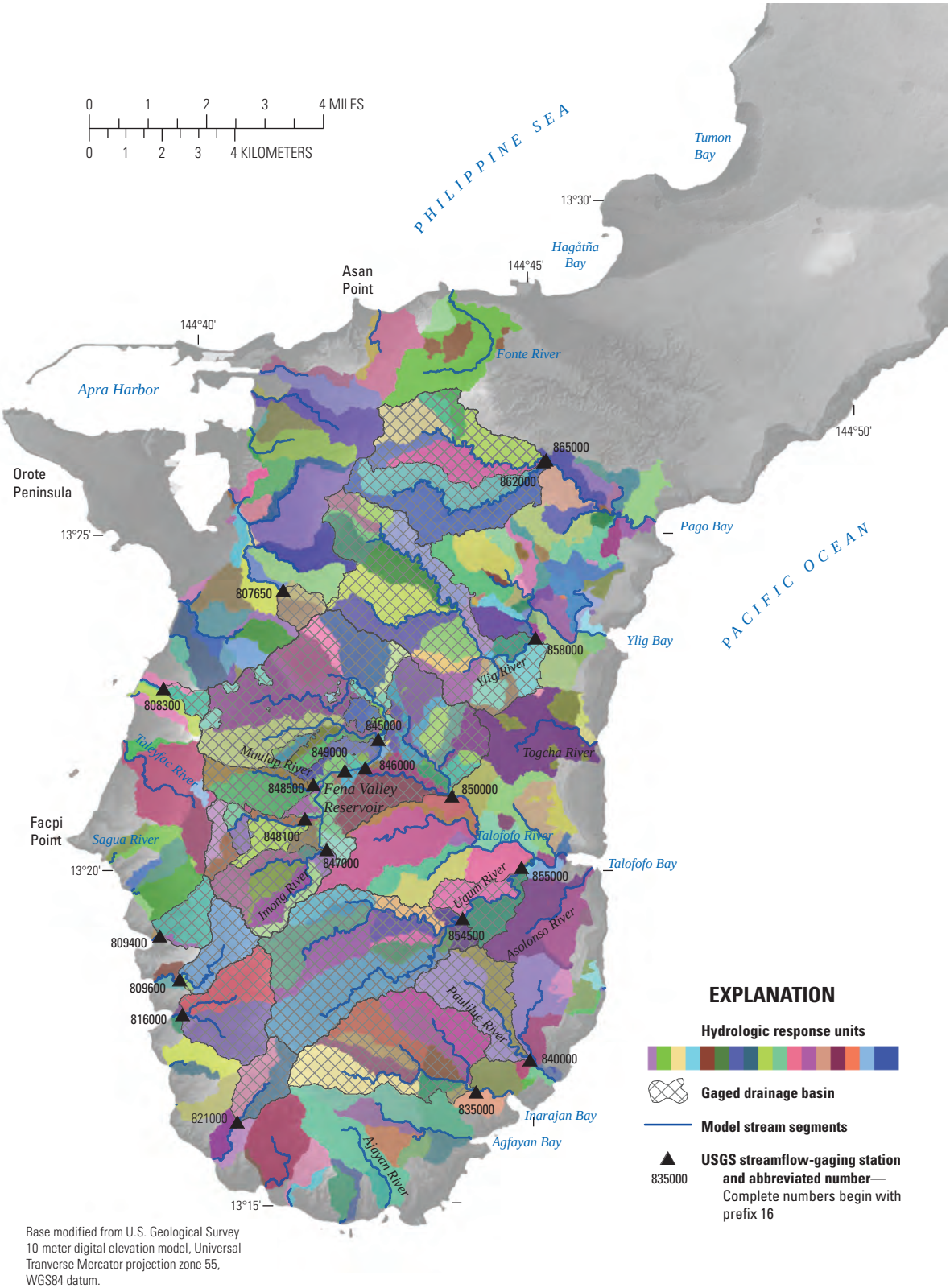

Figure 17. Hydrologic response units, modeled stream segments, and gaged drainage basin areas in the PRMS_2016 model.

Model Parameterization

Distributed parameters representing physical HRU characteristics were estimated using the parameterization methods in the GIS Weasel application (Viger and Leavesley, 2007) and the available datasets described earlier. Descriptions of the major distributed and nondistributed parameters used in the PRMS_2016 model are listed in table 4. Selected physical characteristics of the HRUs for the Fena Valley watersheds and the Ugum watershed in the PRMS_2016 model, two of the most important surface-water resources in southern Guam, are listed in table 5. The remaining physical characteristics of the HRUs listed in table 5, as well as the physical characteristics of the other southern Guam HRUs can be found in the associated USGS data release (Rosa and Hay, 2017; DOI:10.5066/F7HH6HV4). An average depth of 120 in. (3.0 m) was used for each of the HRUs in the model that are internally drained to the subsurface and modeled as closed depression HRUs (table 5; Taborosi and others, 2004). In the PRMS_2016 model the FVR was modeled as an open depression with an average depth of 900 in. (22.9 m) to simulate flows below the Fena Dam spillway (Marineau and Wright, 2015). Either default values within PRMS-IV or values from the previous model (Yeung, 2004) were used as initial parameter values for the nonphysical parameters.

Model Calibration, Verification, and Results

The selection of the calibration and verification periods was largely driven by the availability of concurrent and continuous streamflow and climate data for each of the watersheds modeled. Continuous periods of data eliminated the need to reinitialize the model or the need to synthesize input data. Selection of a calibration period that covers a wide range of flow conditions results in greater confidence that the model is capable of being applied over a range of flow conditions. An additional consideration for the Fena Valley watersheds was that the calibration period needed to include an ENSO (El Niño) event because the performance of the model during periods of drought was important. In the most recent period of data available for calibration (2002–14), Guam experienced four weak to moderately strong El Niño events (National Oceanic Atmospheric Administration, 2016) resulting in reduced rainfall during the year following the El Niño event. The periods selected for calibration and verification are described later in the Simulation Results section of the report.

The PRMS_2016 model was calibrated using an automated parameter-estimation procedure combined with a geographically nested approach. Model parameters were calibrated in two phases, the energy-budget and water-budget phases, with a total of six steps (table 6) using the multiple-objective stepwise-calibration software Luca (Hay and Umemoto, 2007). The PRMS_2016 model was subdivided into areas that may be used and analyzed separately, such as the FVR basin. The PRMS_2016 model was calibrated to obtain the best fit to the data in each of the selected calibration periods and the verification period results represent an independent assessment of the model performance.

Energy-Budget Calibration

The first phase in the calibration procedure was to adjust the energy-budget using available mean monthly SR and PET data. Table 6 lists the parameters used to calibrate the PRMS_2016 model during the SR and PET phase of the calibration. This phase of the calibration focused on the role of these parameters in calculating SR and PET even though they also influence other PRMS-IV calculations. The goal of the calibration was to minimize the objective function. The objective function used by the calibration software Luca to calibrate the mean monthly SR and PET values calculated by PRMS-IV is described as

$$OF = \sum_{m=1}^{12} abs(MSD_m - SIM_m), \quad (1)$$

where

OF	is the objective function,
m	is the month,
abs	is the absolute value,
MSD	are the mean monthly measured values of either SR or PET, and
SIM	are the mean monthly simulated values of either SR or PET.

Water-Budget Calibration

In the second phase of model calibration with the Luca software, the simulated water budget was first adjusted by volume and then by timing, in an attempt to match measured streamflow in the 18 gaged watersheds in southern Guam. Model calibration for the 18 watersheds was divided into two calibration rounds. Data from the Ugum above Talofofo Falls (16854500), Imong (16847000), Almagosa (16848000), Maulap (16848500), and Lonfit (16862000) River gages, which are located near the headwaters of each basin, were used to calibrate the model in round 1 (table 2). Data from the remaining gages were used to calibrate the model in round 2, and parameters that were previously calibrated in round 1 were preserved and not recalibrated in this second round of calibration.

Table 4. List of parameters used in the PRMS_2016 model.

[PRMS, Precipitation-Runoff Modeling System; HRU, hydrologic response unit; GWR, groundwater reservoir; ET, evapostranspiration]

PRMS model parameter	Description of parameter
Distributed (HRU-dependent) parameters	
CAREA_MAX	Maximum possible area contributing to surface runoff (in decimal fraction of HRU area)
COV_TYPE	Vegetation cover type for HRU (bare soil, grasses, shrubs, or trees)
COVDEN_SUM	Summer vegetation cover density for the major vegetation type in each HRU as a decimal fraction
COVDEN_WIN	Winter vegetation cover density for the major vegetation type in each HRU as a decimal fraction
DPRST_AREA	Aggregate sum of surface depression areas of each HRU (acres)
DPRST_DEPTH_AVG	Average depth of storage depressions at maximum storage capacity (inches)
DPRST_ET_COEF	Fraction of unsatisfied potential evapotranspiration to apply to surface depression storage
DPRST_FLOW_COEF	Coefficient in linear flow routing equation for open surface depressions for each HRU
DPRST_FRAC_HRU	Fraction of surface depression areas of each HRU
DPRST_FRAC_INIT	Fraction of maximum surface depression storage that contains water at the start of a simulation
DPRST_FRAC_OPEN	Fraction of open surface depression storage area within an HRU that can generate surface runoff as a function of storage volume
DPRST_SEEP_RATE_CLOS	Coefficient used in linear seepage flow equation for closed surface depressions for each HRU
DPRST_SEEP_RATE_OPEN	Coefficient used in linear seepage flow equation for open surface depressions for each HRU
FASTCOEF_LIN	Linear coefficient in equation to route preferential-flow storage down slope for each HRU preferential-flow storage down slope for each HRU
FASTCOEF_SQ	Non-linear coefficient in equation to route preferential-flow storage down slope for each HRU
HRU_AREA	Area of HRU (acres)
HRU_ASPECT	Aspect of HRU (angular degrees)
HRU_ELEV	Mean land-surface altitude of HRU (meters)
HRU_PERCENT_IMPERV	Decimal fraction of HRU area that is impervious
HRU_SEGMENT	Segment index for HRU lateral inflow
HRU_SLOPE	Slope of each HRU
HRU_X	Longitude (X) for HRU in Albers projection
HRU_Y	Latitude (Y) for HRU in Albers projection
IMPERV_STOR_MAX	Maximum retention storage for HRU impervious area (inches)
JH_COEF_HRU	Air temperature coefficient used in Jensen-Haise potential ET computations for each HRU
OP_FLOW_THRES	Fraction of open depression storage above which surface runoff occurs for each timestep
PREF_FLOW_DEN	Fraction of the soil zone in which preferential flow occurs for each HRU; used if control parameter
RAD_TRNCF	Transmission coefficient for short-wave radiation through winter plant canopy (decimal fraction)
SAT_THRESHOLD	Water holding capacity of the gravity and preferential flow reservoirs; difference between field capacity and total soil saturation for each HRU (inches)
SLOWCOEF_LIN	Linear coefficient in equation to route gravity-reservoir storage down slope for each HRU
SLOWCOEF_SQ	Non-linear coefficient in equation to route gravity reservoir storage down slope for each HRU
SMIDX_COEF	Coefficient in non-linear contributing area algorithm for each HRU (for computing surface runoff)
SMIDX_EXP	Exponent in non-linear contributing area algorithm for each HRU (for computing surface runoff)
SOIL_MOIST_INIT	Initial value of available water in the capillary reservoir (inches)
SOIL_MOIST_MAX	Maximum available water holding capacity of capillary reservoir from land surface to rooting depth of the major vegetation type of each HRU (inches)
SOIL_RECHR_INIT	Initial storage for soil recharge zone (upper part of capillary reservoir where losses occur as both evaporation and transpiration) for each HRU (inches)

Table 4. List of parameters used in the PRMS_2016 model.—Continued

[PRMS, Precipitation-Runoff Modeling System; HRU, hydrologic response unit; GWR, groundwater reservoir; ET, evapostranspiration]

PRMS model parameter	Description of parameter
	Distributed (HRU-dependent) parameters—Continued
SOIL_RECHR_MAX	Maximum storage for soil recharge zone (upper portion of capillary reservoir where losses occur as both evaporation and transpiration) (inches)
SOIL_TYPE	Soil type of each HRU (sand, loam, or clay)
SOIL2GW_MAX	Maximum amount of the capillary reservoir excess that is routed directly to the GWR for each HRU (inches)
SRAIN_INTCP	Summer rain interception storage capacity for the major vegetation type in each HRU (inches)
WRAIN_INTCP	Winter rain interception storage capacity for the major vegetation type in each HRU (inches)
SRO_TO_DPRST	Fraction of pervious surface runoff that flows into surface depression storage; the remainder flows to a stream network for each HRU
SRO_TO_DPRST_IMPERV	Fraction of impervious surface runoff that flows into surface depression storage; the remainder flows to a stream network for each HRU
VA_CLOS_EXP	Coefficient in the exponential equation relating maximum surface area to the fraction that closed depressions are full to compute current surface area for each HRU
VA_OPEN_EXP	Coefficient in the exponential equation relating maximum surface area to the fraction that open depressions are full to compute current surface area for each HRU
	Selected temperature and rainfall related parameters
ADJUST_RAIN	Monthly factor to adjust measured precipitation on each HRU to account for differences in elevation, and so forth
DDAY_INCPT	Monthly (January to December) intercept in degree-day equation
DDAY_SLOPE	Monthly (January to December) slope in degree-day equation
DIST_EXP	Exponent for inverse distance calculations
JH_COEF	Monthly (January to December) air temperature coefficient used in Jensen-Haise potential ET computations
NDIST_PSTA	Number of precipitation measure stations for inverse distance calculations
NDIST_TSTA	Number of air temperature-measurement stations for inverse distance calculations
PRCP_WGHT_DIST	Monthly (January to December) precipitation weighting function for inverse distance calculations
PSTA_ELEV	Altitude of each measurement station that measures precipitation
PSTA_NUSE	Defines which measurement stations will be used in the distribution regression of precipitation
PSTA_X	Longitude (X) for each precipitation measurement station in Albers projection
PSTA_Y	Latitude (Y) for each measurement station that measures precipitation in Albers projection
RADMAX	Maximum fraction of the potential solar radiation that may reach the ground due to haze, dust, smog, and so forth
SOLRAD_ELEV	Elevation of the solar radiation station used for the degree-day curves to distribute temerature
TEMP_WGHT_DIST	Monthly (January to December) temperature weighting function for inverse distance calculations
TMAX_ADJ	Adjustment to maximum air temperature for HRU, estimated on basis of slope and aspect
TMIN_ADJ	Adjustment to minimum air temperature for HRU, estimated on basis of slope and aspect
TRANSP_TMAX	Temperature index to determine the specific date of the start of the transpiration period
TSTA_ELEV	Altitude of each measurement station that measures air temperature
TSTA_NUSE	Defines which measurement stations will be used in distribution regression of air temperatures
TSTA_X	Longitude (X) for each measurement station that measures air temperature in Albers projection
TSTA_Y	Latitude (Y) for each measurement station that measures air temperature in Albers projection

Table 4. List of parameters used in the PRMS_2016 model.—Continued

[PRMS, Precipitation-Runoff Modeling System; HRU, hydrologic response unit; GWR, groundwater reservoir; ET, evapostranspiration]

PRMS model parameter	Description of parameter
Groundwater and subsurface routing related parameters	
GWFLOW_COEF	Linear coefficient in the equation to compute groundwater discharge for each GWR
GWSINK_COEF	Linear coefficient in the equation to compute outflow to the groundwater sink for each GWR
GWSTOR_INIT	Storage in each GWR at the beginning of a simulation
SSR2GW_EXP	Non-linear coefficient in equation used to route water from the gravity reservoirs to the GWR for each HRU
SSR2GW_RATE	Linear coefficient in equation used to route water from the gravity reservoir to the GWR for each HRU
SSSTOR_INIT	Initial storage of the gravity and preferential-flow reservoirs for each HRU

Table 5. Selected physical characteristics of hydrologic response units for the Fena Valley watersheds and Ugum watershed in the PRMS_2016 model.

[Parameter definitions are shown in table 4. HRU, hydrologic response unit; HRUs for the Fena Valley watershed are shown in figure 2]

HRU	COV_TYPE	HRU_AREA (acres)	HRU_ELEV (feet)	HRU_PERCENT_IMPERV	HRU_SLOPE	DPRST_AREA (acres)	DPRST_DEPTH_AVG (inches)	SOIL_TYPE
Maulap River watershed								
1	Trees	230.22	652.72	0.01	4.71	0.00	0	Clay
2	Trees	522.96	485.44	0.00	3.90	0.00	0	Clay
Almagosa River watershed[1]								
1	Trees	73.31	764.24	0.01	2.92	0.00	0	Loam
2	Trees	106.43	806.88	0.00	4.04	0.00	0	Loam
3	Trees	70.44	357.52	0.02	5.63	0.00	0	Clay
4	Trees	296.43	498.56	0.00	3.46	0.00	0	Clay
5	Trees	277.90	1059.44	0.00	2.54	276.51	120	Loam
6	Trees	49.66	931.52	0.00	0.16	49.41	120	Loam
7	Trees	25.98	918.40	0.00	0.19	25.81	120	Loam
8	Trees	170.95	967.60	0.00	2.00	170.10	120	Loam
9	Trees	126.08	908.56	0.00	2.98	125.45	120	Clay
10	Trees	5.41	790.48	0.00	0.28	5.38	120	Loam
11	Trees	6.20	1243.12	0.00	0.18	6.17	120	Loam
Imong River watershed								
1	Trees	44.24	239.44	0.00	4.20	0.00	0	Loam
2	Trees	80.20	298.48	0.00	3.21	0.00	0	Loam
3	Trees	391.86	803.60	0.00	3.26	0.00	0	Loam
4	Trees	191.76	508.40	0.00	3.03	0.00	0	Loam
5	Trees	256.82	534.64	0.00	3.76	0.00	0	Loam
6	Trees	264.97	603.52	0.00	3.25	0.00	0	Loam

Table 5. Selected physical characteristics of hydrologic response units for the Fena Valley watersheds and Ugum watershed in the PRMS_2016 model.—Continued

[Parameter definitions are shown in table 4. HRU, hydrologic response unit; HRUs for the Fena Valley watershed are shown in figure 2]

HRU	COV_TYPE	HRU_AREA (acres)	HRU_ELEV (feet)	HRU_PERCENT_IMPERV	HRU_SLOPE	DPRST_AREA (acres)	DPRST_DEPTH_AVG (inches)	SOIL_TYPE
Ungaged watershed areas								
1	Trees	97.20	200.08	0.05	0.56	0.00	0	Clay
2	Trees	17.35	160.72	0.00	1.92	0.00	0	Clay
3	Trees	83.21	239.44	0.02	1.61	0.00	0	Loam
4	Trees	127.37	203.36	0.00	0.55	0.00	0	Clay
5	Trees	13.28	193.52	0.01	3.06	0.00	0	Clay
6	Trees	104.25	285.36	0.00	1.86	0.00	0	Clay
7	Trees	8.25	154.16	0.00	3.96	0.00	0	Loam
8	Trees	125.43	288.64	0.00	2.63	0.00	0	Loam
Ugum River watershed								
1	Trees	9.03	3.28	0.00	10.00	0.00	0	Clay
2	Trees	16.97	3.28	0.00	8.04	0.00	0	Clay
3	Trees	370.94	180.40	0.00	3.24	0.00	0	Clay
4	Trees	417.56	242.72	0.03	3.55	0.00	0	Clay
5	Trees	699.19	206.64	0.01	2.95	0.00	0	Clay
6	Trees	290.37	419.84	0.00	2.78	0.00	0	Clay
7	Trees	180.15	285.36	0.00	3.44	0.00	0	Sand
8	Trees	376.27	173.84	0.01	3.16	0.00	0	Loam
9	Trees	90.70	364.08	0.00	3.59	0.00	0	Sand
10	Trees	613.68	521.52	0.00	3.25	0.00	0	Loam
11	Trees	56.54	259.12	0.00	3.06	0.00	0	Clay
12	Trees	491.16	449.36	0.00	3.40	0.00	0	Loam
13	Trees	238.29	305.04	0.00	3.34	0.00	0	Clay
14	Grasses	108.16	298.48	0.02	3.92	0.00	0	Loam
15	Trees	11.94	219.76	0.00	8.75	0.00	0	Clay
16	Trees	46.21	265.68	0.00	2.60	0.00	0	Loam
17	Trees	94.99	331.28	0.00	3.58	0.00	0	Clay
18	Trees	153.72	380.48	0.00	2.71	0.00	0	Clay
19	Trees	1321.78	462.48	0.00	2.93	0.00	0	Loam
20	Trees	94.68	328.00	0.00	3.40	0.00	0	Loam
21	Trees	40.71	255.84	0.00	0.12	40.51	120	Loam
22	Trees	7.39	190.24	0.00	0.26	7.35	120	Clay

[1]HRUs 5 and 11 for Almagosa River watershed were added to account for additional groundwater flow from limestone areas.

Table 6. Calibration procedure using the Luca software for the PRMS_2016 model.

[Weight of the objective function is shown in parentheses]

Calibration data set	Objective function(s) and parameter(s) included	Paremeters used to calibrate model state	Parameter range[1]
Phase 1			
Step 1-Solar radiation			
Basin mean monthly solar radiation (SR)	Absolute difference: 1. Mean monthly (1)	dday_intcp dday_slope	-60 to 10 0.2 to 0.9
Step 2-Potential evapotranspiration			
Basin mean monthly potential evapotranspiration (PET)	Absolute difference: 1. Mean monthly (1)	jh_coef	0.001 to 0.09
Phase 2			
Step 1-Annual and monthly water budget			
Annual and monthly streamflow volume	Normalized root mean square error: 1. Mean monthly (1/3) 2. Monthly mean (1/3) 3. Annual mean (1/3)	adjust_rain	-0.75 to 0.75
Step 2-High flows			
High flows	Normalized root mean square error: 1. Mean monthly (0.5) 2. Daily high flows (0.3) 3. Three-day moving average (0.2)	smidx_coef smidx_exp	0.0001 to 1.0 0.2 to 0.8
Step 3-Low flows			
Low flows	Normalized root mean square error: 1. Mean monthly (0.5) 2. Daily low flows (0.3) 3. Three-day moving average (0.2)	gwflow_coef soil2gw_max	0.0006 to 0.08 0.0 to 0.6
Step 4-Daily streamflow timing			
Daily streamflow timing	Normalized root mean square error: 1. Daily high flows (0.3) 2. Daily low flows (0.1) 3. Three-day moving average (0.6)	carea_max fastcoef_lin pref_flow_den slowcoef_sq soil_moist_max radmax tmax_adj tmin_adj soil_rechr_max transp_tmax	0.2 to 0.8 0.01 to 0.3 0.00 to 0.2 0.005 to 0.3 0.05 to 12 0.05 to 1.0 –3.0 to 3.0 –3.0 to 3.0 0.05 to 4 0 to 1.1

[1]The range represents a typical range from other published models.

The parameters that influence simulated streamflow volume and timing were calibrated during this phase using four steps, attempting to match measured (1) annual and monthly water budgets, (2) high flows, (3) low flows, and (4) daily streamflow timing (table 6). Flow regulation and water use in southern Guam potentially impacts the timing and volume of the low flows measured at 6 of the 18 gages during some subperiods of the station's period of record (table 2). Data from 5 of the 6 streamflow-gaging stations with flow regulation during part of their period of record were used directly with no adjustments. Because diversion data were not available to adjust measured discharge at these gages, the calibration scheme was adjusted to only consider periods of nonregulated flow. To account for possible unknown periods of flow alteration, less weight was placed on the calibration of daily flows and more weight on the calibration of mean monthly flows for all gages. The Almagosa streamflow record was adjusted for known diversions, as discussed in the data section. The calibration scheme was designed to avoid calibrating natural-flow model parameters to reflect regulated-flow conditions.

The calibration scheme to fit simulated streamflow volumes to measured streamflow volumes used monthly mean, mean monthly, and annual mean streamflow aggregates of the datasets. The PRMS_2016 model was calibrated for high- and low-flow conditions using mean monthly, daily high and low flows, and a 3-day moving average of daily streamflow. A 3-day moving average was used to prevent the optimization process from overcompensating and adjusting the model parameters to unrealistic values because of the difference in flow timing owing to the possibility of low-flow alterations. The goal of the calibration was to minimize the objective function. The final objective function value in the Luca software for each step is calculated as

$$OF = \sum_{i=1}^{nOF} (w_i \times OF_i), \quad (2)$$

where

OF_i is the objective function value for the *i*th objective function,
w_i is the weight for the *i*th objective function, and
nOF is the total number of objective functions for a given step.

The objective function, parameters included in the objective function, and the weight applied to each objective function used for each step in Phase 2 of the calibration are listed in table 6. These objective functions were calculated using the normalized root mean square error (NRMSE):

$$NRMSE = \sqrt{\frac{\sum_{n=1}^{nstep} \left(MSD_n - SIM_n\right)^2}{\sum_{n=1}^{nstep} \left(MSD_n - \mathrm{MN}\right)^2}}, \quad (3)$$

where

n is the time step,
$nstep$ is the total number of time steps,
MSD_n are the measured streamflow values,
SIM_n are the simulated streamflow values, and
MN is the mean of all streamflow values for the objective function time period.

If NRMSE = 0, then the measured values are equal to the simulated values (MSD=SIM). A value of NRMSE >1 indicates that the average value of all the measured data is as good or better than using the simulated values from the PRMS_2016 model. Selected parameter and coefficient values for the daily mode streamflow calculations for the Fena Valley watersheds and the Ugum watershed in the PRMS_2016 model are listed in tables 7 and 8.

Energy-Budget Verification and Simulation Results

Mean monthly reference ET values that Johnson (2012) calculated to use in conjunction with crop coefficients as an approximation for PET in a water-budget model for Guam ranged from 0.16 inches/day (in/day) in October to 0.20 in/day in April. Johnson (2012) estimated that reference ET is about 82 percent of pan evaporation on Guam, which generally agrees with the approximation for the seasonal pattern of measured PET used in the calibration process for the PRMS_2016 model.

Water-Budget Verification and Simulation Results

Simulation results from the PRMS_2016 model were examined both graphically and statistically. Graphs of simulated basin rainfall and measured and simulated daily streamflow for the calibration and verification periods used for the Fena Valley watersheds and the Ugum watershed are shown in figures 18 through 25. The data are plotted using a semi-logarithmic scale to emphasize the low flows during the dry season, when water availability is of greatest concern for these particular areas of surface-water development. The figures show PRMS_2016 simulates the volume and timing of streamflow in southern Guam well, however the model is sometimes limited in its ability to simulate the complex shape of the baseflow recession hydrographs.

Table 7. Selected parameter and coefficient values for daily mode runoff calculations for the Fena Valley watersheds and Ugum watershed in the PRMS_2016 model.

[Parameter definitions are shown in table 4. HRU, hydrologic response unit]

HRU	CAREA_MAX	COVDEN_SUM	FASTCOEF_LIN	GW-FLOW_COEF	PREF_FLOW_DEN	RAD-MAX	SLOW-COEF_SQ	SMIDX_COEF	SMIDX_EXP	SOIL_MOIST_MAX	SOIL_RECHR_MAX	SOIL-2GW_MAX	SRAIN_INTCP	SSR2GW_RATE	TMAX_ADJ	TMIN_ADJ	TRANSP_TMAX
Maulap																	
1	0.2004	0.7133	0.2527	0.0136	0.0002	0.5329	0.0632	0.0006	0.6169	8.1110	0.7980	0.2266	0.0615	0.0250	2.9830	2.9730	0.3440
2	0.2016	0.9291	0.2527	0.0136	0.0002	0.5329	0.0632	0.0006	0.6169	11.9854	1.0223	0.2266	0.0722	0.0250	2.9830	1.5145	0.3440
Almagosa																	
1	0.2051	1.0000	0.2028	0.0104	0.0000	0.5233	0.0427	0.0122	0.4512	11.4302	2.5586	0.0000	0.0825	0.0250	2.9953	-0.0724	0.9608
2	0.2011	0.8068	0.2028	0.0104	0.0000	0.5233	0.0427	0.0122	0.4512	11.7985	3.4135	0.0000	0.0731	0.0250	2.9953	1.6774	0.9608
3	0.2065	0.7816	0.2028	0.0104	0.0000	0.5233	0.0427	0.0122	0.4512	1.3792	2.1451	0.0000	0.0714	0.0250	2.9953	1.7711	0.9608
4	0.2016	0.6864	0.2028	0.0104	0.0000	0.5233	0.0427	0.0122	0.4512	11.9972	0.4658	0.0000	0.0665	0.0250	2.9953	-2.0733	0.9608
5	0.0010	0.9423	0.2028	0.0204	0.1999	0.5233	0.2886	0.0010	0.0010	10.0245	2.7347	0.5368	0.0794	0.2000	2.9953	-1.6799	0.9608
6	0.2008	0.6353	0.2028	0.0204	0.1999	0.5233	0.2886	0.0131	0.3363	0.4519	0.8523	0.5368	0.0620	0.2000	2.9953	-0.2147	0.9608
7	0.2008	0.7351	0.2028	0.0204	0.1999	0.5233	0.2886	0.0131	0.3363	0.3405	2.4341	0.5368	0.0701	0.2000	2.9953	-1.3205	0.9608
8	0.2008	0.9306	0.2028	0.0204	0.1999	0.5233	0.2886	0.0131	0.3363	0.2208	3.6527	0.5368	0.0787	0.2000	2.9953	-1.7717	0.9608
9	0.0010	0.7204	0.2028	0.0204	0.1999	0.5233	0.2886	0.0010	0.0010	9.6730	0.2829	0.5368	0.0683	0.2000	2.9953	-0.7089	0.9608
10	0.2008	1.0000	0.2028	0.0204	0.1999	0.5233	0.2886	0.0131	0.3363	0.8923	0.1167	0.5368	0.0825	0.2000	2.9953	-0.8244	0.9608
11	0.2008	0.9010	0.2028	0.0204	0.1999	0.5233	0.2886	0.0131	0.3363	0.7896	0.4132	0.5368	0.0746	0.2000	2.9953	2.7361	0.9608
Imong																	
1	0.5297	0.2561	0.0334	0.0175	0.0006	0.7186	0.2644	0.0438	0.2056	1.6090	1.5080	0.3809	0.0569	0.0250	2.9776	2.5556	0.6085
2	0.5297	0.8022	0.0334	0.0175	0.0006	0.7186	0.2644	0.0438	0.2056	1.0937	0.5944	0.3809	0.0874	0.0250	2.9776	2.1895	0.6085
3	0.5297	0.3109	0.0334	0.0175	0.0006	0.7186	0.2644	0.0438	0.2056	3.1281	0.4005	0.3809	0.0587	0.0250	2.9776	2.7762	0.6085
4	0.5297	0.5449	0.0334	0.0175	0.0006	0.7186	0.2644	0.0438	0.2056	2.2820	1.5963	0.3809	0.0713	0.0250	2.9776	2.6646	0.6085
5	0.5297	0.5751	0.0334	0.0175	0.0006	0.7186	0.2644	0.0438	0.2056	1.4029	0.7939	0.3809	0.0747	0.0250	2.9776	1.4271	0.6085
6	0.5297	0.4120	0.0334	0.0175	0.0006	0.7186	0.2644	0.0438	0.2056	3.2979	0.3511	0.3809	0.0645	0.0250	2.9776	2.9437	0.6085
Ungaged																	
1	0.2010	0.6212	0.2527	0.0136	0.0002	0.5329	0.0632	0.0006	0.6169	10.0482	0.9102	0.2266	0.0639	0.0250	2.9830	1.1469	0.3440
2	0.2010	0.5130	0.2527	0.0136	0.0002	0.5329	0.0632	0.0006	0.6169	10.0482	0.9102	0.2266	0.0744	0.0250	2.9830	0.0587	0.3440
3	0.2010	0.9128	0.2527	0.0136	0.0002	0.5329	0.0632	0.0006	0.6169	10.0482	0.9102	0.2266	0.0566	0.0250	2.9830	0.0587	0.3440
4	0.5297	0.5743	0.0334	0.0175	0.0006	0.5329	0.2644	0.0438	0.2056	2.1356	0.8740	0.3809	0.0873	0.0250	2.9830	0.0587	0.6085
5	0.5297	0.7283	0.0334	0.0175	0.0006	0.5329	0.2644	0.0438	0.2056	2.1356	0.8740	0.3809	0.0860	0.0250	2.9830	2.4527	0.6085

Table 7. Selected parameter and coefficient values for daily mode runoff calculations for the Fena Valley watersheds and Ugum watershed in the PRMS_2016 model.—Continued

[Parameter definitions are shown in table 4. HRU, hydrologic response unit]

HRU	CAREA_MAX	COVDEN_SUM	FASTCOEF_LIN	GW-FLOW_COEF	PREF_FLOW_DEN	RAD-MAX	SLOW-COEF_SQ	SMIDX_COEF	SMIDX_EXP	SOIL_MOIST_MAX	SOIL_RECHR_MAX	SOIL-2GW_MAX	SRAIN_INTCP	SSR2GW_RATE	TMAX_ADJ	TMIN_ADJ	TRANSP_TMAX
Ungaged—Continued																	
6	0.5297	0.6535	0.0334	0.0175	0.0006	0.5329	0.2644	0.0438	0.2056	2.1356	0.8740	0.3809	0.0637	0.0250	2.9830	0.0587	0.6085
7	0.2008	0.9749	0.2028	0.0204	0.1999	0.5329	0.2886	0.0131	0.3363	5.3635	1.7336	0.5368	0.0908	0.0250	2.9830	-0.7031	0.9608
8	0.2008	0.9079	0.2028	0.0204	0.1999	0.5329	0.2886	0.0131	0.3363	5.3635	1.7336	0.5368	0.0717	0.0250	2.9830	0.0587	0.9608
Ugum																	
1	0.5999	0.8961	0.0418	0.0227	0.0008	0.8359	0.0095	0.0001	0.2500	3.2943	2.6969	0.6000	0.0717	0.0250	-0.0077	1.1528	0.1140
2	0.5999	0.5517	0.0418	0.0227	0.0008	0.8359	0.0095	0.0001	0.2500	2.8128	2.4121	0.6000	0.0585	0.0250	-0.0077	-0.8691	0.1140
3	0.2743	0.5842	0.0243	0.0163	0.0008	0.5511	0.0096	0.0342	0.2004	3.6674	0.6335	0.0564	0.0564	0.0250	2.9665	2.8625	0.4565
4	0.5999	0.7244	0.0418	0.0227	0.0008	0.8359	0.0095	0.0001	0.2500	2.1267	1.7922	0.6000	0.0657	0.0250	-0.0077	-0.8691	0.1140
5	0.5999	0.6317	0.0418	0.0227	0.0008	0.8359	0.0095	0.0001	0.2500	2.0071	1.6681	0.6000	0.0561	0.0250	-0.0077	-0.8691	0.1140
6	0.3670	0.2881	0.0609	0.0128	0.0036	0.5818	0.0096	0.0668	0.2000	2.6447	0.7451	0.1051	0.0414	0.0250	2.7497	2.7285	0.8643
7	0.3670	0.2907	0.0609	0.0128	0.0036	0.5818	0.0096	0.0668	0.2000	2.1671	0.3882	0.1051	0.0426	0.0250	2.7497	2.9532	0.8643
8	0.2743	0.6445	0.0243	0.0163	0.0008	0.5511	0.0096	0.0342	0.2004	3.2735	0.4040	0.0564	0.0581	0.0250	2.9665	0.5965	0.4565
9	0.3670	0.2692	0.0609	0.0128	0.0036	0.5818	0.0096	0.0668	0.2000	2.6226	0.6527	0.1051	0.0375	0.0250	2.7497	0.4816	0.8643
10	0.3670	0.4134	0.0609	0.0128	0.0036	0.5818	0.0096	0.0668	0.2000	2.1717	0.3520	0.1051	0.0470	0.0250	2.7497	2.7285	0.8643
11	0.3670	0.8932	0.0609	0.0128	0.0036	0.5818	0.0096	0.0668	0.2000	2.2206	0.3765	0.1051	0.0698	0.0250	2.7497	2.9532	0.8643
12	0.3670	0.5586	0.0609	0.0128	0.0036	0.5818	0.0096	0.0668	0.2000	2.1681	0.3329	0.1051	0.0550	0.0250	2.7497	0.4816	0.8643
13	0.3670	0.4587	0.0609	0.0128	0.0036	0.5818	0.0096	0.0668	0.2000	2.2656	0.4350	0.1051	0.0492	0.0250	2.7497	0.4816	0.8643
14	0.3670	0.1716	0.0609	0.0128	0.0036	0.5818	0.0096	0.0668	0.2000	1.9278	0.1930	0.1051	0.0323	0.0250	2.7497	0.4816	0.8643
15	0.3670	0.8829	0.0609	0.0128	0.0036	0.5818	0.0096	0.0668	0.2000	2.1555	0.2542	0.1051	0.0679	0.0250	2.7497	1.6050	0.8643
16	0.3670	0.4849	0.0609	0.0128	0.0036	0.5818	0.0096	0.0668	0.2000	1.9053	0.1216	0.1051	0.0479	0.0250	2.7497	0.4816	0.8643
17	0.3670	0.7141	0.0609	0.0128	0.0036	0.5818	0.0096	0.0668	0.2000	2.6283	0.7023	0.1051	0.0629	0.0250	2.7497	2.9532	0.8643
18	0.3670	0.6585	0.0609	0.0128	0.0036	0.5818	0.0096	0.0668	0.2000	2.6898	0.7322	0.1051	0.0587	0.0250	2.7497	0.4816	0.8643
19	0.3670	0.3999	0.0609	0.0128	0.0036	0.5818	0.0096	0.0668	0.2000	2.3352	0.4832	0.1051	0.0477	0.0250	2.7497	0.4816	0.8643
20	0.3670	0.4959	0.0609	0.0128	0.0036	0.5818	0.0096	0.0668	0.2000	2.2427	0.3496	0.1051	0.0504	0.0250	2.7497	0.4816	0.8643
21	0.7999	0.9318	0.0418	0.0227	0.0008	0.8359	0.0095	0.0001	0.2500	1.8274	1.5050	0.6000	0.0743	0.2000	-0.0077	0.1419	0.1140
22	0.7999	0.9776	0.0418	0.0227	0.0008	0.8359	0.0095	0.0001	0.2500	2.2217	1.8886	0.6000	0.0690	0.2000	-0.0077	-0.8691	0.1140

Table 8. Selected monthly parameter and coefficient values for calculations for the Fena Valley watersheds and Ugum watershed in the PRMS_2016 model.

[Parameter definitions are shown in table 4]

Month	ADJUST_RAIN	DDAY_INTCP	DDAY_SLOPE	JH_COEF
Maulap				
January	-0.116	-55.049	0.336	0.014
February	-0.116	-55.049	0.621	0.009
March	-0.116	-55.049	0.612	0.010
April	-0.116	-55.049	0.605	0.010
May	-0.116	-55.049	0.476	0.012
June	-0.116	-55.049	0.558	0.009
July	-0.116	-55.049	0.347	0.010
August	-0.116	-55.049	0.322	0.007
September	-0.116	-55.049	0.461	0.012
October	-0.116	-55.049	0.587	0.010
November	-0.116	-55.049	0.424	0.010
December	-0.116	-55.049	0.611	0.010
Almagosa				
January	0.177	-50.169	0.776	0.007
February	0.177	-50.169	0.667	0.009
March	0.177	-50.169	0.583	0.011
April	0.177	-50.169	0.566	0.009
May	0.177	-50.169	0.455	0.010
June	0.177	-50.169	0.436	0.010
July	0.177	-50.169	0.447	0.010
August	0.177	-50.169	0.468	0.009
September	0.177	-50.169	0.575	0.008
October	0.177	-50.169	0.571	0.010
November	0.177	-50.169	0.701	0.007
December	0.177	-50.169	0.720	0.008
Imong				
January	-0.008	-57.134	0.405	0.017
February	-0.008	-57.134	0.555	0.015
March	-0.008	-57.134	0.243	0.012
April	-0.008	-57.134	0.536	0.013
May	-0.008	-57.134	0.360	0.013
June	-0.008	-57.134	0.491	0.009
Imong—Continued				
July	-0.008	-57.134	0.550	0.009
August	-0.008	-57.134	0.522	0.010
September	-0.008	-57.134	0.368	0.012
October	-0.008	-57.134	0.547	0.011
November	-0.008	-57.134	0.452	0.010
December	-0.008	-57.134	0.417	0.015
Ungaged				
January	-0.116	-55.049	0.336	0.014
February	-0.116	-55.049	0.621	0.009
March	-0.116	-55.049	0.612	0.010
April	-0.116	-55.049	0.605	0.010
May	-0.116	-55.049	0.476	0.012
June	-0.116	-55.049	0.558	0.009
July	-0.116	-55.049	0.347	0.010
August	-0.116	-55.049	0.322	0.007
September	-0.116	-55.049	0.461	0.012
October	-0.116	-55.049	0.587	0.010
November	-0.116	-55.049	0.424	0.010
December	-0.116	-55.049	0.611	0.010
Ugum				
January	-0.101	-57.014	0.360	0.011
February	-0.101	-57.014	0.531	0.015
March	-0.101	-57.014	0.648	0.008
April	-0.101	-57.014	0.633	0.010
May	-0.101	-57.014	0.469	0.014
June	-0.101	-57.014	0.444	0.008
July	-0.101	-57.014	0.570	0.009
August	-0.101	-57.014	0.421	0.007
September	-0.101	-57.014	0.613	0.013
October	-0.101	-57.014	0.458	0.010
November	-0.101	-57.014	0.565	0.014
December	-0.101	-57.014	0.464	0.010

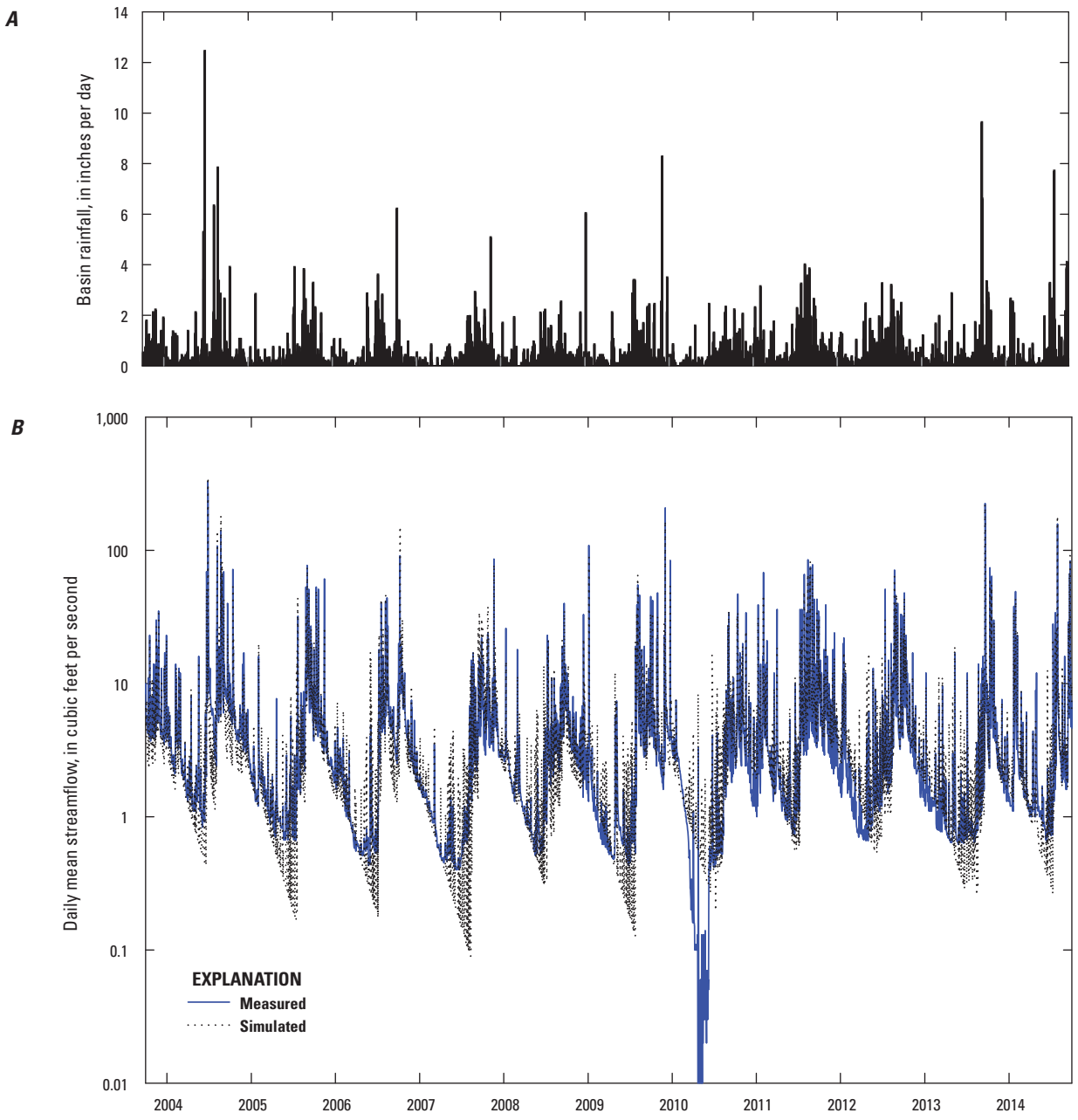

Figure 18. *A*, Simulated basin rainfall for the calibration period, Maulap River watershed, Guam, from October 1, 2003 to September 30, 2014. *B*, Measured and simulated daily streamflow for the calibration period, Maulap River watershed, Guam, from October 1, 2003 to September 30, 2014.

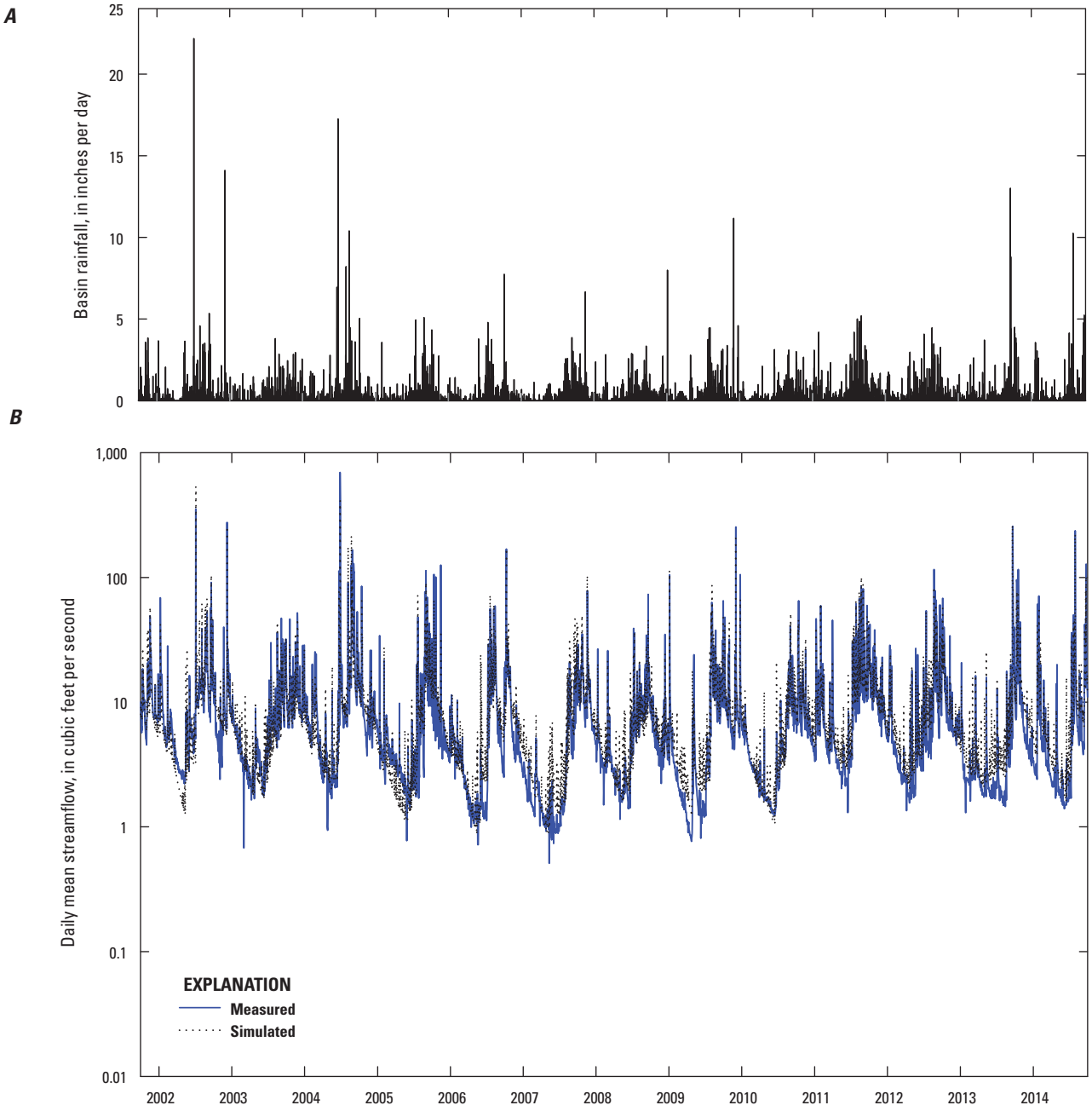

Figure 19. *A*. Simulated basin rainfall for the calibration period, Almagosa River watershed, Guam, from October 1, 2001 to September 30, 2014. *B*. Measured and simulated daily streamflow for the calibration period, Almagosa River watershed, Guam, from October 1, 2001 to September 30, 2014.

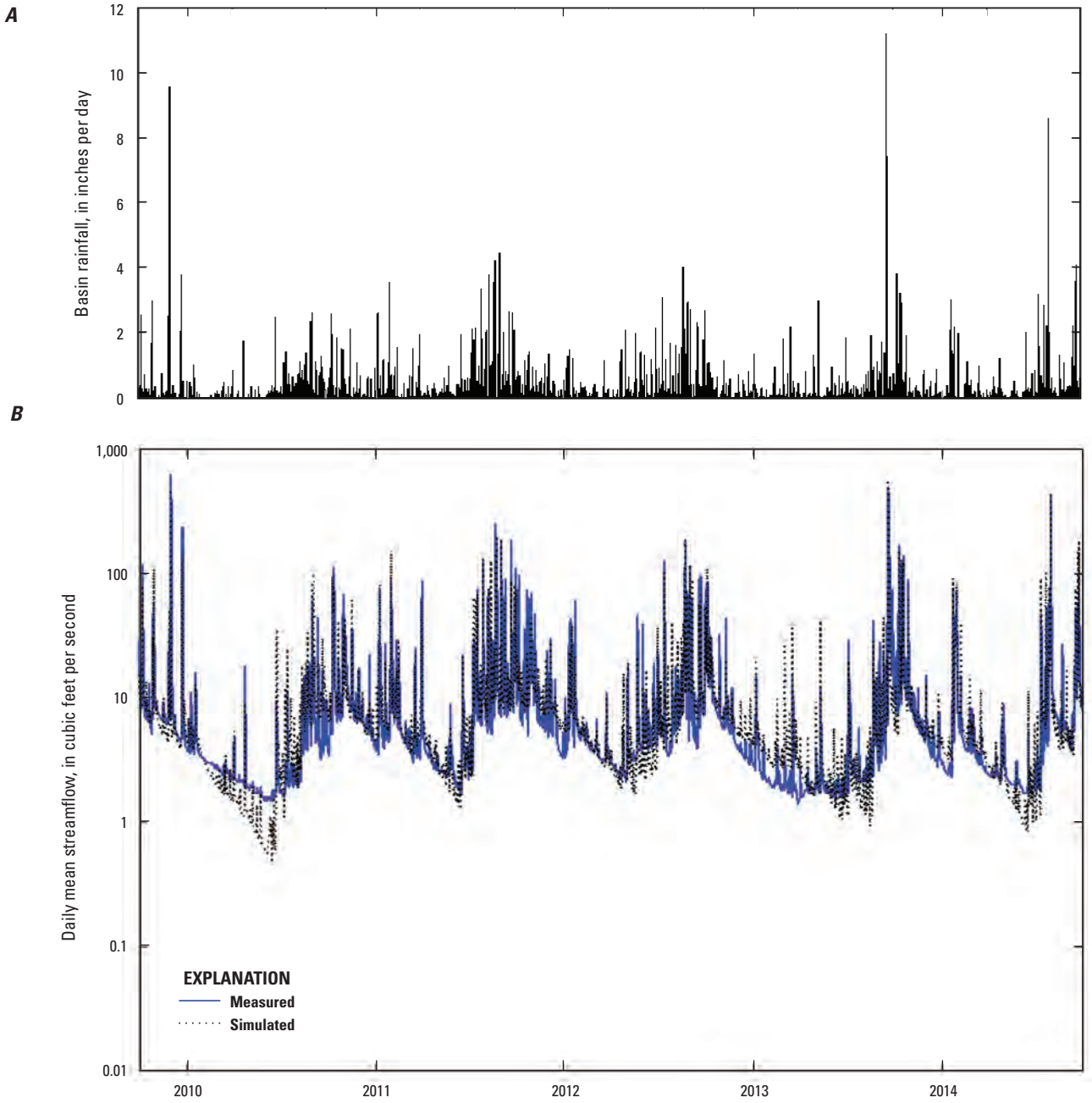

Figure 20. *A*, Simulated basin rainfall for the calibration period, Imong River watershed, Guam, from October 1, 2009 to September 30, 2014. *B*, Measured and simulated daily streamflow for the calibration period, Imong River watershed, Guam, from October 1, 2009 to September 30, 2014.

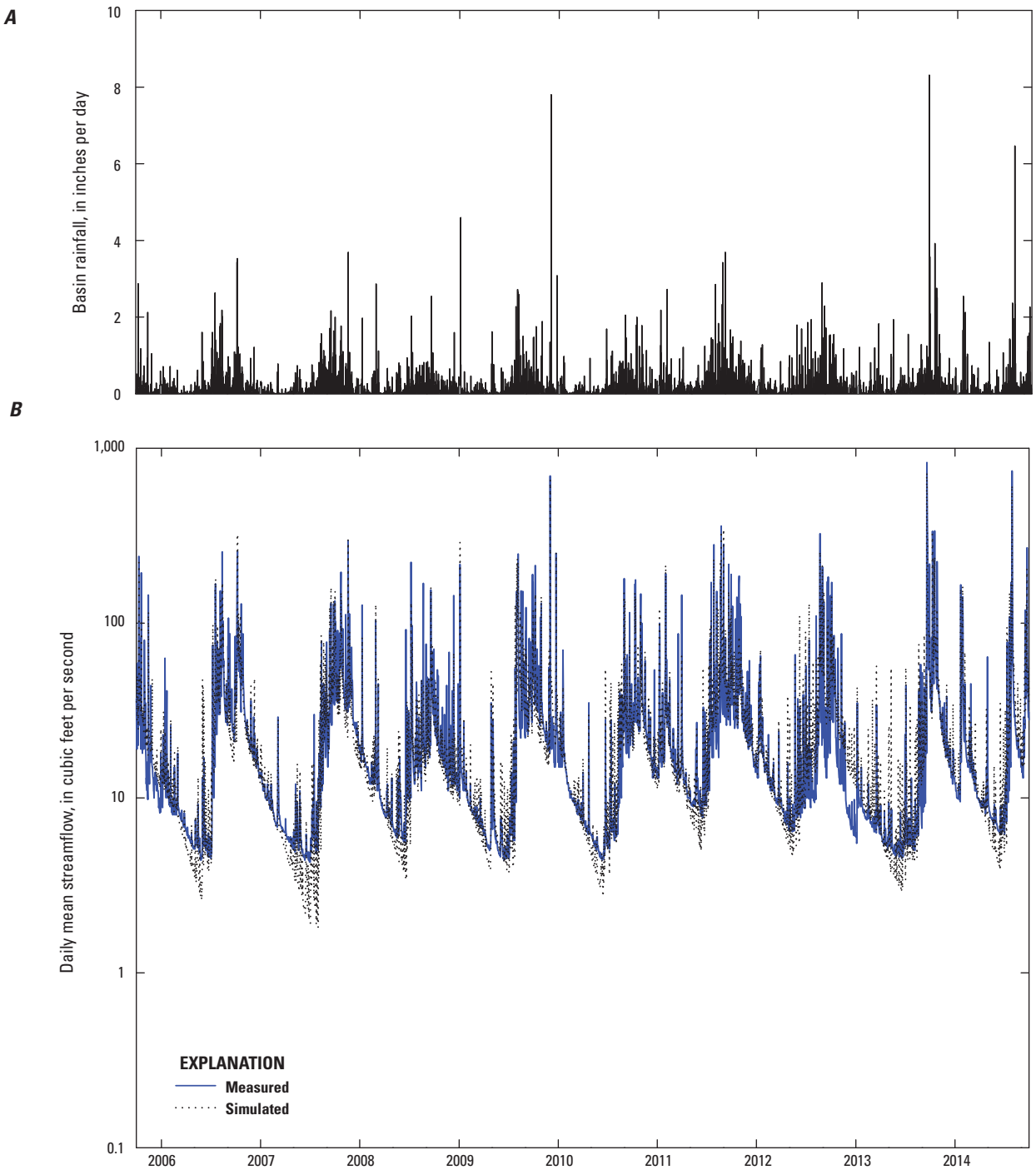

Figure 21. *A*, Simulated basin rainfall for the calibration period, Ugum River above Talofofo Falls, Guam, from October 1, 2005 to September 30, 2014. *B*, Measured and simulated daily streamflow for the calibration period, Ugum River above Talofofo Falls, Guam, from October 1, 2005 to September 30, 2014.

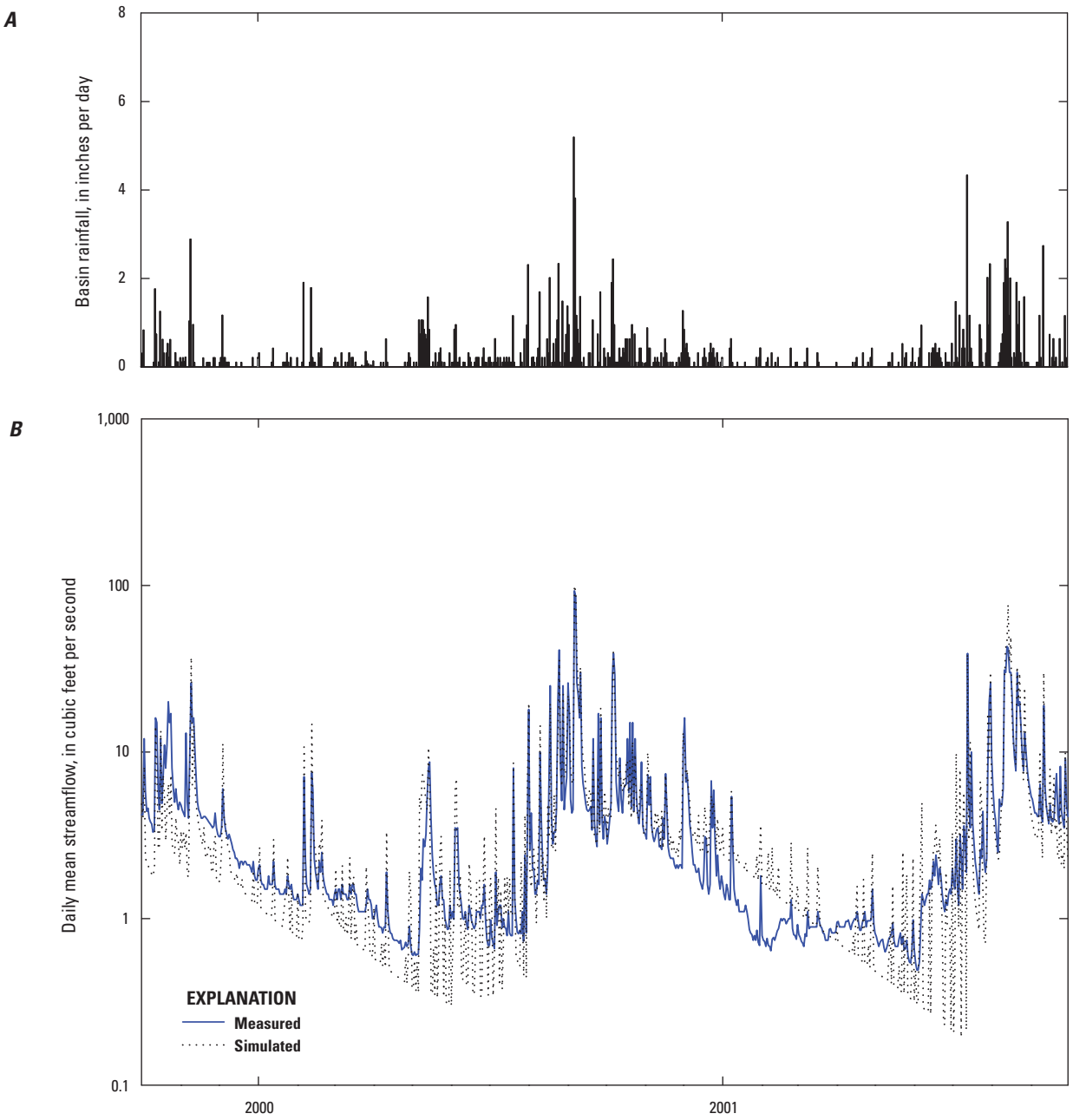

Figure 22. *A*, Simulated basin rainfall for the verification period, Maulap River watershed, Guam, from October 1, 1999 to September 30, 2001. *B*, Measured and simulated daily streamflow for the verification period, Maulap River watershed, Guam, from October 1, 1999 to September 30, 2001.

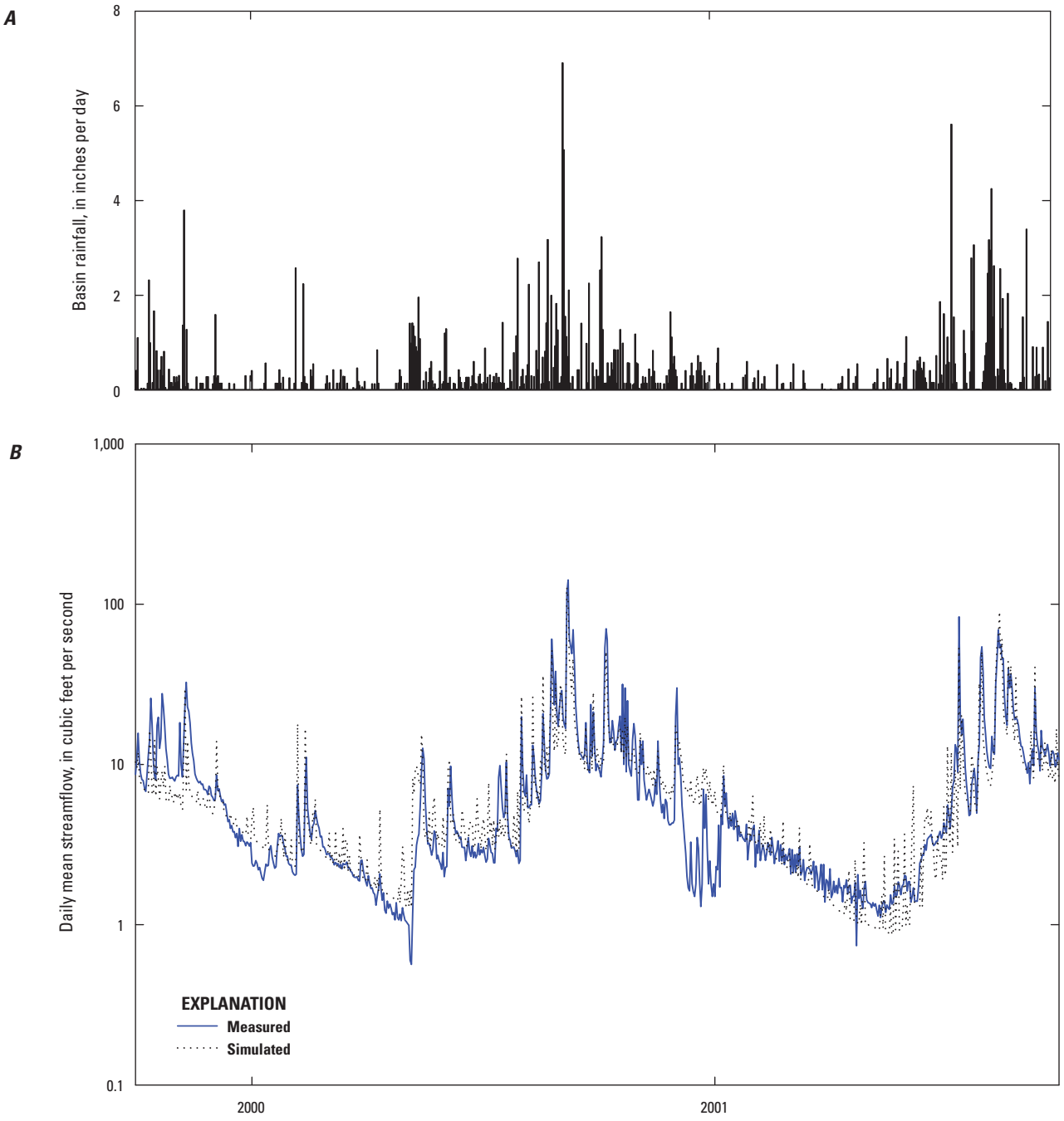

Figure 23. *A*, Simulated basin rainfall for the verification period, Almagosa River watershed, Guam, from October 1, 1999 to September 30, 2001. *B*, Measured and simulated daily streamflow for the verification period, Almagosa River watershed, Guam, from October 1, 1999 to September 30, 2001.

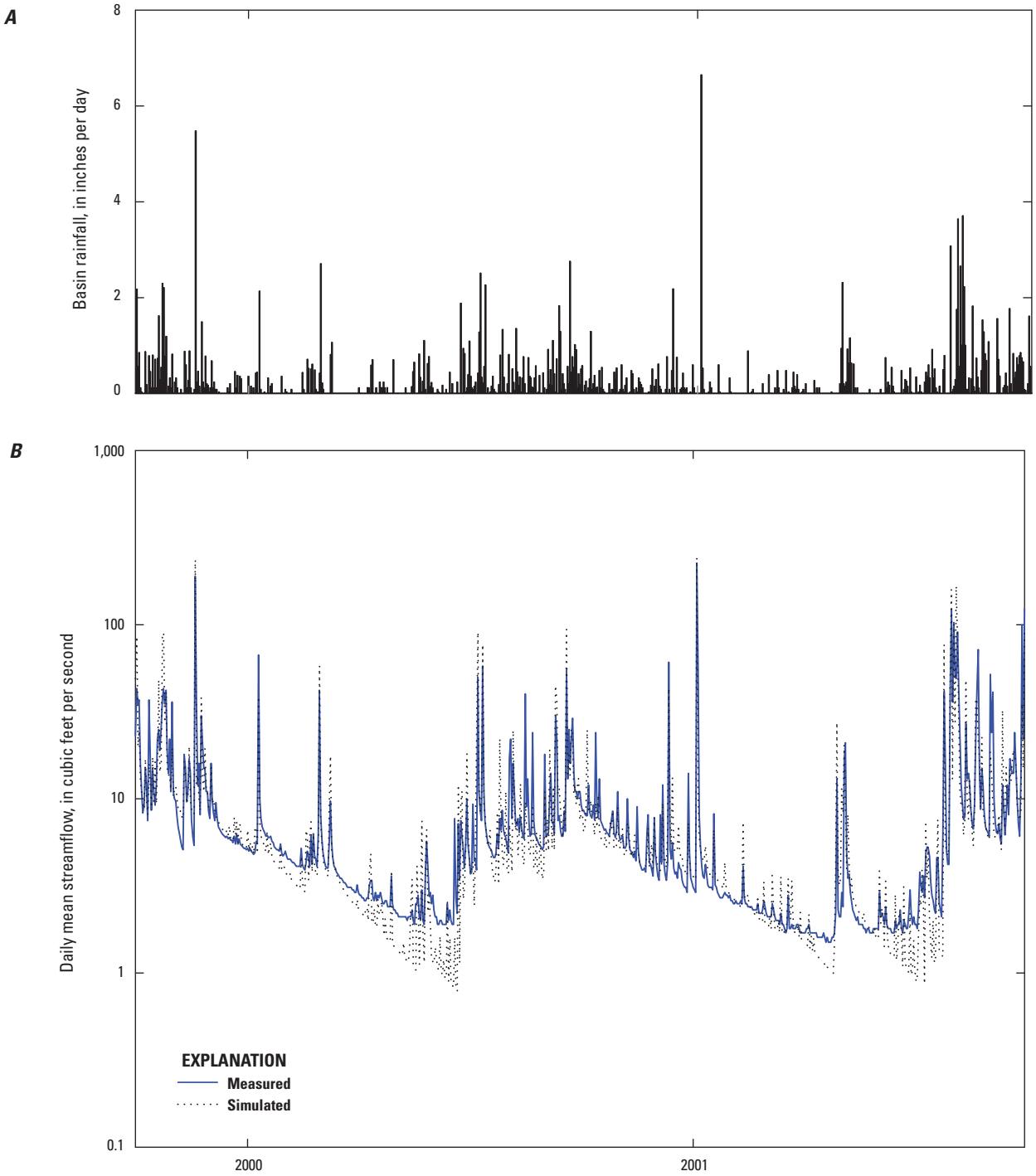

Figure 24. *A*. Simulated basin rainfall for the verification period, Imong River watershed, Guam, from October 1, 2007 to September 30, 2009. *B*. Measured and simulated daily streamflow for the verification period, Imong River watershed, Guam, from October 1, 2007 to September 30, 2009.

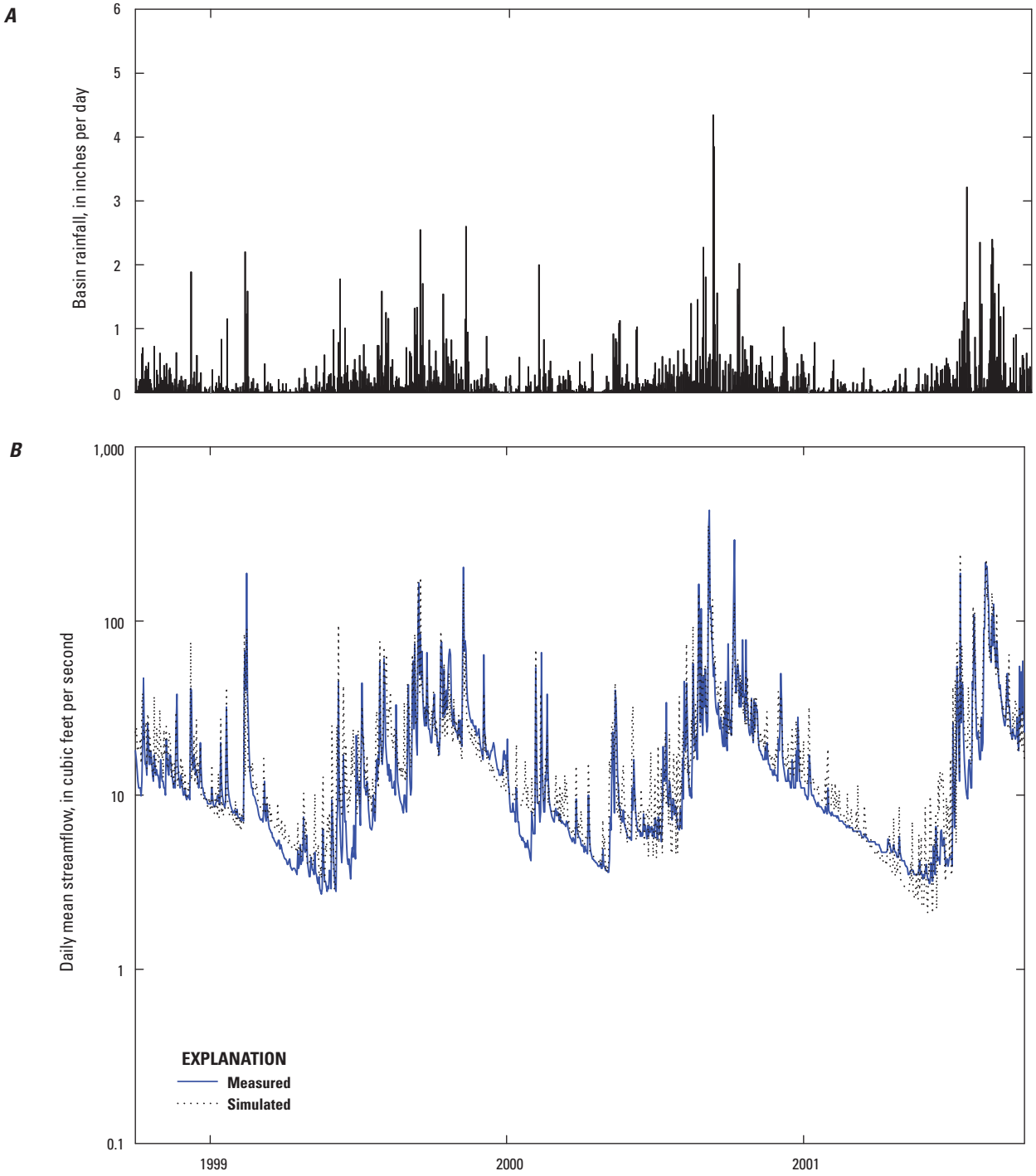

Figure 25. *A*. Simulated basin rainfall for the verification period, Ugum River above Talofofo Falls, Guam, from October 1, 1998 to September 30, 2001. *B*. Measured and simulated daily streamflow for the verification period, Ugum River above Talofofo Falls, Guam, from October 1, 1998 to September 30, 2001.

Statistical summaries of the accuracy of simulated daily and monthly mean streamflow for the calibration and verification periods are shown in tables 9 and 10. Models were evaluated using the Nash-Sutcliffe model efficiency index (NSE; Nash and Sutcliffe [1970]) and the model bias (P_{bias}, expressed as a percentage) equations below (the terms used in equations 4 and 5 were previously defined for equation 3):

$$NSE = 1.0 - \frac{\sum_{n=1}^{nstep}\left(MSD_n - SIM_n\right)^2}{\sum_{n=1}^{nstep}\left(MSD_n - MN\right)^2} \text{ , and} \qquad (4)$$

$$P_{bias} = \frac{\sum_{n=1}^{n_{step}}\left(SIM_n - MSD_n\right)}{\sum_{n=1}^{n_{step}}\left(MSD_n\right)} \times 100 , \qquad (5)$$

The NSE statistic or coefficient of efficiency was examined as a measure of the overall quality of model fit, with a value of 1 representing a perfect fit between the measured and simulated data. A value of 0 indicates that using the average value of all of measured data is as good as the model. A negative NSE statistic indicates that the average value of all of the measured data provides a better fit than the simulated model results. The coefficient of efficiency is a widely used relative measure of a model's predictive power (Markstrom and others, 2008). Model bias was calculated to determine whether the model consistently overestimated or underestimated streamflow. A bias of 0 indicates that the model does not have a tendency to either overestimate or underestimate streamflow. A positive value indicates a tendency to overestimate streamflow, whereas a negative value indicates a tendency to underestimate streamflow. Monthly model simulations with a coefficient of efficiency equal to or greater than 0.5 and a bias between +25 and –25 percent are commonly rated as having a satisfactory performance. Monthly model simulations with a coefficient of efficiency greater than 0.65 and a bias between +15 and –15 percent are commonly rated as having a good performance. Finally, monthly model simulations with a coefficient of efficiency greater than 0.75 and a bias between +10 and –10 percent are commonly rated as having a very good performance (Moriasi and others, 2007).

The coefficient of efficiency based on simulated and measured daily streamflows in the PRMS_2016 model ranges from 0.28 to 0.90 for the calibration period and from 0.26 to 0.99 for the verification period (table 9). These values indicate that the PRMS_2016 model provides a better estimate of daily streamflow than the mean measured value of streamflow for each of the 18 watersheds that were used in the calibration. The bias in the PRMS_2016 model ranges from –16.71 to 4.99 percent for the calibration period and from –17.81 to 38.06 percent for the verification period (table 9). The model generally is expected to perform better in the calibration period than in the verification period because the model parameter values are optimized for the calibration period. In this study, the most heavily weighted calibration target of the PRMS_2016 model was the simulation of monthly flows (table 6). Model-evaluation statistics calculated using monthly values (determined from aggregated daily values) generally indicate better performance than statistics calculated using the daily values. The statistics from the daily models are rated (table 9) according to the same statistical ranges provided by Moriasi and others (2007) for monthly model-evaluation statistics. The monthly coefficient of efficiency in the PRMS_2016 model ranges from 0.62 to 0.98 for the calibration period and from 0.70 to 0.98 for the verification period (table 10). These values indicate that the PRMS_2016 model provides a better estimate of monthly streamflow than the mean monthly measured value of streamflow for each of the 18 watersheds that were used in the calibration process. The bias in the PRMS_2016 model for monthly values ranges from –16.71 to 5.73 percent for the calibration period and from –17.81 to 38.06 percent for the verification period (table 10). According to the criteria of Moriasi and others (2007), the PRMS_2016 model has a "satisfactory" to "very good" rating for all but two of the gaged watersheds during the verification period, the Talofofo (16850000) and Lonfit (16862000) watersheds (table 10). The verification periods for both of these watersheds rely on temperature and rainfall data from the only available climate station during 1953–56, the Fena Filter Plant (fig. 1, table 1). The verification period for the Tolaeyuus near Agat (16845000) watershed, which has a good rating, also uses data from this climate station as input to the model. However, the Tolaeyuus stream gage is located in closer proximity to the Fena Filter Plant station, and therefore the better model performance for the Tolaeyuus gaging station is expected.

The accuracy of monthly simulation results is especially important because the FVR water-balance model is run using a monthly time step with monthly streamflow totals from the Fena Valley watersheds as input. The following discussion of the accuracy of model simulations is therefore focused primarily on monthly results for the Fena Valley watershed. PRMS_2016 simulated streamflow volume on a monthly scale for all three gaged Fena Valley watersheds reasonably well. The monthly coefficient of efficiency for both the calibration and verification periods was greater than 0.87 for all three watersheds. Bias for the calibration and verification periods ranged from underestimating flow by 6.96 percent in the Almagosa River watershed to overestimating flow by 0.60 percent in the Maulap River watershed. Overall, simulation errors were greatest in the Almagosa River watershed, most likely due to the added complexity of the closed depression area simulations and the reconstructed streamflow record to account for the diversion at the Almagosa Springs. Simulation errors for the Imong River watershed were the smallest of all three watersheds. A summary of measured and simulated streamflow volumes for each simulation period (table 11) indicates that the cumulative streamflow volume for the Almagosa River watershed was underestimated by 6.96 percent for the verification period, whereas the Maulap watershed was within 0.57 percent for the same period. The model calculated total

Table 9. Errors in simulated daily mean streamflow for gaged watersheds used to calibrate the PRMS_2016 model.

[abv, above; nr, near; –, not applied to any region]

USGS stream gaging station	Calibration				Verification				Region model calibration applied[2]
	Period	Coefficient of efficiency	Bias (percent)	Performance rating[1]	Period	Coefficient of efficiency	Bias (percent)	Performance rating[1]	
16807650 (Aplacho)	10/1/2007–9/30/2009	0.28	–5.30	Unsatisfactory	10/1/2009–9/30/2011	0.80	0.04	Very good	A
16808300 (Finile)	10/1/1976–9/30/1982	0.44	1.19	Unsatisfactory	10/1/1962–9/30/1976	0.59	–0.36	Satisfactory	D
16809400 (Cetti)	10/1/1964–9/30/1966	0.70	–1.29	Good	10/1/1961–9/30/1964	0.26	–3.25	Unsatisfactory	–
16809600 (La Sa Fua)	10/1/2007–9/30/2013	0.89	0.56	Very good	10/1/2001–9/30/2007	0.82	–14.04	Good	G
16816000 (Umatac)	10/1/2004–9/30/2010	0.83	–16.71	Satisfactory	10/1/2010–9/30/2011	0.39	1.49	Unsatisfactory	–
16821000 (Geus)	10/1/1971–9/30/1974	0.41	–2.17	Unsatisfactory	10/1/1974–9/30/1975	0.34	8.65	Unsatisfactory	–
16835000 (Inarajan)	10/1/1972–9/30/1982	0.64	2.34	Satisfactory	10/1/1970–9/30/1972	0.55	–17.81	Satisfactory	–
16840000 (Tinaga)	10/1/1975–9/30/1985	0.74	0.01	Good	10/1/1965–9/30/1971	0.52	0.74	Satisfactory	H
16845000 (Tolaeyuus nr Agat)	10/1/1956–9/30/1959	0.57	–16.01	Satisfactory	10/1/1954–9/30/1956	0.99	–13.75	Good	–
16847000 (Imong)	10/1/2009–9/30/2014	0.88	0.34	Very good	10/1/2007–9/30/2009	0.72	–0.43	Good	Imong
16848100 (Almagosa)	10/1/2001–9/30/2014	0.75	–0.67	Very good	10/1/1999–9/30/2001	0.82	–6.96	Very good	Almagosa
16848500 (Maulap)	10/1/2003–9/30/2014	0.83	0.60	Very good	10/1/1999–9/30/2001	0.87	0.57	Very good	Maulap
16850000 (Talofofo)	10/1/1957–9/30/1961	0.51	4.99	Satisfactory	10/1/1953–9/30/1957	0.72	35.19	Unsatisfactory	E
16854500 (Ugum abv Talofofo Falls)	10/1/2005–9/30/2014	0.87	0.84	Very good	10/1/1998–9/30/2001	0.79	7.37	Very good	F
16855000 (Ugum nr Talofofo)	10/1/1961–9/30/1969	0.58	1.27	Satisfactory	10/1/1969–9/30/1970	0.46	–17.27	Unsatisfactory	–
16858000 (Ylig)	10/1/1999–9/30/2001	0.90	–0.25	Very good	4/1/1998–9/30/1999	0.68	–15.33	Good	C
16862000 (Lonfit)	10/1/1956–9/30/1959	0.72	2.43	Good	10/1/1954–9/30/1956	0.61	38.06	Unsatisfactory	–
16865000 (Pago)	10/1/2008–9/30/2014	0.85	0.55	Very good	10/1/2006–9/30/2008	0.82	1.19	Very good	B

[1]Performance ratings as described by Moriasi and others, 2007.

[2]Regions are shown in figure 26.

Table 10. Errors in simulated monthly mean streamflow for gaged watersheds used to calibrate the PRMS_2016 model.

[abv, above; nr, near; –, not applied to any region]

USGS stream gaging station	Calibration				Verification				Region model calibration applied[2]
	Period	Coefficient of efficiency	Bias (percent)	Performance rating[1]	Period	Coefficient of efficiency	Bias (percent)	Performance rating[1]	
16807650 (Aplacho)	10/1/2007–9/30/2009	0.62	–0.65	Satisfactory	10/1/2009–9/30/2011	0.78	0.04	Very good	A
16808300 (Finile)	10/1/1976–9/30/1982	0.84	1.19	Very good	10/1/1962–9/30/1976	0.80	–0.36	Very good	D
16809400 (Cetti)	10/1/1964–9/30/1966	0.86	–1.29	Very good	10/1/1961–9/30/1964	0.70	–3.25	Good	–
16809600 (La Sa Fua)	10/1/2007–9/30/2013	0.95	0.56	Very good	10/1/2001–9/30/2007	0.92	–14.04	Good	G
16816000 (Umatac)	10/1/2004–9/30/2010	0.89	–16.71	Satisfactory	10/1/2010–9/30/2011	0.79	1.49	Very good	–
16821000 (Geus)	10/1/1971–9/30/1974	0.71	–2.17	Good	10/1/1974–9/30/1975	0.90	8.65	Very good	–
16835000 (Inarajan)	10/1/1972–9/30/1982	0.90	2.34	Very good	10/1/1970–9/30/1972	0.73	–17.81	Satisfactory	–
16840000 (Tinaga)	10/1/1975–9/30/1985	0.93	0.01	Very good	10/1/1965–9/30/1971	0.85	0.74	Very good	H
16845000 (Tolaeyuus nr Agat)	10/1/1956–9/30/1959	0.84	–16.01	Satisfactory	10/1/1954–9/30/1956	0.72	–13.75	Good	–
16847000 (Imong)	10/1/2009–9/30/2014	0.94	0.50	Very good	10/1/2007–9/30/2009	0.94	–0.43	Very good	Imong
16848100 (Almagosa)	10/1/2001–9/30/2014	0.87	–0.67	Very good	10/1/1999–9/30/2001	0.92	–6.96	Very good	Almagosa
16848500 (Maulap)	10/1/2003–9/30/2014	0.92	0.60	Very good	10/1/1999–9/30/2001	0.94	0.57	Very good	Maulap
16850000 (Talofofo)	10/1/1957–9/30/1961	0.80	5.73	Very good	10/1/1953–9/30/1957	0.84	35.19	Unsatisfactory	E
16854500 (Ugum abv Talofofo Falls)	10/1/2005–9/30/2014	0.97	0.84	Very good	10/1/1998–9/30/2001	0.93	7.37	Very good	F
16855000 (Ugum nr Talofofo)	10/1/1961–9/30/1969	0.87	1.27	Very good	10/1/1969–9/30/1970	0.75	–17.27	Satisfactory	–
16858000 (Ylig)	10/1/1999–9/30/2001	0.98	–0.25	Very good	4/1/1998–9/30/1999	0.87	–15.33	Good	C
16862000 (Lonfit)	10/1/1956–9/30/1959	0.94	2.43	Very good	10/1/1954–9/30/1956	0.75	38.06	Unsatisfactory	–
16865000 (Pago)	10/1/2008–9/30/2014	0.93	–0.28	Very good	10/1/2006–9/30/2008	0.98	0.02	Very good	B

[1]Performance ratings as described by Moriasi and others, 2007.

[2]Regions are shown in figure 26.

streamflow volume for the Maulap, Almagosa, and Imong River watersheds within 0.60, –1.43, and 0.27 percent of measured values, respectively, over the entire simulation period.

Of particular interest are the monthly dry-season flows for the Fena Valley watersheds. Measured and simulated monthly mean streamflow for the dry season (January to June) for months during which concurrent data are available for the three Fena Valley gaged watersheds are summarized in table 12. Months with estimated values of streamflow in the measured record were not included in the analysis. The differences between measured and simulated monthly mean streamflow for the Maulap River watershed ranged from –38.1 percent (May 2014) to 91.7 percent (March 2012) in the calibration period and from –22.0 percent (January 2000) to 81.6 percent (January 2001) in the verification period. For the Almagosa River watershed, the differences ranged from –18.9 (January 2014) to 48.0 percent (April 2012) in the calibration period and from –15.2 (April 2001) to 45.5 percent (May 2000) in the verification period. For the Imong River watershed, the differences ranged from –47.3 percent (May 2010) to 135.6 percent (March 2013) in the calibration period and from –18.8 percent (January 2008) to 17.8 percent (May 2009) in the verification period.

Table 11. Summary of measured and simulated cumulative streamflow for the gaged watersheds in the Fena Valley watershed, Guam.

Period	Measured[1] (inches)	Simulated[1] (inches)	Percentage difference[2]
Maulap River watershed			
Calibration (10/1/2003–9/30/2014)	604.90	608.56	0.61
Verification (10/1/1999–9/30/2001)	93.05	93.58	0.57
Entire period	**697.95**	**702.14**	**0.60**
Almagosa River watershed			
Calibration (10/1/2001–9/30/2014)	836.84	831.27	–0.67
Verification (10/1/1999–9/30/2001)	115.84	107.78	–6.96
Entire period	**952.68**	**939.05**	**–1.43**
Imong River watershed			
Calibration (10/1/2009–9/30/2014)	365.73	367.57	0.50
Verification (10/1/2007–9/30/2009)	121.19	120.66	–0.44
Entire period	**486.92**	**488.23**	**0.27**

[1]Cumulative streamflow depth= total volume of streamflow/area of watershed

[2]Percentage difference = 100 x (simulated - measured)/measured

The large over-estimation error during March 2013 for the Imong River watershed is probably related to error in the rainfall estimate. Rainfall input to the model is estimated using the inverse distance and elevation module in PRMS-IV with data collected from Fena pump and Almagosa rain gages. During March 2013, the rainfall distribution from these gages probably overestimated rainfall in the Imong River watershed located farther south. Measured rainfall records at the Almagosa and Fena rain gages indicated a localized storm occurred in the northern part of the study area in March 2013. Monthly total rainfall for March 2013 at the Fena pump and Almagosa rain gages averaged about 7.4 in.; farther to the south, the Umatac rain gage received only about 4.6 in.

Total measured and simulated streamflow volumes during the dry seasons for each simulation period are summarized in table 13. The PRMS_2016 model simulated the total volume of dry season streamflow for the entire simulation period at Almagosa River watershed within 0.54 percent of the measured volume. Simulation errors for the Maulap and Imong River watersheds were higher at 6.39 and 6.06 percent, but were still within the limit of the accuracy of the measured streamflow record. Over-simulation rates (number of over-estimated months divided by the total number of monthly simulations) for all three watersheds were close to 50 percent, which indicated that the positive and negative errors were distributed evenly.

Table 12. Summary of measured and simulated dry season monthly mean discharge and associated error for the gaged watersheds in the Fena Valley watershed, Guam.

[ft^3/s, cubic feet per second; percentage difference = 100 x (simulated - measured)/measured; gray shading, months that include estimated measured data; n/a, not available]

Month	Maulap watershed			Almagosa watershed			Imong watershed		
	Monthly mean discharge			Monthly mean discharge			Monthly mean discharge		
	Simulated ft^3/s	Measured ft^3/s	Percentage difference	Simulated ft^3/s	Measured ft^3/s	Percentage difference	Simulated ft^3/s	Measured ft^3/s	Percentage difference
Calibration period									
2010									
January	2.91	3.17	–8.3	6.91	5.81	18.8	4.84	4.93	–1.9
February	1.43	1.62	–11.9	3.74	3.35	11.7	2.57	2.99	–13.9
March	1.15	0.55	109.9	2.58	2.56	1.0	1.94	2.53	–23.5
April	1.09	0.27	308.6	2.35	2.11	11.3	1.79	2.75	–34.9
May	0.55	0.04	1,259.0	1.60	1.56	2.4	0.94	1.78	–47.3
2011									
January	6.51	5.85	11.2	10.59	9.90	7.0	12.58	11.07	13.6
February	6.54	7.62	–14.2	10.85	11.34	–4.4	12.98	11.62	11.7
March	2.95	2.79	5.6	5.91	4.84	22.3	6.17	5.00	23.5
April	2.92	3.08	–5.0	5.46	6.29	–13.2	6.43	6.55	–1.9
May	1.93	1.35	42.9	4.23	2.87	47.3	2.74	3.01	–8.8
2012									
January	5.38	4.93	9.3	9.11	9.95	–8.5	9.57	11.92	–19.7
February	2.63	1.60	64.7	5.14	3.63	41.5	4.73	4.54	4.3
March	1.95	1.02	91.7	3.67	2.72	34.9	3.71	3.78	–2.0
April	1.69	0.90	88.0	3.12	2.11	48.0	2.99	2.70	10.5
May	2.29	1.69	35.2	4.72	4.24	11.5	4.11	5.72	–28.2
2013									
January	2.53	1.79	41.6	4.86	4.36	11.4	4.96	3.29	50.7
February	1.69	1.20	40.3	3.39	2.57	32.2	3.44	2.10	63.8
March	2.28	1.67	36.1	4.31	3.61	19.4	5.65	2.40	135.6
April	1.07	0.79	36.0	2.75	2.13	28.9	2.29	1.84	24.8
May	1.82	1.54	18.4	4.04	2.86	41.4	4.06	2.46	65.1
2014									
January	7.28	7.33	–0.7	11.49	14.18	–18.9	16.72	12.99	28.7
February	4.52	3.57	26.7	8.64	6.43	34.4	7.45	5.23	42.5
March	1.71	1.68	2.2	4.79	3.38	41.5	4.17	3.32	25.5
April	1.55	2.11	–26.5	3.68	3.41	7.9	2.95	2.85	3.4
May	0.77	1.24	–38.1	2.60	2.12	22.7	1.72	2.27	–24.1
Verification period									
2000									
January	1.23	1.57	–22.0	3.26	2.62	24.6	N/A	N/A	N/A
February	2.32	2.13	8.5	4.30	3.98	8.0	N/A	N/A	N/A
March	1.04	1.33	–21.8	2.56	2.29	11.8	N/A	N/A	N/A
April	0.72	0.86	–16.9	1.88	1.42	31.7	N/A	N/A	N/A
May	2.41	2.06	16.9	5.02	3.45	45.5	N/A	N/A	N/A

Table 12. Summary of measured and simulated dry season monthly mean discharge and associated error for the gaged watersheds in the Fena Valley watershed, Guam.

[ft³/s, cubic feet per second; percentage difference = 100 x (simulated - measured)/measured; gray shading, months that include estimated measured data; n/a, not available]

Month	Maulap watershed			Almagosa watershed			Imong watershed		
	Monthly mean discharge			Monthly mean discharge			Monthly mean discharge		
	Simulated ft³/s	Measured ft³/s	Percentage difference	Simulated ft³/s	Measured ft³/s	Percentage difference	Simulated ft³/s	Measured ft³/s	Percentage difference
Verification period—Continued									
2001									
January	2.40	1.32	81.6	4.74	3.98	18.9	N/A	N/A	N/A
February	1.54	0.85	80.9	3.04	2.91	4.4	N/A	N/A	N/A
March	1.03	0.85	22.3	1.95	2.21	-11.9	N/A	N/A	N/A
April	0.79	0.96	-17.7	1.39	1.64	-15.2	N/A	N/A	N/A
May	0.67	0.72	-6.9	1.31	1.43	-8.9	N/A	N/A	N/A
2008									
January	N/A	N/A	N/A	N/A	N/A	N/A	6.24	7.68	-18.8
February	N/A	N/A	N/A	N/A	N/A	N/A	5.95	5.87	1.4
March	N/A	N/A	N/A	N/A	N/A	N/A	4.18	4.12	1.5
April	N/A	N/A	N/A	N/A	N/A	N/A	2.23	2.74	-18.6
May	N/A	N/A	N/A	N/A	N/A	N/A	2.11	2.47	-14.4
2009									
January	N/A	N/A	N/A	N/A	N/A	N/A	11.82	12.39	-4.6
February	N/A	N/A	N/A	N/A	N/A	N/A	2.64	2.50	5.5
March	N/A	N/A	N/A	N/A	N/A	N/A	2.09	1.99	4.7
April	N/A	N/A	N/A	N/A	N/A	N/A	2.35	2.07	13.6
May	N/A	N/A	N/A	N/A	N/A	N/A	3.90	3.31	17.8

Table 13. Summary of measured and simulated dry season streamflow (January to May) for the gaged watersheds in the Fena Valley watershed, Guam.

Period	Measured[1] (inches)	Simulated[1] (inches)	Percentage difference[2]	Over-simulation rate[3] (percent)
Maulap River watershed				
Calibration (10/1/2003–9/30/2014)	106.18	112.36	5.82	54.5
Verification (10/1/1999–9/30/2001)	12.12	13.51	11.42	40.0
Entire period	**118.31**	**125.87**	**6.39**	**52.3**
Almagosa River watershed				
Calibration (10/1/2001–9/30/2014)	152.55	149.53	–1.98	58.5
Verification (10/1/1999–9/30/2001)	15.44	17.56	13.67	70.0
Entire period	**167.99**	**167.08**	**–0.54**	**60.0**
Imong River watershed				
Calibration (10/1/2009–9/30/2014)	70.01	76.86	9.78	56.0
Verification (10/1/2007–9/30/2009)	26.62	25.63	–3.71	60.0
Entire period	**96.63**	**102.49**	**6.06**	**57.1**

[1]Cumulative streamflow depth = total volume of streamflow/area of watershed

[2]Percentage difference = 100 x (simulated - measured)/measured

[3]Number of overestimated months divided by the total number of monthly simulations

For ungaged areas within each modeled region, model parameters were determined from a selected and representative gaged area with similar physical watershed characteristics within that region. The modeled regions, model stream segments, and the gaged drainage basins that were used to calibrate the PRMS_2016 model are shown in figure 26. The ungaged regions to which the parameters from each gaged model calibration were applied are listed in the last column in tables 9 and 10. The parameters for each of the FVR ungaged areas were derived from one of the nearby Fena Valley watershed gaged areas. Calibrated parameters from the gaged areas were transferred to the ungaged HRUs in closest proximity to the outlet of the gaged Fena Valley watershed areas (tables 7 and 8).

Model Uncertainties

PRMS-IV is a practical tool that makes it possible to simulate complex natural systems through sets of mathematical equations and empirical relations representing and approximating the major components of the hydrologic cycle and hydrologic processes involved. As a result of the assumptions and simplifications that must be made, error and uncertainty are built into the model. Even though the 317 HRUs in the PRMS_2016 model capture some of the heterogeneity of the watershed characteristics, these characteristics still must be simplified into these assumed homogenous units. Models in general are also limited by errors associated with the input data. The quality and accuracy of time-series data for rainfall, temperature, streamflow, diversion, SR, and PET impact the accuracy of the simulation results. Calibration and verification were done for a specific time period and range of streamflow and therefore it is uncertain how the PRMS_2016 model will perform under different conditions.

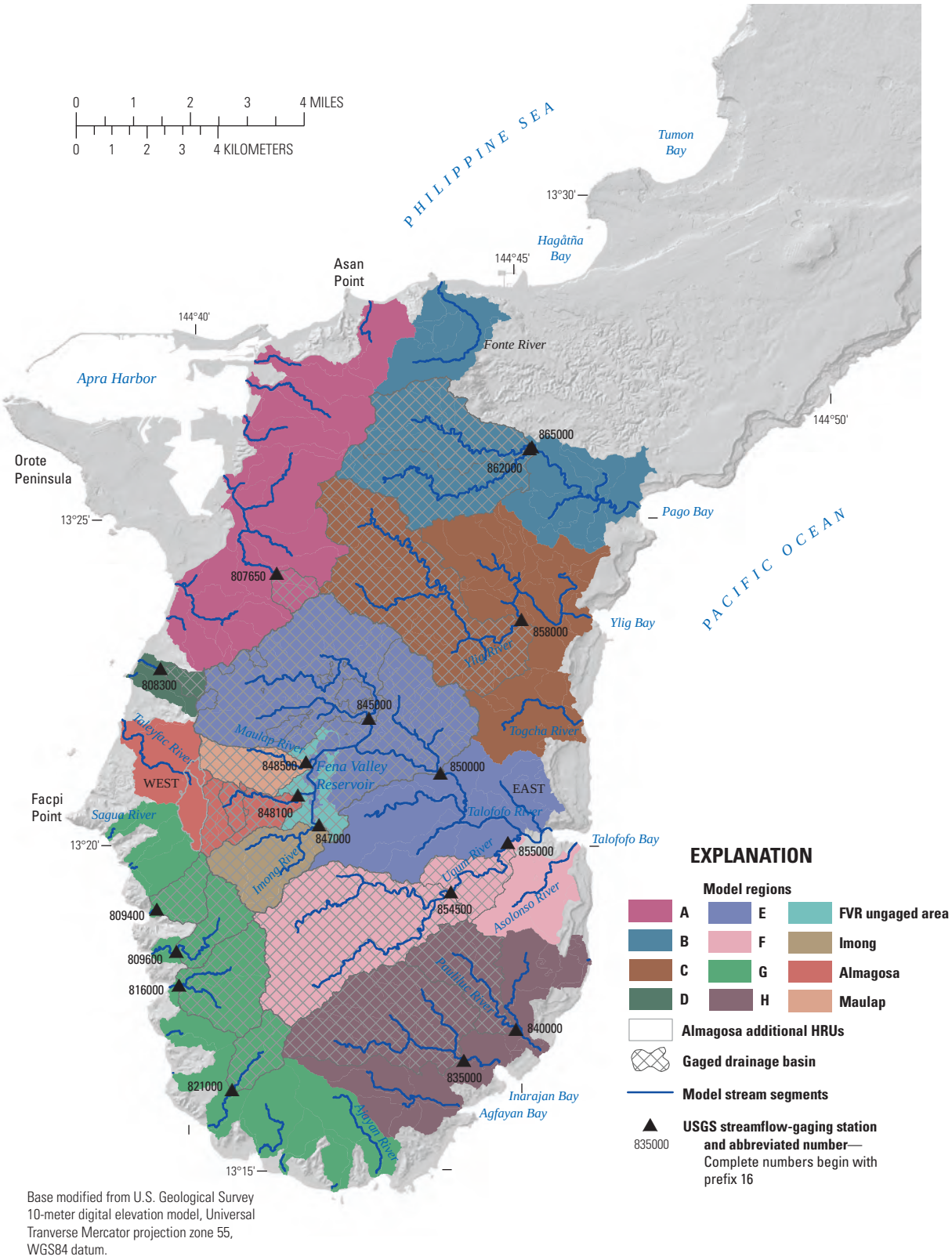

Base modified from U.S. Geological Survey 10-meter digital elevation model, Universal Tranverse Mercator projection zone 55, WGS84 datum.

Figure 26. Modeled regions, model stream segments, and gaged drainage-basin areas in the PRMS_2016 model. FVR, Fena Valley Reservoir; HRU, hydrologic response unit.

Comparison to Previous Fena Valley Reservoir Water Model

Many of the limitations identified in the PRMS_1994 model of the Fena Valley watershed developed by Nakama (1994) were addressed in the PRMS_2004 model developed by Yeung (2004). Yeung (2004) calibrated the Almagosa River watershed model and accounted for the diversion from the Almagosa Springs to reflect natural streamflow conditions necessary for model calibration and an area of limestone terrain outside of the topographically based divide for the Almagosa River watershed that contributes groundwater discharge to the watershed. Yeung (2004) improved the geographical representation of rainfall data and modeled the ungaged areas of the watershed to improve the estimation of total watershed streamflow draining into the FVR. Furthermore, the PRMS_2004 model included a period of three moderately strong to severe El Niño events, from 1990 to 2001, giving modeled examples of these important climate drivers.

As well as modeling all of southern Guam, PRMS_2016 contains a model of the Fena Valley watersheds that improved on the Fena Valley watershed (only) PRMS_2004 model. The new model considers the most recent hydrologic conditions in the watershed, including ENSO events (weak, moderate, and strong) in both the calibration and verification periods; it also used a longer period of data (1951–2015) to achieve a more representative model of each watershed. The PRMS_2016 model improved upon the simulated basin rainfall by using the inverse distance and elevation (ide_dist) distribution module instead of an arithmetic average of the Almagosa and Fena rain gages. A small improvement was made in PET calculation accuracy by calibrating to solar radiation data, whereas the PRMS_2004 model used possible hours of sunshine (Yeung, 2004). Lastly, closed depressions were included in the PRMS_2016 model to more appropriately address internally drained limestone areas near the headwaters of the Almagosa watershed that substantially add to the subsurface and groundwater flow measured at the outlet. These additional closed depression HRUs added 280 acres of contributing area to the Almagosa watershed (table 5).

The common verification periods of the Maulap and Almagosa watersheds were compared to evaluate the performances of the PRMS_2004 model and PRMS_2016 model of the Fena Valley watersheds. The PRMS_2016 model simulated cumulative streamflow in the Maulap basin more accurately than the PRMS_2004 model (0.57 percent difference compared to 8.2 percent difference). The PRMS_2004 model simulated cumulative streamflow more accurately in the Almagosa watershed (–2.9 percent difference compared to –6.96 percent difference). However, the PRMS_2016 model simulated dry season monthly mean streamflows more accurately in the Almagosa watershed and less accurately in the Maulap watershed. The discrepancies in the PRMS_2016 model performance for the Maualp and Almagosa watersheds may be due to the decreased number of HRUs in the Maualp watershed and inclusion of the closed depressions in the Almagosa watershed.

Although results of the PRMS_2004 and PRMS_2016 models were only directly compared for the Maulap and Almagosa watersheds, the average monthly coefficients of efficiency for the PRMS_2004 model and the coefficients of efficiency for the PRMS_2016 model provide another measure of comparison. In the PRMS_2004 model, the average monthly coefficients of efficiency for the Maulap, Almagosa, and Imong River watersheds' second verification period were 0.93, 0.96, and 0.88, respectively (table 9 in Yeung [2004]). In the PRMS_2016 model, the average monthly coefficients of efficiency for the Maulap, Almagosa, and Imong River watersheds' verification periods were 0.94, 0.92, and 0.94, respectively (table 10). Values for the PRMS_2016 model were higher for the Maulap and Imong watershed, but slightly lower for the Almagosa watershed.

Fena Valley Reservoir Water-Balance Model

This section describes the transformation of the FVR_2004 water-balance model from Yeung (2004) into the FVR_2016 model. The FVR_2016 model is not a redeveloped model structure, but instead the same model structure is used with updated reservoir stage-surface area and reservoir stage-storage capacity curves (Marineau and Wright, 2015), and the model is recalibrated. Yeung (2004) provides a detailed description of the water-balance model and development. The sections here describing the model and the model development are largely taken from that report.

Description of Model

The water-balance model developed for FVR simply accounts for the interactions between various forms of water going into and out of the reservoir over monthly intervals. Water levels above spillway crest level were not simulated because measured bathymetric information was available only up to spillway crest level and flow-over-spillway data were not available. Fennessey (1995) determined that a monthly time step provides accurate reservoir-yield estimates. The model is based upon a simple water-balance equation:

CHANGE IN STORAGE = GAGED STREAMFLOW
+ UNGAGED STREAMFLOW + RAINFALL -
WITHDRAWALS - EVAPORATION

The components of the reservoir water-balance model are shown in figure 27. Inflow components include streamflow from the three gaged tributary rivers (draining 80 percent of the watershed), streamflow from the ungaged land area (15 percent of the watershed area), and direct rainfall on the

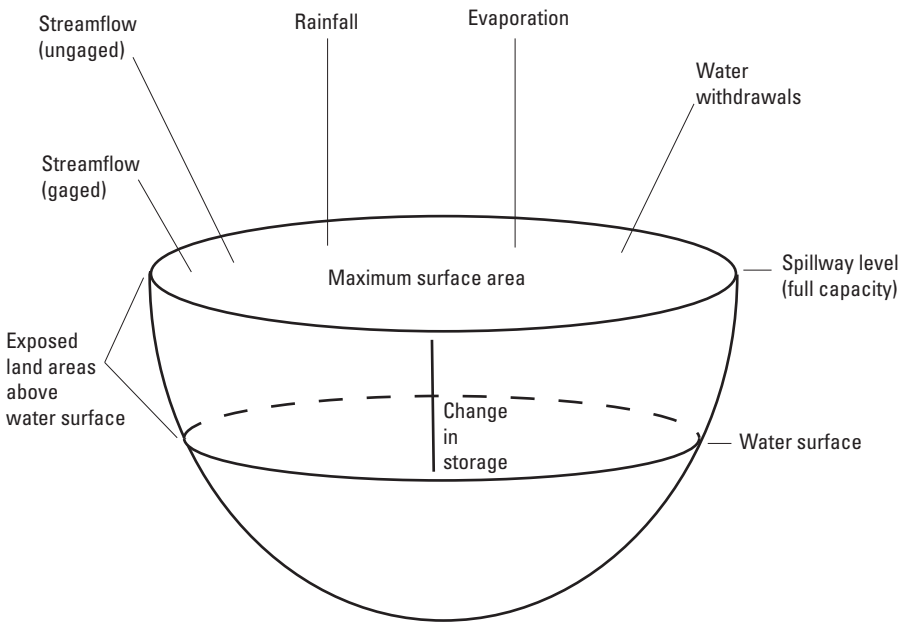

Figure 27. Components of the water-balance model for the Fena Valley Reservoir, Guam (Yeung, 2004).

reservoir water surface (5 percent). Outflows from the reservoir include withdrawals for water supply, and direct evaporation from the water surface of the reservoir. Limited understanding of groundwater exchange in Fena Valley Reservoir prevented the estimation of the loss or gain of groundwater. Groundwater inflow and outflow were assumed negligible relative to other inflow and outflow components. The low permeability of the clayey soil and volcanic rocks underlying the reservoir probably do not allow for appreciable water exchange between the reservoir and the groundwater body (Roumasset and others, 2010).

Model Development

The data required for an accurate calibration of the water-balance model are reservoir bathymetry, reservoir-wide average evaporation, reservoir-wide average rainfall, monthly water levels, tributary inflows, and water-withdrawal data.

Recent relations between reservoir water level and water-surface area, and water level and storage volume were developed (fig. 28) on the basis of the new bathymetric survey of the FVR (Marineau and Wright, 2015). The FVR_2016 water-balance model incorporated these relations to convert simulated month-end storage volume to water level and to determine month-end reservoir surface area.

Information pertaining to evaporation losses from the Fena Valley Reservoir is limited. Because pan-evaporation data are no longer collected in the vicinity of the reservoir, PET generated from the PRMS_2016 model, using the Jensen and Haise (1963) method, was applied in the water-balance model. Measured PET data were adjusted downward by 30 percent and these adjusted values were used as an approximation for the seasonal pattern and absolute magnitude of measured PET during the calibration process. The simulated average monthly PET rate was multiplied by the corresponding month-start reservoir surface area to estimate volume of reservoir evaporation loss for the month.

Rain falling on the water surface of the reservoir was considered a component of inflow. The simulated rainfall in the PRMS_2016 model of the Almagosa watershed was used to estimate rainfall inflow in the water-balance model. Monthly rainfall was estimated using the PRMS_2016 simulated basin rainfall with a rainfall adjustment factor applied. Direct inflow to the reservoir from rainfall was calculated as the monthly average rainfall times the maximum water-surface area of the reservoir. Maximum water-surface area was assigned the area when the water level in the reservoir was at the spillway crest. The water-surface area was held constant in the calculations because according to field observations during dry seasons, reservoir land area above the water surface and below spillway level remained nearly saturated. It was assumed that all rain falling on these saturated areas ran off and contributed directly to reservoir inflow.

Data for the remainder of the inflow and outflow components in the water-balance model, including gaged and ungaged streamflow and water withdrawals, were applied without adjustment. Gaged streamflow was calculated as the recorded streamflow from the three gaged rivers. Adjustment was not necessary for the Almagosa River data because recorded discharge at the gage reflected actual streamflow going into the reservoir. Streamflow from the ungaged land area was estimated using the PRMS_2016 model. Monthly total withdrawal data were metered and available from the U.S. Navy, (at the time of publication, data had not been published by the U.S. Navy). Accuracy of the recorded withdrawal data is not known.

Actual month-end reservoir volumes were compared with the simulated month-end reservoir volumes to assess the accuracy of the water-balance model. Reservoir volume (water storage) was calculated using month-end water-level measurements collected at the USGS reservoir water-level gage (16849000; fig. 17) at the Fena Dam spillway and the documented relation between water level and reservoir storage volume (Marineau and Wright, 2015; fig. 28). The accuracy ratings of the measured water-level data ranged from “poor” to “good.” Records were usually rated “good” except for periods of estimated data that were rated “poor.”

The monthly reservoir water-balance calculations are summarized in the following steps:

1. Given the reservoir water level at the beginning of a month, determine the initial reservoir volume (V_i) and surface area for the month using relations illustrated in figure 28.
2. Calculate the reservoir evaporation volume for the month (E) based on initial surface area times the estimated evaporation rate for the month as calculated by the PRMS_2016 model.
3. Determine the volume of water withdrawn (W) from the reservoir during the month based on data recorded by the U.S. Navy, Guam.
4. Estimate the volume of rain falling directly on the reservoir (R) during the month based on the surface area of the reservoir at spillway level times the monthly average rainfall.
5. Determine the volume of streamflow input to the reservoir from the gaged watersheds using data from the three gaged rivers (S_g).
6. Determine the volume of streamflow input to the reservoir from the ungaged areas using output from the PRMS_2016 model (S_u).
7. Determine volume of water in the reservoir at the end of the month (V_f) using the reservoir water-balance equation: $V_f = V_i + R + S_g + S_u - E - W$.

Model Calibration, Verification, and Results

The selection of periods used for calibration and verification of the water-balance model were dictated by the availability of concurrent data, similar to procedures used for the PRMS_2016 model. Periods of missing streamflow data and periods of questionable withdrawal data (owing to pumpmeter failure) limited model calibration and verification to four discontinuous periods between 2003 and 2009. Data for the periods September 2006 through September 2007 and September 2008 through September 2009 were used for model calibration, and data for the periods September 2003 through September 2004 and September 2007 through September 2008 were used for model verification. Calibration and verification periods were selected so that each included a drought period,

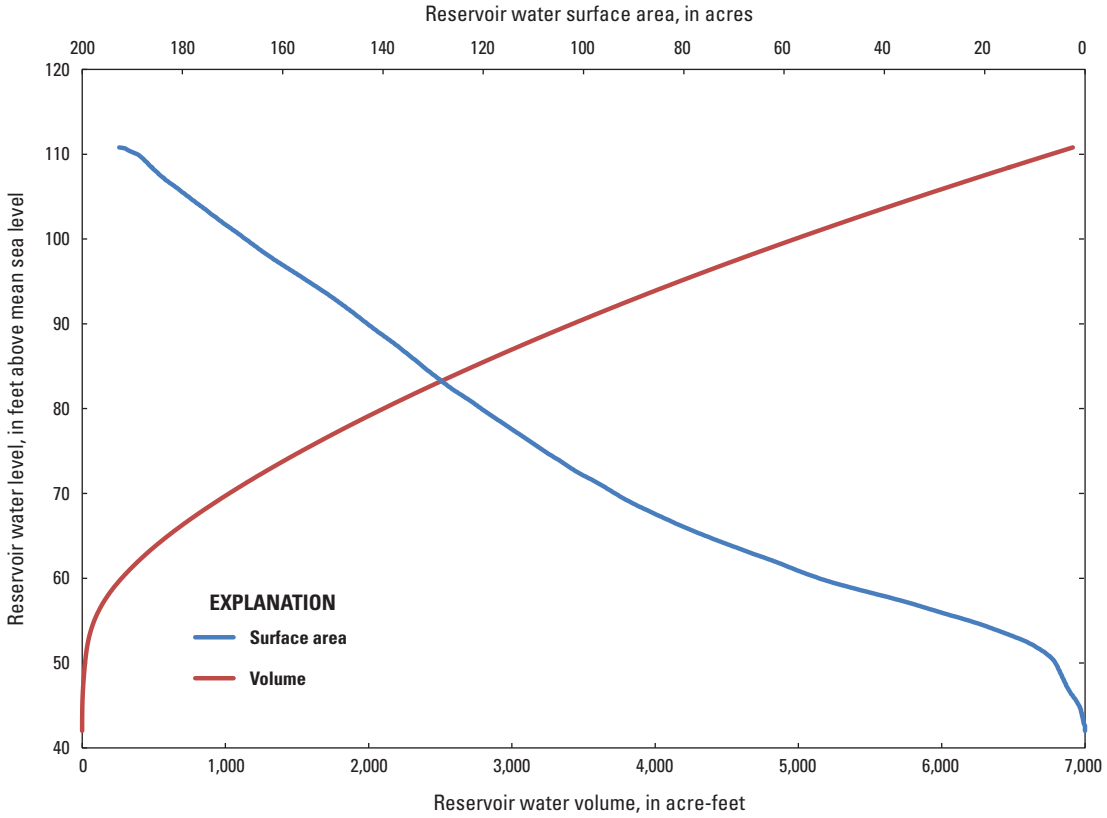

Figure 28. Water level-surface area and water level-capacity curves for the Fena Valley Reservoir, Guam (Marineau and Wright, 2015).

as the ability of the water-balance model to accurately simulate steep water-level declines during extreme dry conditions is critical to its utility as a management tool.

A relatively simple process was used to calibrate the water-balance model. Among all the water-balance components, direct evaporation and rainfall were the most uncertain and difficult to estimate. Because other components were comparatively well known, calibration involved adjusting only the correction coefficients associated with direct water-surface evaporation and rainfall. The coefficients were adjusted manually in a trial-and-error manner to fit simulated reservoir volumes to measured reservoir volumes.

Calibration and Verification Results

Calibration results indicated a rainfall correction coefficient of 1.17, which is similar to the adjustment applied in the Almagosa watershed model (table 8). A coefficient of 0.7 was applied to PET to estimate reservoir evaporation. The coefficient was expected to be close to 1.0 because evaporation from a large water surface is considered to be approximately equivalent to PET (Jones, 1992).

Monthly results for the calibration and verification periods are presented graphically in figures 29 and 30. The water-balance model generally simulated monthly reservoir storage volume with reasonable accuracy. For the calibration periods, errors associated with simulated month-end reservoir-storage volume for individual months ranged from 6.04 percent (284.6 acre-feet or 92.7 Mgal) to –5.70 percent (–240.8 acre-feet or –78.5 Mgal). For the verification periods, errors for individual months ranged from 4.22 percent (280.2 acre-feet or 91.3 Mgal) to 0.08 percent (5.7 acre-feet or 1.9 Mgal). Simulated month-end volumes for March 2008 to June 2008 were not included in the error analysis because reservoir water levels from the USGS gaging station for those months were estimated. Bias and relative errors also were calculated to evaluate model performance during both calibration and verification periods. Results are summarized in table 14. Monthly simulation bias ranged from –0.48 percent for the calibration period to 0.87 percent for the verification period; relative error ranged from –0.60 to 0.88 percent for the calibration and verification periods, respectively. Relatively small bias indicated that the model did not consistently overestimate or underestimate reservoir storage volume. Out of the 44 monthly simulations, 26 (59 percent) of the simulations resulted in overestimation and 10 (23 percent) resulted in underestimation. Water-balance model errors did not display any systematic patterns, therefore supporting the assumption that groundwater inflows and outflows were negligible relative to other model components. Because water levels above spillway crest level were not simulated, the model assumed any simulated volume greater than the reservoir capacity to be 6,915 acre-feet (2,253 Mgal).

Model Uncertainties

Although the water-balance equation is fairly simple, measures of accuracy regarding hydrologic phenomena are uncertain. The difference between simulated and measured reservoir volume reflects errors associated with measuring tributary inflow, change in storage, and water withdrawal; estimating streamflow from ungaged areas, rainfall, and reservoir evaporation; and neglecting flow between the reservoir and the groundwater body. Lacking meteorological measurements over the reservoir surface, evaporation was the most difficult component to quantify and had the highest uncertainty among all the water-balance components. Because evaporation is typically less than 7 percent of total outflow (table 15), errors associated with evaporation, however, are considered to have a relatively small effect on overall simulation results.

In terms of magnitude, the two largest water-budget components in the water-balance model are total watershed streamflow and water withdrawal (table 15). The magnitudes of these two components vary seasonally (fig. 31). Total watershed streamflow, the sum of gaged tributary inflow and simulated ungaged area streamflow, is much greater than the other components during the wet season. As a result, inflow during the wet season is overwhelmingly greater than outflow and the reservoir remains at full capacity during most of the wet season. The accuracies of rainfall and evaporation estimates during the wet season are therefore not very critical from a reservoir management perspective. From the onset of the dry season, reservoir volumes start to decline as total streamflow decreases and water withdrawals become more significant, around 94 percent of the outflow (fig. 31). A small error in the water-withdrawal data could have a substantial effect on the simulation results (table 15). This implies that the accuracy of the model calibration during the dry season is highly dependent on the accuracy of the water-withdrawal data.

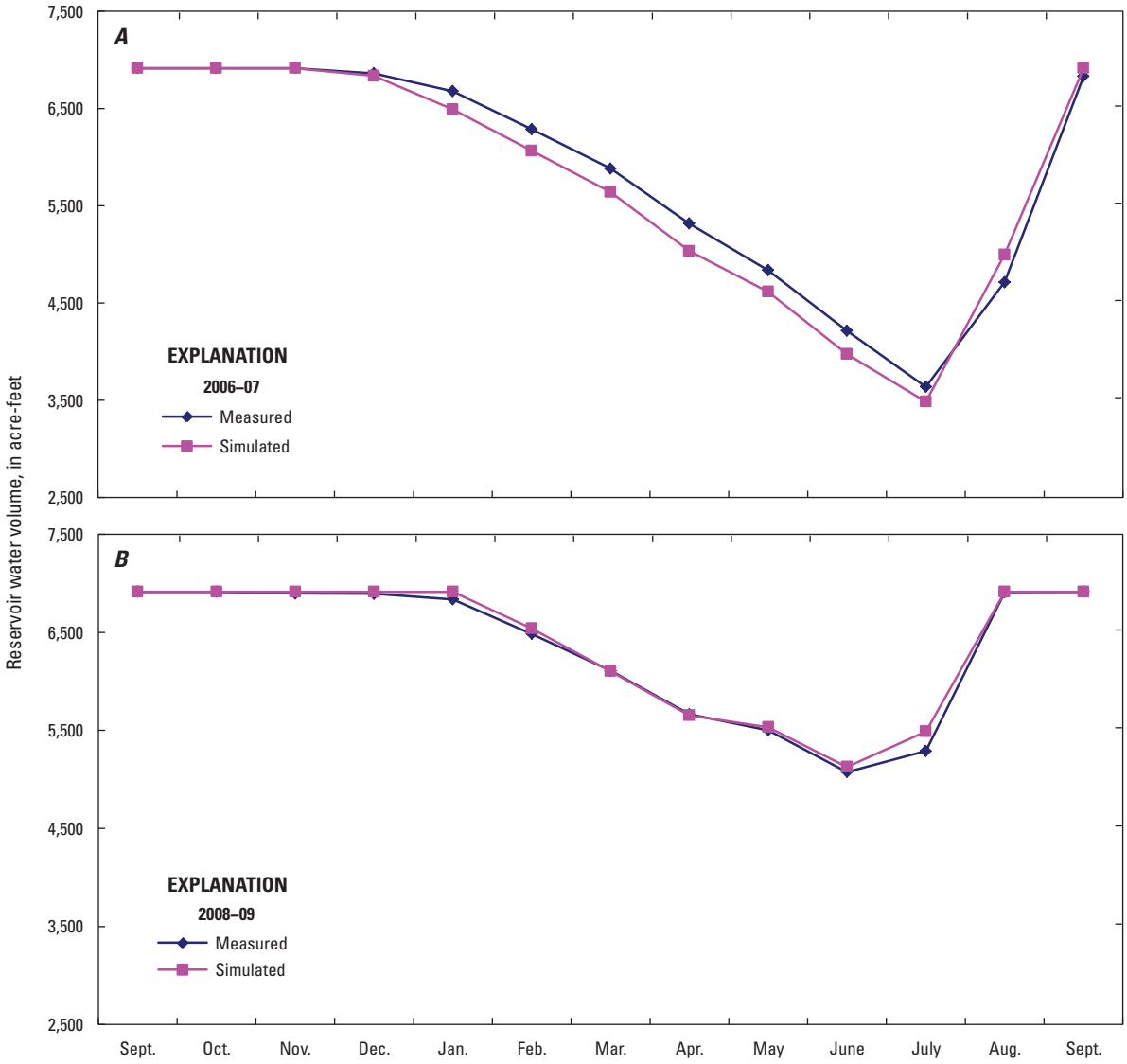

Figure 29. Measured and simulated month-end reservoir volume for the calibration periods, Fena Valley Reservoir, Guam, for (*A*) September 2006 to September 2007 and (*B*) September 2008 to September 2009.

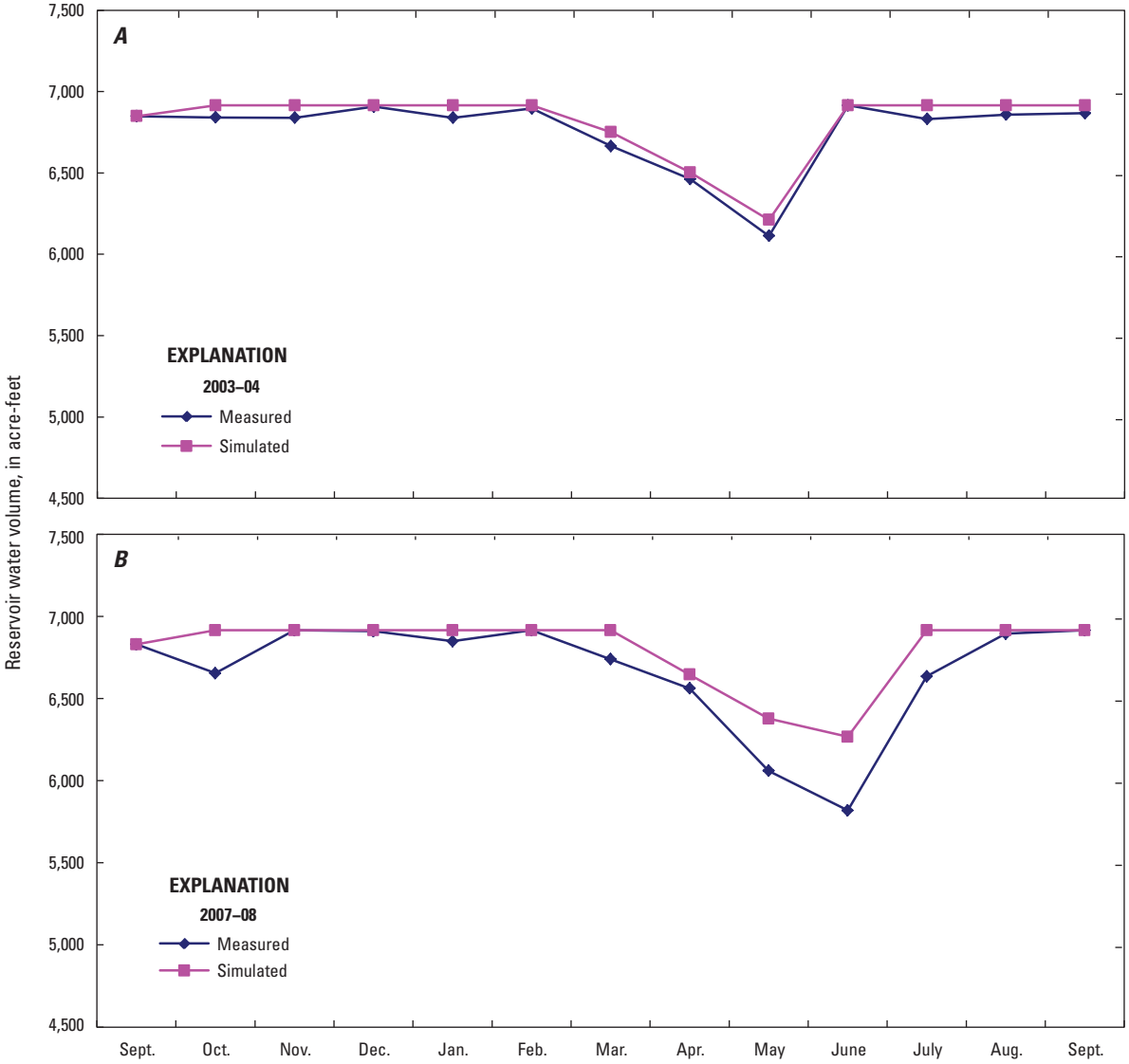

Figure 30. Measured and simulated month-end reservoir volume for the verification periods, Fena Valley Reservoir, Guam, for (*A*) September 2003 to September 2004 and (*B*) September 2007 to September 2008.

Table 14. Errors in simulated month-end storage volume in the Fena Valley Reservoir, Guam.

Period	Relative error[1] (percent)	Bias[2] (percent)	Over-simulation rate[3] (percent)
Calibration	–0.60	–0.48	42
Verification	0.88	0.87	80
Entire period	**0.08**	**0.18**	**59**

[1]Relative error: $\sum_{i=1}^{N}((SIM_i - MSD_i) / MSD_i) / N \times 100$

where,

SIM_i is simulated month-end storage volume for month i

MSD_i is measured month-end storage volume for month i

N is number of observed values

[2]Bias, as a percentage of mean observed storage volume,

$$= \left(\frac{\sum_{i=1}^{N} (SIM_i - MSD_i)}{\sum_{i=1}^{N} (MSD_i)} \right) \times 100$$

[3]Number of overestimated months divided by the total number of monthly simulations

Table 15. Water budget for the Fena Valley Reservoir during calibration and verification periods

Period	Inflows (percentage of total inflow)		Outflows (percentage of total outflows)	
	Total streamflow	Direct-rainfall	Evaporation	Water withdrawals
Calibration period				
September 2006– 2007	88.39	11.61	5.65	94.35
September 2008– 2009	88.69	11.31	6.41	93.59
Verification period				
September 2003– 2004	92.68	7.32	5.97	94.03
September 2007– 2008	89.25	10.75	7.14	92.86

Two-Step Modeling Procedure for Fena Valley Reservoir

The two-step modeling procedure (fig. 2) is used as a management tool by the U.S. Navy to estimate the response of the FVR to a variety of rainfall and water-withdrawal scenarios. The PRMS_2016 model of the Fena Valley watersheds can be used in conjunction with the FVR_2016 model, which incorporates a reservoir water balance (Yeung, 2004) and updated FVR capacity curves (Marineau and Wright, 2015), to estimate reservoir water levels. The first step involves application of the PRMS_2016 model to estimate monthly total streamflow for the three gaged watersheds and ungaged areas in the Fena Valley watershed. The second step involves use of the monthly streamflow and potential evapotranspiration estimates from the PRMS_2016 model as input to the FVR_2016 model to estimate water-level changes in the reservoir. Estimates of future water availability in the reservoir vary depending on the range of rainfall and water-withdrawal scenarios being evaluated.

Model Development

Rainfall scenarios commonly applied in the PRMS_2016 and FVR_2016 models are long-term average monthly rainfall and current ENSO rainfall projections provided by the Pacific ENSO Application Center at the University of Hawaii (http://www.weather.gov/peac/update). ENSO rainfall projections are reported as a percentage of long-term average monthly rainfall. The long-term average monthly rainfall for the updated model was calculated using the entire period of record for the Almagosa (1992–2015) and Fena (1993–2015) rain gages. The long-term average monthly rainfall values can be used directly in the water-balance model because the model is run using a monthly time step. The PRMS_2016 model, however, is applied on a daily time step and requires daily rainfall data to calculate monthly streamflow and potential evapotranspiration. Monthly rainfall projections are partitioned into daily time steps by following historical rainfall patterns recorded at the Almagosa and Fena rain gages. The pattern used to partition rainfall projections for the month of June, for example, is based on the June during which the recorded rainfall at each gage was the closest to the long-term average June rainfall for each respective rain gage. The same technique is applied to each of the remaining months. This method assumes that the historical rainfall patterns at the Almagosa and Fena Pump rain gages are reasonable representations of daily rainfall patterns for the monthly rainfall projections being modeled. The historical daily rainfall pattern is used to distribute the monthly ENSO rainfall projections for both the Almagosa and Fena rain gages and then used as input to the PRMS_2016 model to produce the streamflow estimates to evaluate future water availability. The long-term average minimum and maximum daily temperature data needed as input to run the

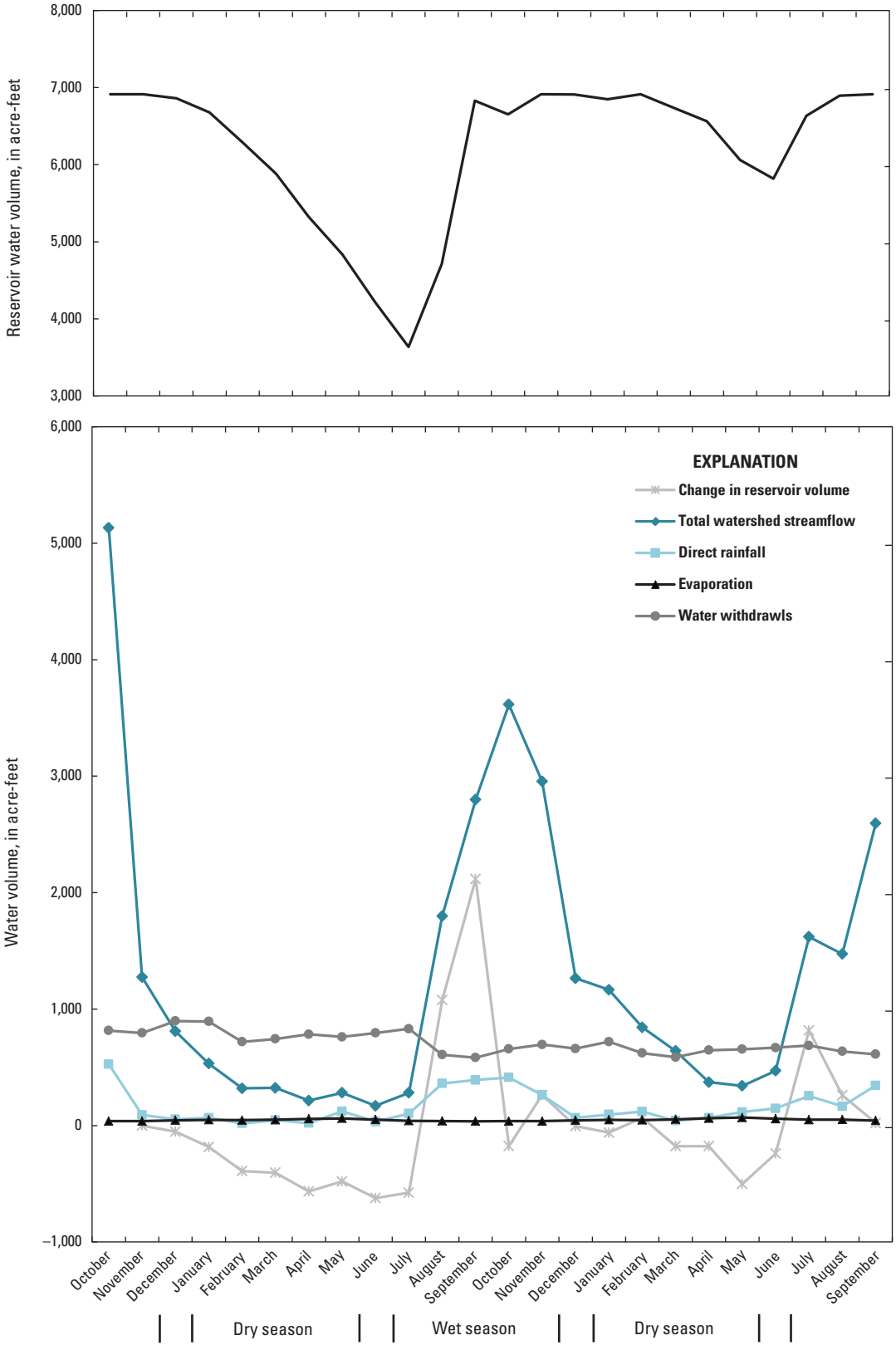

Figure 31. Monthly reservoir volume and water budget, Fena Valley Reservoir, Guam, from October 2006 to September 2008.

watershed model were from the NAS-Tiyan station using data from the last 30 years (1986–2015).

Model Verification

Earlier parts of this report focus on the accuracies of the PRMS_2016 model and FVR_2016 models individually. Measured daily rainfall was used as input in the evaluation of the PRMS_2016 model, and measured monthly rainfall and streamflow data were used as input in the evaluation of the FVR_2016 model. To evaluate the performance of the two-step modeling procedure as a whole, streamflow simulated using the PRMS_2016 model was used as input in the FVR_2016 model. Daily rainfall applied in the PRMS_2016 model was simulated by distributing the measured monthly total using the method as discussed above.

Periods in 2006–07 and 2008–09, each including a moderate ENSO event, were selected for the evaluation of the two-step modeling procedure. Monthly reservoir storage volumes computed using both measured and simulated daily rainfall were compared to measured reservoir storage volumes (fig. 32). Differences between calculated results using measured and simulated rainfall were used to indicate errors associated with using simulated rainfall patterns in the modeling procedure. The modeling procedure performed reasonably well when measured rainfall patterns were used. Results based on simulated rainfall using the ENSO forecasts (as updated every three months), however, consistently overestimated reservoir storage volumes in both evaluation periods. Overall in the two evaluation periods, monthly reservoir storage volumes computed from measured and simulated rainfall patterns were within 13.21 percent (622.7 acre-feet or 202.9 Mgal) and

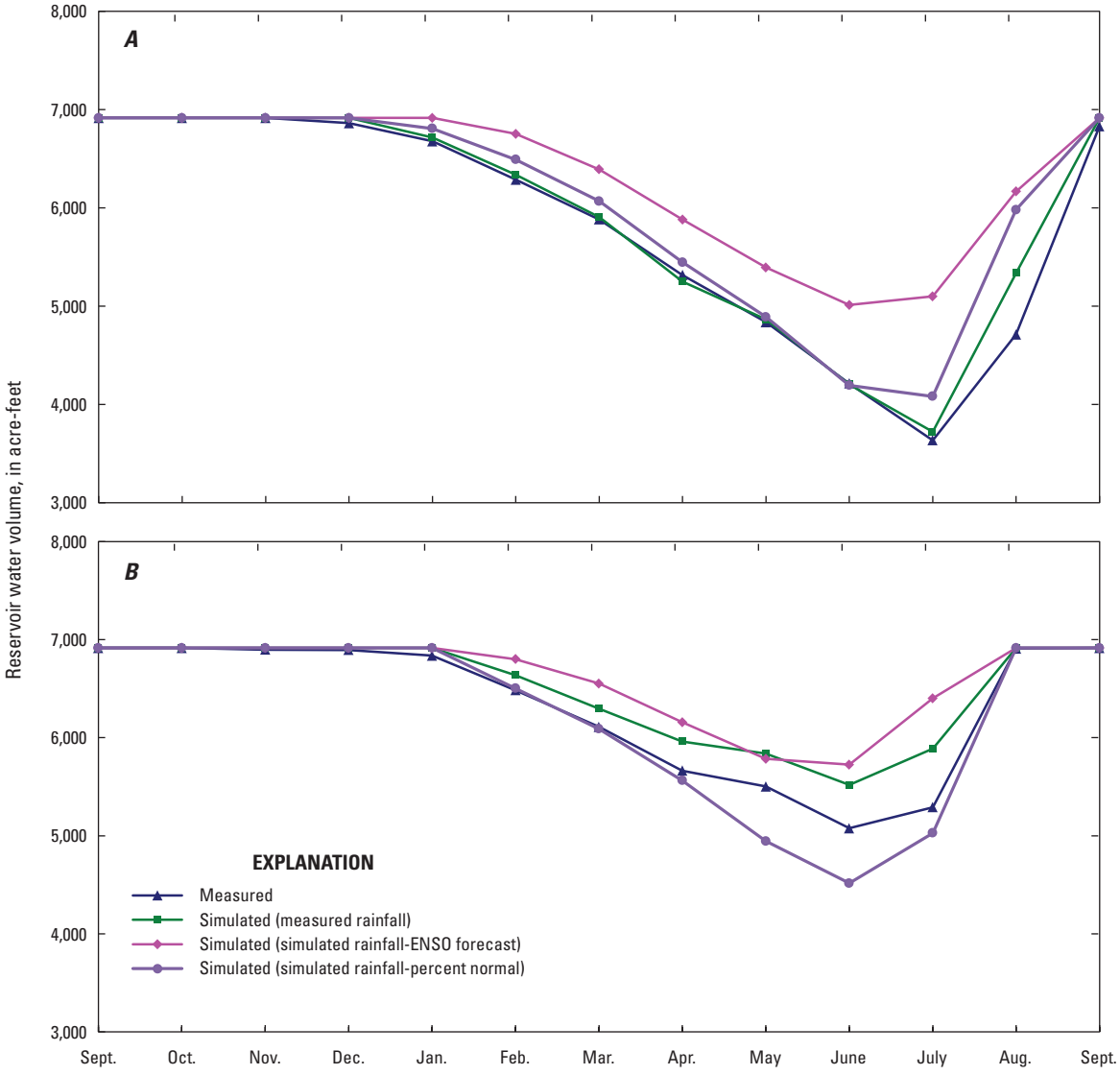

Figure 32. Measured and simulated month-end reservoir volume for the evaluation periods, Fena Valley Reservoir, Guam, from (*A*) September 2006 to September 2007 and (*B*) September 2008 to September 2009. ENSO, El Niño Southern Oscillation.

40.20 percent (1462.2 acre-feet or 476.5 Mgal), respectively. The water balance was re-run using the monthly values of observed percent normal of the long-term rainfall in the ENSO forecast bulletins instead of the ENSO forecast percent normal to eliminate the accuracy of the ENSO forecast and only evaluate the simulation of daily rainfall patterns. Daily rainfall values are still being estimated for input to PRMS_2016, however the observed percent normal are being used to represent the monthly rainfall values instead of the ENSO forecasts. Overall in the two evaluation periods, monthly reservoir storage volumes computed from the simulated rainfall patterns using the observed percent normal from the ENSO bulletin were estimated within 26.90 percent (1268.0 acre-feet or 413.2 Mgal) and 11.04 percent (560.0 acre-feet or 156.8 Mgal) of the measured reservoir storage volumes. It should be noted, however, that this does not measure the actual forecast capabilities of the procedure because the accuracy of a forecast is heavily dependent on the accuracy of rainfall and water-withdrawal projections being applied.

Summary and Conclusions

A two-step modeling procedure developed by the U.S. Geological Survey will allow estimates of monthly water levels in the FVR in response to various combinations of projected water-withdrawal rates and rainfall conditions. The first step in this predictive modeling procedure involves the use of the USGS PRMS_2016 model, a physically based, distributed-parameter watershed model designed to analyze the effects of rainfall, temperature, and land use on watershed streamflow. The second step of the procedure is to use streamflow estimates from the PRMS_2016 model as input to the FVR_2016 model to estimate changes in water levels in the reservoir.

The PRMS_2004 model (Yeung, 2004) was updated and recalibrated for the Maulap, Almagosa, and Imong River watersheds, and also expanded to all of southern Guam. The parameters from gaged watersheds were applied to the ungaged areas by transferring model parameters from nearby representative watersheds. The PRMS_2016 model also improved upon the simulated basin rainfall by using the inverse distance and elevation (ide_dist) distribution module. A small improvement was made in PET calculation accuracy by calibrating to solar radiation data, whereas the PRMS_2004 model used possible hours of sunshine (Yeung, 2004). Lastly, closed depressions were included in the PRMS_2016 model to more appropriately address internally drained limestone areas.

In the entirety of southern Guam, the watershed model has a "satisfactory" to "very good" rating, according to the criteria of Moriasi and others (2007), when simulating monthly mean streamflow for all but one of the gaged watersheds during the verification period. Statistical analyses of monthly measured and simulated streamflow for the three gaged rivers in the Fena Valley watershed and the Ugum River watershed indicated "very good" model performance for the PRMS_2016 model in these valuable surface-water resource areas. Model performance in the ungaged areas could not be evaluated. For the Fena Valley watersheds, bias in simulating monthly mean streamflow ranged from –0.67 to 0.60 percent for the calibration period and from –6.96 to 0.57 percent for the verification period; the coefficient of efficiency ranged from 0.87 to 0.94 percent for the calibration period and from 0.92 to 0.94 percent for verification period. The total streamflow-volume error for the entire simulation period ranged from -1.43 to 0.60 percent for the Fena Valley watersheds. For the Ugum River above Talofofo Falls watershed, bias in simulating monthly mean streamflow was 0.84 percent for the calibration period and 7.37 percent for the verification period; the coefficient of efficiency was 0.97 for the calibration period and 0.93 for the verification period. These statistics indicate that the PRMS_2016 model performance is "very good" in the Ugum River watershed. The only area where the PRMS_2016 model's monthly performance is rated "unsatisfactory" is the Talofofo River watershed, owing to the large bias during the verification period, which is most likely caused by the limited data available in southern Guam to run the model in the early 1950s.

Because reliable simulations of monthly dry season flows were of greatest concern, the focus of the PRMS_2016 model calibration was on monthly dry season conditions. Dry season model results for the entire simulation period indicated that streamflow can be predicted within 6.39 percent in the Maulap River watershed, within -0.54 percent in the Almagosa River watershed, and within 6.06 percent in the Imong River watershed. Although model error for the Maulap and Imong River watersheds was higher than for the other gaged watersheds, the results were still within the limits of the accuracy of the streamflow records used to develop the model.

The month-end reservoir volumes simulated by the FVR_2016 model for both calibration and verification periods compared closely with measured reservoir volumes. For the calibration periods, errors associated with month-end reservoir-storage simulation for individual months ranged from 6.04 percent (284.6 acre-feet or 92.7 Mgal) to –5.70 percent (–240.8 acre-feet or –78.5 Mgal). For the verification periods, errors for individual months ranged from 4.22 percent (280.2 acre-feet or 91.3 Mgal) to 0.08 percent (5.7 acre-feet or 1.9 Mgal). Monthly simulation bias ranged from –0.48 percent for the calibration period to 0.87 percent for the verification period; relative error ranged from –0.60 to 0.88 percent for the calibration and verification periods. Relatively small bias indicated that the model did not consistently overestimate or underestimate reservoir volume.

The PRMS_2016 model of the Fena Valley watersheds developed as part of this study represents a reliable tool for estimating streamflow contributions to the FVR. The PRMS_2016 model, in conjunction with the reservoir water-balance model, which was also recalibrated in this study, provide accurate and reliable estimates of future availability of water supply in the FVR for a broad range of projected climatic and water-withdrawal scenarios. This information is

critical to the U.S. Navy to make timely decisions regarding the amount of water that can reliably be withdrawn from the reservoir. The updated and expanded PRMS_2016 model is a useful tool to evaluate changes in streamflow and recharge owing to climate change or land-cover change in other watersheds of interest in southern Guam, such as the Ugum River. Datasets of projected climate could be used as input to PRMS_2016 to evaluate potential climate-change impacts to Guam's surface-water resources.

References Cited

Daly, C., and Halbleib, M., 2006, Pacific Islands (Guam) average monthly and annual minimum and maximum temperature and mean dewpoint temperature, 1971–2000: PRISM Group at Oregon State University, accessed June 22, 2011, at http://www.prism.oregonstate.edu/products/pacisl.phtml.

Donnegan, J.A., Butler, S.L., Grabowiecki, Walter, Hiserote, B.A., and Limtiaco, David, 2004, Guam's forest resources, 2002: U.S. Department of Agriculture, Forest Service, Resources Bulletin PNW-RB-243, 32 p.

Fennessey, N.M., 1995, Sensitivity of reservoir-yield estimates to model time step surface-moisture fluxes: Journal of Water Resources Planning and Management, v. 121, no. 4, p. 310–317.

Gingerich, S.B., 2013, The effects of withdrawals and drought on groundwater availability in the Northern Guam Lens Aquifer, Guam: U.S. Geological Survey Scientific Investigations Report 2013–5216, 76 p. [Also available at http://dx.doi.org/10.3133/sir20135216.]

Guard, C., Hamnett, M.P, Neuman, C.J., Lander, M.A., and Siegrist, H.G, 1999, Typhoon vulnerability study for Guam, University of Guam, Water and Environmental Research Institute Technical Report no. 85-2, 23 p.

Hamon, W.R., 1961, Estimating potential evapotranspiration: Proceedings of the American Society of Civil Engineers, Journal of the Hydraulics Division, v. 87, no. 3, p. 107–120

Hay, L.E., and Umemoto, Makiko, 2007, Multiple-objective stepwise calibration using Luca: U.S. Geological Survey Open-File Report 2006–1323, 25 p.

Heitz, L.F., 2015, Digital atlas of southern Guam—Rainfall distribution (variation in precipitation): University of Guam, Water and Environmental Research Institute, accessed May 2015, at http://south.hydroguam.net/map-climate-precipitation.php.

Intergovernmental Panel on Climate Change, 2013, Climate change 2013—The physical science basis, *in* Stocker, T.F., Qin, D., Plattner, G.-K., Tignor, M., Allen, S.K., Boschung, J., Nauels, A., Xia, Y., Bex, V., and Midgley, P.M., eds., Contribution of Working Group I to the Fifth Assessment Report of the Intergovernmental Panel on Climate Change: Cambridge, United Kingdom, Cambridge University Press, 1,535 p.

Jensen, M.E., and Haise, H.R., 1963, Estimating evapotranspiration from solar radiation: Proceedings of the American Society of Civil Engineers, Journal of Irrigation and Drainage, v. 89, p. 15–41.

Jocson, J.M.U., Jenson, J.W., and Contractor, D.N., 2002. Recharge and aquifer response—Northern Guam lens aquifer, Guam, Mariana Islands: Journal of Hydrology, v. 260, no. 1, p.231–254.

Johnson, A.G., 2012, A water-budget model and estimates of groundwater recharge for Guam: U.S. Geological Survey Scientific Investigations Report 2012–5028, 53 p. [Also available at http://pubs.usgs.gov/sir/2012/5028/.]

Jones, F.E., 1992, Evaporation of water with emphasis on applications and measurements: Michigan, Lewis Publishers, Inc., 188 p.

Keener, V.W., Marra, J.J., Finucane, M.L., Spooner, D., and Smith, M.H., 2012, Climate change and Pacific Islands—Indicators and impacts: Report for the 2012 Pacific Islands Regional Climate Assessment (PIRCA), 170 p.

Kubota, Hisayuki, and Wang, Bin, 2009, How much do tropical cyclones affect seasonal and interannual rainfall variability over the Western North Pacific?: Journal of Climate, v. 22, p. 5495–5510.

Lander, M.A., 1994, Meteorological factors associated with drought on Guam: University of Guam Water and Energy Research Institute of Western Pacific Technical Report no. 75, 39 p.

Lander, M.A., and Guard, C.P., 2003, Creation of a 50-year rainfall database, annual rainfall climatology, and annual rainfall distribution map for Guam: Mangilao, Guam, University of Guam, Water and Environmental Research Institute Technical Report no. 102, 20 p. plus appendixes.

Marineau, M.D., and Wright, S.A, 2015, Storage capacity of the Fena Valley Reservoir, Guam, Mariana Islands, 2014: U.S. Geological Survey Scientific Investigations Report 2015–5128, 31 p. [Also available at http://dx.doi.org/10.3133/sir20155128.]

Markstrom, S.L., Niswonger, R.G., Regan, R.S., Prudic, D.E., and Barlow, P.M., 2008, GSFLOW—Coupled groundwater and surface-water flow model based on the integration of the Precipitation-Runoff Modeling System (PRMS) and the Modular Ground-Water Flow Model (MODFLOW–2005): U.S. Geological Survey Techniques and Methods, book 6, chap. D1, 240 p.

Markstrom, S.L., Regan, R.S., Hay, L.E., Viger, R.J., Webb, R.M.T., Payn, R.A., and LaFontaine, J.H., 2015, PRMS-IV, the precipitation-runoff modeling system, version 4: U.S. Geological Survey Techniques and Methods, book 6, chap. B7, 158 p. [Also available at http://dx.doi.org/10.3133/tm6B7.]

Mink, J.F., 1976, Groundwater resources of Guam; Occurrence and development: Water and Environmental Research Institute of the Western Pacific, University of Guam, Technical Report no. 1, 276 p.

Moriasi, D.N., Arnold, J.G., Van Liew, M.W., Bingner, R.L., Harmel, R.D., and Veith, T.L., 2007, Model evaluation guidelines for systematic quantification of accuracy in watershed simulations: American Society of Agricultural and Biological Engineers, v. 50, no. 3, p. 885–900.

Nakama, L.Y., 1992, Storage capacity of Fena Valley Reservoir, Guam, Mariana Islands, 1990: U.S. Geological Survey Water-Resources Investigations Report 92-4114, 17 p.

Nakama, L.Y., 1994, Application of the precipitation-runoff modeling system model to simulate dry season runoff for three watersheds in south-central Guam: U.S. Geological Survey Water-Resources Investigations Report 93-4116, 38 p.

Nash, J.E., and Sutcliffe, J.V., 1970, River flow forecasting through conceptual models—Part 1–A discussion of principles: Journal of Hydrology, v. 10, p. 282–290.

National Oceanic and Atmospheric Administration, 2007, Joint Airborne Lidar Bathymetry Technical Center of Expertise (JALBTCX) tobobathy lidar: Guam, National Ocean Service's Office for Coastal Management, accessed May 2015, at https://coast.noaa.gov/htdata/lidar1_z/geoid12a/data/551.

National Oceanic and Atmospheric Administration, 2015, National Weather Service Cooperative Observer Program: National Oceanic and Atmospheric Administration web page, accessed February 2015, at http://www.nws.noaa.gov/om/coop.

National Oceanic and Atmospheric Administration, 2016, National Weather Service Climate Prediction Center: National Oceanic and Atmospheric Administration web page, accessed July 2016, at http://www.cpc.noaa.gov/products/precip/CWlink/MJO/enso.shtml.

National Renewable Energy Laboratory, 2007, Digital solar radiation data for the United States and its territories: National Renewable Energy Laboratory web page, accessed February 25, 2010, at http://rredc.nrel.gov/solar/old_data/nsrdb/.

Regan, R.S., and LaFontaine, J.H., 2017, Documentation of the dynamic parameter, water-use, stream and lake flow routing, and two summary output modules and updates to surface-depression storage simulation and initial conditions specification options with the Precipitation-Runoff Modeling System (PRMS): U.S. Geological Survey Techniques and Methods, book 6, chap. B8, 60 p., https://doi.org/10.3133/tm6B8.

Rosa, S.N., and Hay, L.E., 2017, Supporting data for Fena Valley Reservoir watershed and water-balance model, southern Guam: U.S. Geological Survey data release, https://doi.org/10.5066/ F7HH6HV4.

Roumasset, J., Burnett, K.M., and Balisacan, A.M., 2010, Sustainability science for watershed landscapes, sustainable water quality management for Pacific Island watersheds—Illustrations from American Samoa, Hawaii, and Micronesia: Institute of Southeast Asian Studies, 346 p.

Schroeder, T.A., Chowdhury, Md R., Lander, M.A., Guard, C.C., Felkley, C., and Gifford, D., 2012, The role of the Pacific ENSO Applications Climate Center in reducing vulnerability to climate hazards—Experience from the US-affiliated Pacific Islands: Bulletin of the American Meteorological Society, v. 93, p. 1003–1015, doi:10.1175/BAMS-D-11-00109.1.

Siegrist, H.G., Jr., Reagan, M.K., Randall, R.H., and Jenson, J.W., 2007 Geologic map and sections of Guam, Mariana Islands: Water and Environmental Research Institute of the Western Pacific, University of Guam, map, scale 1:50,000, accessed May 2015, at http://www.weriguam.org/pdf/geologic-maps/map-of-guam.pdf.

Taborosi, Danko, 2006, Karst inventory of Guam, Mariana Islands: Water and Environmental Research Institute of the Western Pacific, University of Guam, Technical Report no. 112, 141 p.

Taborosi, D., Jenson, J.W., and Mylroie, J.E., 2004, Karst features of Guam Marianas Islands: Water and Environmental Research Institute of the Western Pacific, University of Guam, Technical Report no. 104, 29 p.

Taylor, C.J., and Nelson, H.L., Jr., 2008, A compilation of provisional karst geospatial data for the Interior Low Plateaus physiographic region, central United States: U.S. Geological Survey Data Series 339, 26 p.

Tracey, J.I., Jr., Schlanger, S.O., Stark, J.T., Doan, D.B., and May, H.G., 1964, General geology of Guam: U.S. Geological Survey Professional Paper 403–A, 104 p., 3 pl.

U.S. Department of Agriculture, 2006, Detailed vegetation map for the Island of Guam: U.S. Department of Agriculture, Forest Service Region 5, State and Private Forestry, Forest Health Protection, accessed March 29, 2010, at http://www.fs.fed.us/r5/spf/fhp/fhm/landcover/islands/index.shtml.

U.S. Department of Agriculture, 2009, Soil survey geographic (SSURGO) database for Territory of Guam: U.S. Department of Agriculture, Natural Resources Conservation Service, accessed March 31, 2010, at http://soildatamart.nrcs.usda.gov/Survey.aspx?County=GU010.

U.S. Geological Survey, 2015, USGS water data for Guam: U.S. Geological Survey National Water Information System Web page, accessed May 26, 2015, at http://waterdata.usgs.gov/gu/nwis/nwis.

Viger, R.J., and Leavesley, G.H., 2007, The GIS Weasel user's manual: U.S. Geological Survey Techniques and Methods, book 6, chap. B4, 201 p.

Ward, P.E, Hoffard, S.H., and Davis, D.A., 1965, Hydrology of Guam, *in* Geology and hydrology of Guam, Mariana Islands: U.S. Geological Survey Professional Paper 403–H, 28 p., 1 pl.

Ward-Garrison, C., Markstrom, S.L., and Hay, L.E., 2009, Downsizer—A graphical user interface-based application for browsing, acquiring, and formatting time-series data for hydrologic modeling: U.S. Geological Survey Open-File Report 2009–1166, 27 p.

Yeung, C.W., 2004, Rainfall-runoff and water-balance models for management of the Fena Valley Reservoir, Guam: U.S. Geological Survey Scientific Investigations Report 2004–5287, 52 p.

Young, F.J., 1988, Soil survey of territory of Guam: U.S. Department of Agriculture Soil Conservation Service, 166 p.

Menlo Park and Lafayette Publishing Service Centers
Manuscript approved August 30, 2017
Edited by Katherine Jacques
Design and layout by James E. Banton

ISSN 2383-0328 (online)
https://doi.org/10.3133/sir20175093